5-27-2013 12:00 AM

Elucidating the Role of Menin During Islet Cell Development in the Human Fetal Pancreas

Jessica L. Dubrick
The University of Western Ontario

Supervisor
Dr. Rennian Wang
The University of Western Ontario

Graduate Program in Pathology
A thesis submitted in partial fulfillment of the requirements for the degree in Master of Science

ELUCIDATING THE ROLE OF MENIN DURING ISLET CELL DEVELOPMENT IN THE HUMAN FETAL PANCREAS

(Thesis format: Monograph)

by

Jessica L. Dubrick

Graduate Program in Pathology

A thesis submitted in partial fulfillment
of the requirements for the degree of
Master of Science

The School of Graduate and Postdoctoral Studies
The University of Western Ontario
London, Ontario, Canada

Abstract

Studies show that Menin, a tumour suppressor encoded by the multiple endocrine neoplasia type 1 (*Men1*) gene, is required during murine pancreatic development. In humans, mutation results in the MEN1 tumourigenic syndrome; however, knowledge of menin in human pancreatic development is limited. This study examined the expression pattern and functional role of menin during human fetal islet development. Immunostaining revealed the presence of nuclear menin within pancreatic cells from the 1st through 2nd trimester co-localizing with various developmental factors. Knockdown of *MEN1* in human fetal islet-epithelial cells significantly increased apoptosis, reduced proliferation, and decreased SOX9, NKX2.2, and NKX6.1 mRNA levels (transcription factors required in maintenance of the progenitor pool and endocrine differentiation). Overexpression of *MEN1* confirmed these results suggesting that menin promotes cell survival and proliferation, maintains the islet progenitor pool, and regulates islet differentiation in the human fetal pancreas: a different function compared to its anti-tumourigenic role during adulthood.

Keywords: *MEN1*, Menin, human fetal pancreas, islet-epithelial cell clusters, endocrine differentiation, *MEN1* overexpression, *MEN1* knockdown

Dedication

I would like to dedicate this thesis to my family. To my parents, for encouraging my interest in science at a young age and for bringing the world of medicine to life at the dinner table every night. For instilling in me the spirit to always shoot for the stars, for that even if you stumble at least you'll end up on the moon. With your unconditional love and support throughout my studies, I can never truly express my gratitude towards you both. To my brother, who keeps me smiling no matter the circumstance. Finally, to my grandparents, who also supported and believed in me, that I could do anything if I put my mind to it, to never settle for anything less than the best.

Acknowledgements

I would like to express my gratitude to my supervisor, Dr. Rennian Wang, who provided me this opportunity to pursue a graduate degree in her lab and who devised a thesis project that combined both my interests of diabetes and oncology research. Her experience, understanding, and patience have added considerably to my graduate experience. I am very grateful for this amazing opportunity and for the financial and technical support she has provided me throughout my period of study.

I would like to thank Jinming Li, our lab technician; without his technical support and guidance this project would not have been completed. I am deeply grateful for his assistance with various aspects of my project, for his knowledge of various techniques, his understanding, his patience and for our conversations at the lab bench which brought a smile on many occasions.

I would like to thank the members of the Wang Lab especially Zhi Chao Feng, Matt Riopel, and Jamie Belo, for your advice, ongoing support, assistance with various tasks, and for making my experience in the Wang Lab what it was. I have enjoyed our random discussions at our desks and on the bench while waiting for experiments, and our entertaining antics outside of the lab and during lab lunches. To our various fourth year undergraduate students throughout the years, you have also been a source of support and have offered your help whenever needed.

I would also like to thank the members of my advisory committee, Dr. Alison Allan and Dr. Chandan Chakraborty, for their experience, advice and support throughout my project. Many thanks to Dr. Chakraborty for all the time he has spent reading my thesis drafts, his comments and advice in the midst of his other important commitments are very much appreciated.

To my friends in London and back at home who have encouraged me and helped me through these years during graduate school in a new city. To Kim Beaucage and Mario Elia, who have spent countless hours editing this thesis; your support and encouragement during this process has been abundant and extremely appreciated. And finally, to my

family who continue to offer me unconditional love, support and encouragement throughout my life and in whatever I decide to pursue.

In conclusion, I would like to recognize that this research would not have been possible without the financial assistance of the Canadian Institutes of Health Research, the Canadian Diabetes Association, the Children's Health Research Institute and the Department of Pathology at the University of Western Ontario; to these agencies I express my gratitude.

Table of Contents

List of Tables

List of Figures

List of Appendices

List of Abbreviations

°C	degrees Celsius
%	percent
18S	ribosomal RNA subunit, 18 Svedburg units
28S	ribosomal RNA subunit, 28 Svedburg units
µg	microgram
µL	microliter
AKT (PKB)	protein kinase B
ANOVA	analysis of variance
ASK	activator S-phase kinase
ATR	ataxia telangiectasia and Rad3 related
bHLH	basic helix-loop-helix
BM-MSC	bone-marrow derived mesenchymal stem cell
BMP	bone morphogenetic protein
Btc	betacellulin
bp	base pairs
BRCA1	breast cancer 1, early onset
BSA	bovine serum albumin
CASP8	caspase-8
CDK	cyclin-dependent kinase

cDNA	complimentary DNA
CK19	cytokeratin 19
cm	centimeter
CNS	central nervous system
Ctrl	control
DAPI	4’-6’-diamidino-2-phenylindol
DNA	deoxyribonucleic acid
DNase I	deoxyribonuclease I
DEPC	diethylpyrocarbonate
dH_2O	distilled H_2O
dNTP	deoxyribonucleotide triphoshate
DSHB	developmental studies hybridoma bank
DTT	DL-Dithiothreitol; Clelands reagent
e	embryonic day
E_2	estradiol
EBs	embryoid bodies
ECL	enhanced chemiluminescence
EGFP	enhanced green fluorescent protein
ER	estrogen receptor
ERK	extracellular signal-regulated kinase

ES cells	embryonic stem cells
FAK	focal adhesion kinase
FancD2	fanconi anemia, complementation group D2
FBS	fetal bovine serum
FoxA1	fork head box A1
FoxA2	fork head box A 2
FoxO1	fork head box O 1
GTP	guanosine triphosphate
HBSS	Hank’s balanced salt solution
HES1	hairy and enhancer of split 1
HEPES	N-2-Hydroxyethylpiperazine-N’-2-Ethanesulfonic Acid
HDAC	histone deacetylase complex
HMTC	histone methyl transferase complex
HOX	homeobox
hr(s)	hour(s)
hTERT	human telomerase reverse transcriptase
IAPP	islet amyloid polypeptide
Igf2	insulin growth factor 2
IGFBP2	insulin-like growth factor binding protein 2
IQGAP1	IQ motif containing GTPase activating protein 1

ISL1	islet-1
kDa	kilodalton
KI67	proliferation index
JRL	Jackson immunoresearch labs
m	months
mA	milliamp
Men1	multiple endocrine neoplasia type 1
mg	milligrams
mL	milliliter
MLL	mixed-lineage leukemia
mM	millimol/liter
mol	mole
MODY4	maturity onset diabetes of the young type 4
mRNA	messenger RNA
NES	nuclear export signal
NFκB	nuclear factor kappa B
ng	nanogram
NGN3	neurogenin 3
NKX2.2	NK2 related transcription factor related, locus 2
NKX6.1	NK6 related transcription factor related, locus 1

NLS	nuclear localization signal
nM	nanomole/liter
p	p value
PBS	phosphate-buffered saline
PCR	polymerase chain reaction
PC1/3	prohormone convertase 1/3
PDX1	pancreatic duodenal homeobox 1
PFA	paraformaldehyde
PI3K	phosphoinositide 3-kinase
POLR2B	polymerase (RNA) II (DNA directed) polypeptide B
PP	pancreatic polypeptide
PTH	parathyroid hormone
qRT-PCR	quantitative real-time reverse transcription PCR
Rb	retinoblastoma
RbBP5	retinoblastoma binding protein 5
RelA	v-rel reticuloendotheliosis viral oncogene homolog A
RNA	ribonucleic acid
RPA2	replication protein A2
rpm	revolutions per minute
Runx2	runt-related transcription factor 2

SDS-PAGE	sodium dodecyl sulfate-polyacrylamide gel electrophoresis
SEM	standard error of the mean
siRNA	small interfering RNA
SOX9	SRY box 9
SRY	sex determining region Y
ss	single stranded
TBST	tris-buffered saline with 0.1% Tween 20
TCF	T-cell factor
TFF1	trefoil factor 1
TGFβ	transforming growth factor, beta
TUNEL	terminal deoxynucleotidyl transferase dUTP nick end labeling
vs.	versus
UTP	uridine triphosphate
Wnt	wingless integration 1
wk(s)	week(s) of fetal age
yr(s)	year(s)

Chapter 1

Introduction

Chapter 1 – **Introduction**

1.1 **Significance of the Study**

The increasing prevalence of diabetes mellitus worldwide continues to be a growing concern. In the past decade, the prevalence has more than doubled with projections to increase another 54% from 2010 to 2030 (Chen et al., 2012). This will amount to 7.7% of the total adult population worldwide (ages 20-79 years old), illustrating the need for continued development of cost-effective and efficient treatments, as well as a potential cure for diabetes.

Diabetes mellitus is a chronic metabolic disease characterized by an abnormally high blood glucose level (hyperglycemia), where the body in unable to use or uptake glucose adequately. Insulin, a hormone produced and secreted by pancreatic beta-cells (found in islets of Langerhans), is involved in lowering blood glucose levels. The two main types of diabetes are classically described as either a deficiency in insulin production due to an auto-immune destruction of islet beta-cells (Type 1) or the inability of target cells to respond to insulin (called insulin resistance, Type 2) (Kim and Hebrok, 2001; Sander and German, 1997). However, type 2 has a complex pathophysiology encompassing insulin resistance, loss of normal beta-cell function and a reduction in beta-cell mass (all of which vary to certain degrees between patients) resulting in a relative insulin deficiency similar to Type 1 (Donath and Halban, 2004). Insulin-replacement therapy is used to treat type 1 patients. Some type 2 patients will also require insulin-replacement therapies if target glucose control cannot be maintained with oral hypoglycemic medications (Kim and Hebrok, 2001; Riethof et al., 2012; Tan et al., 2011). Over the past few decades, the leading edge in insulin-replacement therapy research has focused on beta-cell replacement therapy through the transplantation of islets and overcoming the numerous obstacles involved in this procedure. Some drawbacks have included the lack of donor islet material, the need for life-long immunosuppression, and the declining survival and function of the grafted beta-cells (Senior et al., 2012).

My specific research focus contributes to the broader goal of enhancing the production of more viable and functionally efficient islet beta-cells from existing pancreatic cells,

pancreatic progenitor cells, or stem cells. Current research in the production of functional insulin-secreting cells has noted that engineered cells showed insufficient functionally, low differentiation efficiency, and numerous side effects post transplantation (Liu et al., 2013; Seymour and Sander, 2011). By understanding fetal beta-cell development, its intricate process, and the network of factors and pathways involved, this will give insight into furthering the production and overcoming the obstacles of engineered beta-cells (Seymour and Sander, 2011; Wells, 2003). My research aims to further the understanding of transcription factor expression patterns, functions, and the network involved in islet differentiation during human fetal pancreatic development. Specifically, this project looks at the involvement of the transcription factor menin in the developing human fetal pancreas and its interactions. Menin is encoded by the *MEN1* gene, named for the disease which its mutation causes, Multiple Endocrine Neoplasia type 1, in adult tissues (Bertolino et al., 2003a; Stewart et al., 1998). Studies in the developing rodent pancreas have revealed a requirement for the protein menin in progenitor and endocrine differentiation; an altered function compared to its anti-tumourigenic role within adult tissues (Fontaniere et al., 2008). We have recently characterized the transcriptional profiles of islet progenitor cells during human fetal pancreatic development (Lyttle et al., 2008) and our microarray investigation of 8-21 week human fetal pancreata revealed that *MEN1* is highly expressed relative to adult pancreatic islets. Genes encoding proteins involved in Menin-regulated signaling pathways in the developing mouse pancreas (e.g. Wnt/β-catenin, TGF-β) are highly upregulated in parallel cells, suggesting that Menin may play a role in regulating endocrine cell differentiation. This study will examine whether this altered function between fetal and adult tissues is recapitulated in the developing human fetal pancreas as was seen in rodents and provide us with a better sense of how human islet cells develop.

1.2 Pancreatic Development

1.2.1 The Human Pancreas

The human pancreas is a vital complex organ functioning to produce hormones and enzymes regulating nutrient homeostasis. It can be found in the retroperitoneal region and is comprised of four distinct regions: the head, neck, body and tail. The head is located on the right side of the body adjacent to the duodenum (the first section of the small intestine) where the main pancreatic duct connects to the common bile duct and the narrow pancreatic tail extends to the left side of the body to lie adjacent to the spleen (Slack, 1995). In humans, this organ can weigh between 70 to 150 grams and measure 15-25 cm in length. The pancreas is composed of two distinct glandular tissues: the exocrine compartment which is comprised of ducts and acini makes up over 90% of the pancreas and produces digestive enzymes, and the endocrine compartment (approximately 1-2%) which is organized into structures known as islets of Langerhans (Cleaver, 2010; Slack, 1995).

Islets are embedded within the exocrine tissue and are responsible for producing and secreting hormones into the blood stream for regulation of glucose homeostasis (Slack, 1995). The islets of Langerhans are composed of 5 principle cell types including glucagon secreting alpha (α)-cells, beta (β)-cells secreting insulin, delta (δ)-cells secreting somatostatin, epsilon (ε)-cells secreting ghrelin, and pancreatic polypeptide (PP)-containing PP-cells. The various hormones function such that insulin reduces blood glucose, glucagon increases blood glucose, somatostatin regulates alpha- and beta-cell secretion, PP suppresses exocrine enzyme secretion and appetite, and ghrelin acts to inhibit insulin secretion and increase appetite (Lin and Chance, 1974; Pusztai et al., 2008; Rovasio, 2010; Ueno et al., 1999). Unlike murine islets which are structured with a beta-cell core, human islets have a distinct morphology where beta-cells are intermingled with various endocrine cells throughout the islet. This yields fewer beta-cells in the human pancreas and more alpha-cells such that there are approximately 60% beta-cells, 30% alpha-cells, 10% delta-cells, <5% PP-cells, and fewer still epsilon-cells, however proportions vary throughout the organ. The human islet also differs both morphologically

and physiologically from the murine islet in that all of the endocrine cell types (in no particular order or layer) are closely associated with the islet's microcirculation (Cabrera et al., 2006). Apart from the production of hormones, endocrine cells can also express gene products characteristic of neuroendocrine cells, and can be found throughout the gastrointestinal tract (Slack, 1995).

1.2.2 **Morphological Development of the Human Pancreas**

The pancreas initially develops with the outcropping of a dorsal and ventral bud at the mid-foregut boundary on either side of the primitive gut tube, an endoderm-derived structure. Budding is induced by various extracellular environmental signals emanating from the adjacent notochord, dorsal aorta, and lateral plate mesoderm which lead to the expression of various pancreatic genes (Jorgensen et al., 2007; Piper et al., 2004; Wells, 2003). In humans, pancreatic bud development is initiated at two to three weeks of fetal age whereby the dorsal bud first emerges, sprouting into the surrounding mesenchyme, followed by the ventral bud a few days later (Jeon et al., 2009; Lyttle et al., 2008). A human pancreatic developmental timeline is shown in **Figure 1.1**. The partially-differentiated epithelium of the two buds begins to form a ductal tree through branching morphogenesis, resulting in two predominantly ductal preliminary pancreata (Habener et al., 2005; Rutter et al., 1968). Between weeks 5 and 7 the gut tube (duodenal loop) rotates, translocating the ventral rudiment into contact with the dorsal bud where they fuse and their ductal systems become interconnected, forming the definitive pancreas (Polak et al., 2000). The ventral bud forms the posterior portion of the pancreatic head (the uncinate process) while the dorsal bud gives rise to the major portion of the head as well as the body and tail of the future pancreas (Slack, 1995).

Hormone-expressing endocrine cells can be detected by around 8 weeks of fetal age (wks), expressing insulin and often co-expressing glucagon or somatostatin (Jeon et al., 2009; Polak et al., 2000). At about 9 wks, PP-expressing cells appear and the percentage of hormone co-expression drops dramatically (Polak et al., 2000). These initial endocrine cells appear mainly as single cells, dispersed throughout the central epithelial ductal

Figure 1.1. Human Pancreatic Developmental Timeline.

An approximate gestational timeline outlining the major morphological changes occurring during human pancreatic development. The fetal age in weeks (wks) is shown where the first and second trimesters of pregnancy are key to pancreatic development. The first trimester of pregnancy occurs until the end of the 11^{th} wk of fetal age, the second trimester is designated from 12 to 24 wks, and the third trimester is the gestational period from the 25^{th} week up until birth (approximately 40 wks). Figure by Dr. Rennian Wang.

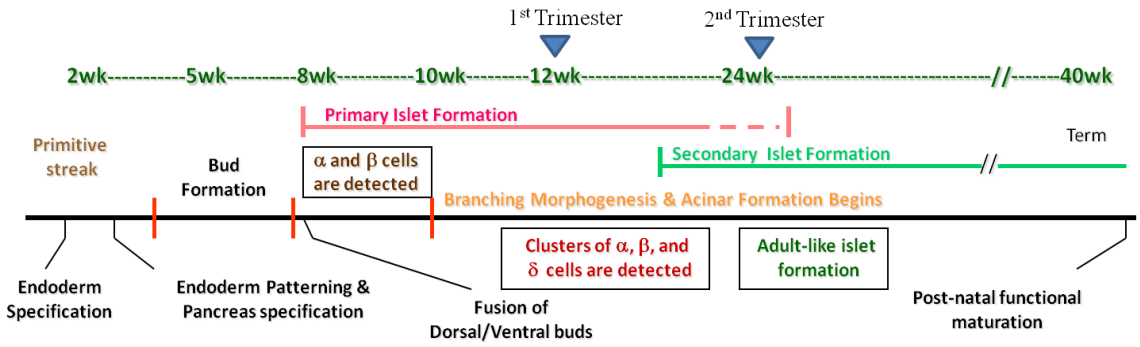
1st Trimester
2nd Trimester
2wk----------5wk---------8wk----------10wk--------12wk----------24wk----------//------40wk
Primary Islet Formation
Primitive streak
Bud Formation
α and β cells are detected
Secondary Islet Formation
Term
Branching Morphogenesis & Acinar Formation Begins
Clusters of α, β, and δ cells are detected
Adult-like islet formation
Endoderm Specification
Endoderm Patterning & Pancreas specification
Fusion of Dorsal/Ventral buds
Post-natal functional maturation

Figure 1.1.

structure, either within the ducts themselves or in small groups in contact with the duct. Thus, endocrine progenitors are thought to arise from pancreatic progenitors or stem cells within the ductal epithelium and not through endocrine proliferation (Bouwens et al., 1997; Polak et al., 2000). Early endocrine progenitors may divide into distinct lineages but may not necessarily generate mature endocrine cells (Fontaniere et al., 2008; Habener et al., 2005; Herrera, 2000). For exocrine cell differentiation, mesenchymal signals are required; without these signals, cells will resort to an endocrine cell fate (Habener et al., 2005). As development proceeds, endocrine cell density increases within the center of the pancreas and expands towards the periphery of the pancreas (Jeon et al., 2009; Polak et al., 2000). During the period of 10 to 12 weeks of fetal age, proliferation of branched tubules continues into exocrine acini, islets, and ducts with limited differentiation (Lyttle et al., 2008).

From 12 to 16 wks, there is a dramatic increase in insulin and glucagon expression suggesting that this period is especially important for endocrine cell development and hormonal expression (Lyttle et al., 2008). Differentiation is brought on by a drastic increase in pancreas-specific protein synthesis and a decrease in cellular proliferation (Jorgensen et al., 2007; Rutter et al., 1968). Analysis of 14 to 16 wk pancreata shows the appearance of vascularized parenchymatous lobules containing small islet clusters expressing all four hormones (insulin, glucagon, somatostatin, and PP) (Gupta V, 2002; Piper et al., 2004). Mature beta-cell markers such as prohormone convertase 1/3 (PC1/3) and islet amyloid polypeptide (IAPP) are first detected centrally in islets during this time period denoting that these beta-cells may be able to process and secrete insulin (Piper et al., 2004). The exocrine cell populations, embedded in dense mesenchymal tissue, differentiate and aggregate together at the lateral and terminal ends of the primitive ducts, forming acinar cells. Within acinar cells at this stage, zymogen granules, exocrine enzyme activity, and acinar cell markers are detectable (Bouwens et al., 1997; Rovasio, 2010). All epithelial cells at this point express CK19 (Cytokeratin 19: a ductal and epithelial cell marker), which includes most endocrine cells since most endocrine cells are still in close contact or within the ductal epithelium at 16 wks of fetal age (Bouwens et al., 1997).

From 18-24 wks, islets show a decrease in CK19 intensity staining (immunofluorescence staining), where single cells and small aggregates still stain strongly for CK19 (Bouwens et al., 1997). This denotes a transitional period as the endocrine cells begin to lose their ductal cell marker as they migrate through the basal membrane and into the surrounding mesenchyme (Bouwens et al., 1997; Kim and Hebrok, 2001). By the end of the second trimester of pregnancy (24 wks of fetal age), the pancreas is almost fully developed showing adult-like islets characterized by larger, well-encapsulated, closely-packed cells with all endocrine granules well established in the cytoplasm. The pancreas has an extensive vascular network, mesenchymal tissue is reduced due to acinar proliferation, and the parenchyma overall is well organized into lobes and lobules throughout the pancreas (Gupta V, 2002; Lyttle et al., 2008).

During the 3rd trimester until birth (25 to approximately 40 wks) the pancreas continues to mature, where connective tissue condenses and compacts around the ducts, islets increase in number and are widely distributed (lose their ductal association, CK19^{-}), with some islets close to acini while few lie within interlobular connective tissue. At birth a well-defined architecture characteristic of a fully-formed and functional pancreas is observed with dense hormone granules present in endocrine cells with well formed acini and ductal systems (Bouwens et al., 1997; Gupta V, 2002).

Throughout development and into adulthood, beta-cells and alpha-cells show very low proliferation activity which may demonstrate the importance of islet neogensis from hormone-negative cells or pancreatic progenitor cells during these time periods (Bouwens et al., 1997). It has been suggested that these pancreatic progenitors, from development into adulthood, reside around the ductal epithelium due to the high proliferation capacity of CK19^{+} cells, as well as the subsequent co-localization and loss of the CK19 marker in endocrine cells. The differentiation of hormone-negative pancreatic cells and pancreatic stem cells are both possible opportunities to further pancreatic cell-based therapeutics (Bouwens et al., 1997; Wells, 2003).

1.2.3 **Transcriptional Profiling of Pancreatic Development**

Pancreatic development and beta-cell differentiation is an intricate process which consists of multiple transcription factors precisely regulated temporally and spatially (Lyttle et al., 2008). Studies using mouse models, as well as cultured or differentiated cell lines, and primary cell cultures have provided the necessary tools to study and elucidate the function of various transcription factors and signalling molecules involved in development. Based on the information and function from these studies, I will highlight the main transcription factors analyzed in my study, focusing on pancreatic and endocrine progenitors as well as the network involved in endocrine lineage determination (**Figure 1.2**). These critical transcription factors include PDX1, NGN3, HES1, ISL1, SOX9, NKX2.2, and NKX6.1.

PDX1 (Pancreatic Duodenal Homeobox 1)

The *PDX1* gene, which has various alternative names including *IPF-1*, *IDX-1*, and *STF-1*, is a member of the ParaHox group of homeodomain transcription factors (Habener et al., 2005; Kim and Hebrok, 2001). Studies have shown that PDX1 is required for pancreas development in both rodents and humans, where it serves to play a role in endoderm specification of the two pancreatic buds as well as pancreatic progenitor differentiation. As development proceeds, PDX1 also plays a role in beta-cell maturation, maintenance, and function (Kim and Hebrok, 2001; Lyttle et al., 2008). It is first detected around 3.5 wks or embryonic day 8.5 in mice (e8.5) in a narrow band of fore-gut endoderm, soon after it is seen in both dorsal and ventral buds and expressed throughout the ductal tree. From 6-11 wks of fetal age, PDX1 is detected in all types of pancreatic epithelial cells which are destined to form islets, ductal structures, and acini (Lyttle et al., 2008; Piper et al., 2004). As development proceeds and islets begin to form into hormone-producing cells, co-localization becomes restricted to the endocrine compartment such that by e18.5 (~16 wks) PDX1 is mostly restricted to mature beta-cells with lower levels in $CK19^{+}$ ductal cells (Habener et al., 2005; Lyttle et al., 2008; Piper et al., 2004). During development PDX1 is expressed in a few glucagon-producing cells early on in develop-

Figure 1.2. Schematic Diagram of Endocrine Lineage Determination

This figure outlines the lineage of endocrine determination from progenitors to fully differentiated cells and the transcription factors involved. Diagram is based on studies outlined in the main text and describes only transcription factors that are addressed in this study. Even though many of these transcription factors play a role at different times throughout pancreatic development, one time point is depicted here, indicating the predominant timing of its function. The colours shown are representative of the different cell types during lineage determination. Adapted from Habener, Kemp, and Thomas, 2005 as well as Cleaver and MacDonald, 2010.

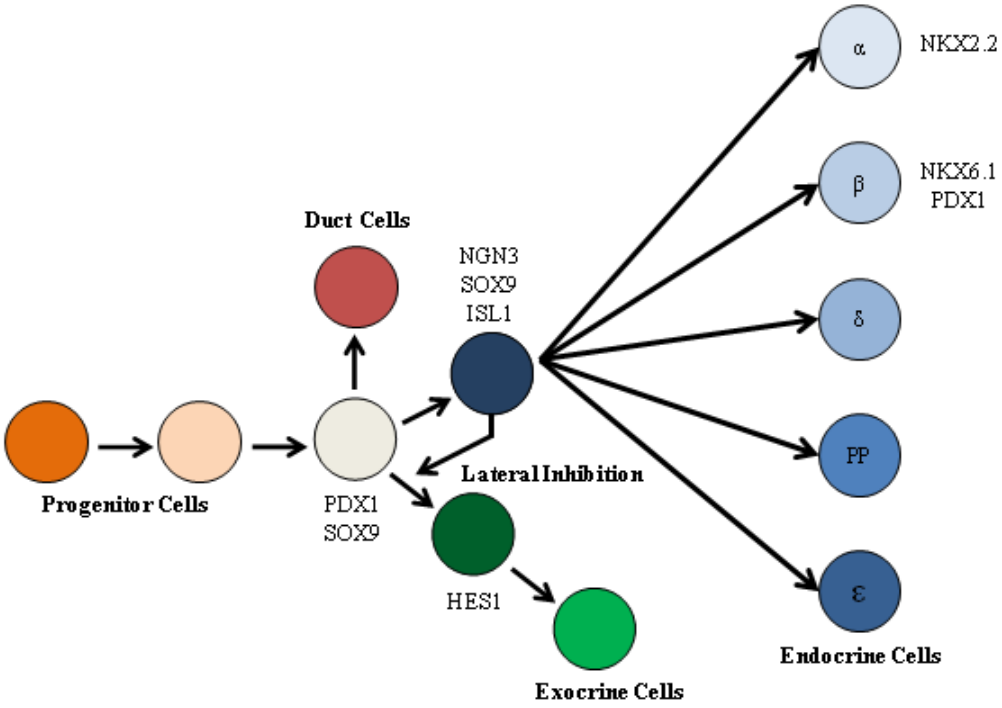
α
NKX2.2
β
NKX6.1
PDX1
δ
PP
ε
Endocrine Cells
Duct Cells
NGN3
SOX9
ISL1
Lateral Inhibition
Progenitor Cells
PDX1
SOX9
HES1
Exocrine Cells

Figure 1.2.

ment, where its expression is weaker than in both progenitor and beta-cells; however no PDX1-glucagon co-localization is seen later in development and into adulthood (Habener et al., 2005; Jeon et al., 2009; Lyttle et al., 2008).

Expression of PDX1 in the adult pancreas is undetectable in the exocrine compartment with expression in sub-populations of somatostatin and PP-cells (Habener et al., 2005). Although its expression remains in ductal cells, PDX1 is more strongly expressed in islets as studies have shown that it regulates the expression of islet-specific genes. In beta-cells PDX1 regulates glucose-induced insulin gene expression (Habener et al., 2005; Piper et al., 2004). *Pdx1* null mice are viable but die soon after birth as a result of pancreatic agenesis where preliminary buds form but then regress during development. Normal pancreatic mesenchyme is detected but the pancreatic epithelium is unable to respond to these mesenchymal signals which are required for differentiation of all pancreatic cell types. This suggests that Pdx1 is required for the endodermal response to signals emanating from the mesenchyme (Habener et al., 2005; Kim and Hebrok, 2001). Similarly, a child born without a pancreas could be homozygous for an inactivating mutation of *PDX1* (Habener et al., 2005). Due to the involvement of PDX1 in insulin production, a heterozygous mutation results in islet defects ranging from impaired glucose regulation to insulin-dependent diabetes such as MODY4 (maturity onset diabetes of the young type 4) (Habener et al., 2005; Wells, 2003). In these cases, diabetes is the result of a *PDX1* haploinsufficiency or a dominant negative inhibition of the normal allele (Habener et al., 2005). These studies have demonstrated the important role of PDX1 at different developmental stages and its requirement throughout pancreatic development and into adulthood for both the murine and human pancreas (Habener et al., 2005; Kim and Hebrok, 2001).

SOX9 (SRY (Sex Determining Region Y)-Box 9)

SOX9 is a member of the SRY homeobox family of transcription factors and has been implicated in the development of various organs. Humans and mice with a SOX9 haploinsufficiency develop Campomelic dysplasia and die either during development or

at term (rare). Analysis of their pancreata illustrates reduced islet size, loosely packed islets, and a reduction of mature insulin cell markers, suggesting a role for SOX9 in endocrine development (Piper et al., 2002; Seymour et al., 2008). Studies have shown that SOX9 is initially highly expressed in the pancreatic primordium at around 3.5 wks of fetal age, highly expressed as the two buds fuse, at 10-12 wks its expression declines, and is even further reduced at 19-21 wks. At 19-21 wks SOX9 expression is mainly restricted to a subpopulation within ductal cells and is excluded from lineage-committed endocrine progenitors. This expression pattern suggests that SOX9 must be down-regulated for endocrine differentiation to proceed and demonstrates a lack of expression in mature endocrine cells (McDonald et al., 2012; Piper et al., 2002; Seymour et al., 2007). SOX9-expressing cells reside in a pool of proliferating progenitor cells, co-localizing with various endocrine-specific factors such as NGN3, NKX2.2, NKX6.1, and ISL1 (McDonald et al., 2012; Seymour et al., 2007). SOX9 has been shown to bind the *NGN3* promoter and studies have revealed that its expression is SOX9-dependent, suggesting that SOX9 is involved in kick-starting endocrine differentiation (McDonald et al., 2012; Seymour et al., 2008). *Sox9* null mice present with agenesis of the pancreas, where embryos at e11.5 (before endocrine differentiation) show an increased ratio of $Glucagon^{+}/Pdx1^{+}$ cells, increased $Isl1^{+}$ cells, reduced $Hes1^{+}$ exocrine cells, reduced proliferation, and increased apoptosis, all of which suggest a crucial role of SOX9 in maintaining the pancreatic progenitor pool (Seymour et al., 2007). Human knockdown studies using SOX9 siRNA in human fetal islet-epithelial cell clusters also show reduced proliferation, reduced endocrine markers, and reduced insulin expression with an increase in alpha-cells demonstrating a necessary role in pancreatic development (McDonald et al., 2012). Overall, these studies outline the requirement of SOX9 in maintenance of the progenitor pool as well as endocrine differentiation for both the murine and human pancreas.

NGN3 (Neurogenin 3)

The transcription factor NGN3, is a member of the basic helix-loop-helix (bHLH) family and is essential for the establishment of endocrine cell differentiation. It is first observed co-localizing with PDX1, insulin, and glucagon in early development (8-10 wks) with significant decreases in NGN3 co-localization as development proceeds (Lyttle et al., 2008). In the rodent pancreas, Ngn3 expression begins at e9-9.5, peaks at e15.5 during the major wave of endocrine neogensis, and is greatly reduced at birth with little or no expression in the adult pancreas (Gradwohl et al., 2000). In rodents, Ngn3 can induce endocrine gene expression (i.e. Insulin), but unlike in humans, it is not observed co-localizing with Insulin or Glucagon (Gradwohl et al., 2000; Lyttle et al., 2008). In the fully developed or adult human pancreas, NGN3 expression in alpha- and beta-cells is minimal but NGN3 can be found around the periphery of islet cell clusters; this suggests the presence of endocrine precursor populations surrounding the adult islet (Lyttle et al., 2008).

The Notch signalling pathway has been shown to be involved in endocrine and exocrine differentiation in a lateral inhibition model similar to neurogenesis, whereby a cell destined to become endocrine ($NGN3^{+}$) inhibits adjacent cells driving them towards exocrine cell fates. The expression of NGN3 leads to the expression of notch ligands which activate notch receptors on adjacent cells. Upon notch activation the transcription factor, HES1 (see below for description), becomes expressed in the adjacent cell which acts to repress NGN3 expression and other target genes to repress the endocrine cell phenotype and promote the exocrine cell fate. Thus, HES1 is not expressed in the endocrine compartment of the pancreas (Habener et al., 2005). Additionally, the timing of NGN3 is key in pancreatic development. Mice with *Ngn3* overexpression exhibit small, poorly branched buds (at e12) with accelerated endocrine differentiation and reduction in pancreatic progenitors with specific reduction in the ability to form the exocrine pancreas (Habener et al., 2005; Kim and Hebrok, 2001). The ectopic induction of PDX1 and NGN3 expression was able to induce pancreatic endocrine gene expression and insulin production in various cells including human embryonic stem cells, pancreatic ductal cells, hepatocytes, and bone-marrow derived mesenchymal stem cells (BM-MSCs)

(Limbert et al., 2011). Reduced or null *Ngn3* expression results in distorted hypoplastic islets with impaired glucose homeostasis where endocrine cells are few or absent and accumulated secretory granules are observed, outlining a role for *Ngn3* in normal exocrine differentiation as well (Kim and Hebrok, 2001). These studies outline the requirement of NGN3 expression for the establishment of all endocrine cell lineages, thus NGN3 can be used as a marker of islet precursor cells (Habener et al., 2005).

ISL1 (Islet-1)

ISL1 is a LIM homeodomain protein downstream of NGN3. In humans, its expression is progressively increased from 8-21 wks co-localizing with endocrine cell markers (PDX1, insulin, glucagon, somatostatin, and PP but not amylase^{+} (exocrine cells)). The same co-localization is observed in adulthood suggesting that ISL1 is required for endocrine differentiation and their functional maintenance (Lyttle et al., 2008). Inactivation of *Isl1* has been shown to cause developmental arrest and death at around e9.5, whereby the dorsal mesenchyme has failed to develop resulting in complete agenesis of the dorsal aorta and the dorsal pancreatic bud with the absence of all endocrine cells (Habener et al., 2005; Jensen, 2004). These studies suggest that ISL1 is required for formation of the dorsal (not ventral) pancreatic mesenchyme, dorsal budding, endocrine differentiation, and maintenance of their function through adulthood (Jensen, 2004; Jeon et al., 2009).

NKX2.2 (NK2 Homeobox 2/NK2 Related Transcription Factor Related, Locus 2)

NKX2.2 is a member of the NK2 family of homeobox protein transcription factors and is also known as NKX2B (Habener et al., 2005; Sussel et al., 1998). In the murine pancreas, Nkx2.2 is found in the early buds (e9.5) where it is expressed by all pancreatic cells until endocrine and exocrine differentiation becomes apparent and then becomes restricted to endocrine cells. In humans, NKX2.2 is up-regulated from 8-21 wks in all endocrine cell types with highest expression in alpha- and beta-cells at 14-16 wks (Habener et al., 2005; Lyttle et al., 2008; Sussel et al., 1998). Knockout *Nkx2.2* mice are

viable but present with severe hyperglycemia a few days after birth and die soon after. Analysis of their pancreas revealed an altered endocrine lineage program, where all beta-cells, few alpha-cells, and a subset of PP-cells failed to differentiate and were replaced by an increase in ghrelin-producing endocrine cells (Prado et al., 2004; Sussel et al., 1998; Wells, 2003). Within endocrine progenitors Nkx2.2 and Ngn3 are co-expressed, where in the absence of *Ngn3*, *Nkx2.2* expression is absent, and within the *Nkx2.2* null pancreata, *Ngn3* expression is reduced (consistent $Ngn3^{+}$ cell population). This suggests that Nkx2.2 and Ngn3 could regulate each other in a feedback loop (Anderson et al., 2009). The exocrine compartment is not affected by Nkx2.2 loss of function and heterozygous mutations of *Nkx2.2* show no significant changes when compared to their wild-type litter mates (Sussel et al., 1998). *Nkx2.2* mutations have shown that this gene is responsible for repressing the beta- to alpha-cell transition in both developmental stages and postnatally (Papizan et al., 2011). NKX2.2 has also been shown in the adult islet to be responsible for mature beta-cell function (Doyle and Sussel, 2007; Lyttle et al., 2008). All of these previous studies outline a crucial role for NKX2.2 both during pancreatic development and in the adult pancreas.

NKX6.1 (NK6 homeobox 1/NK6 related transcription factor related locus 1)

NKX6.1 is a member of the NK6 family of homeobox protein transcription factors. Its expression occurs at increasing levels in beta-cells only through development from 7-21 wks, and it is not expressed in any other pancreatic cell type in humans (Jeon et al., 2009; Lyttle et al., 2008; Rudnick et al., 1994). Conversely, in murine models, Nkx6.1 is also shown to be initially expressed at low levels in the pancreatic buds and in all epithelial cells. Upon the appearance of endocrine cells, its expression is reduced further in non-beta-cells and dramatically increased in beta-cells, such that Nkx6.1 is only detectable in beta-cells at the major wave of endocrine differentiation (Oster et al., 1998; Sander et al., 2000). In *Nkx6.1* knockout murine models, Nkx6.1 suppresses Glucagon expression and enhances Insulin secretion showing that Nkx6.1 is involved in alpha- and beta-cell differentiation (Lyttle et al., 2008). In these knockouts, mice at birth have a reduction of

only beta-cells with a normal assortment of other endocrine cell types, normal bud formation, and no change in the exocrine compartment (Habener et al., 2005; Sander et al., 2000). Analysis of the early null pancreas show no alteration in beta-cell numbers until after the major wave of differentiation (e13) suggesting that Nkx6.1 may be exclusively required for this second wave (the major wave) of beta-cell differentiation, downstream of Nkx2.2 (Sander et al., 2000). It has also been suggested that Nkx6.1 may work in combination with Nkx2.2 to repress the beta- to alpha-cell transition during development and into adulthood (Papizan et al., 2011). These various studies demonstrate the requirement of NKX6.1 during beta-cell differentiation as well as during adulthood where it maintains β-cell function.

HES1 (Hairy and Enhancer of Split 1)

HES1, also known as HRY (Hairy), is expressed in non-endocrine cells and denotes cells destined to become the exocrine compartment of the pancreas. HES1 is dominantly expressed from 7-21 wks of fetal age in pancreatic buds and pancreatic epithelial precursors with levels gradually decreasing (Jeon et al., 2009). As aforementioned, activation of Notch receptors, by NGN3-encoded ligands, signals the expression of HES1. This expression encodes a bHLH repressor capable of repressing the *NGN3* gene promoter, thereby suppressing the downstream endocrine signalling program. Thus, HES1 is not expressed in endocrine cells (Habener et al., 2005; Jensen, 2004; Kim and Hebrok, 2001). Mice homozygous for *Hes1* disruption show characteristics similar to that of *Ngn3* overexpression mice with an overabundance of endocrine cells, rapid declines in pancreatic progenitor cells, acinar apoptosis, and hypoplasia (Habener et al., 2005; Kim and Hebrok, 2001). Overall, these experiments suggest that HES1 is required for normal endocrine and exocrine differentiation from pancreatic precursor cells.

1.3 The Transcription Factor Menin

1.3.1 Menin Expression and the MEN1 Disease

Current research in murine species has implicated the transcription factor Menin, encoded by the *MEN1* gene, as a necessity throughout pancreatic development and has provided insight into its possible function (Bertolino et al., 2003a; Stewart et al., 1998). The human *MEN1* gene was initially isolated, characterized, and named for the disease that its mutation causes, Multiple Endocrine Neoplasia type 1 (MEN1) (Larsson et al., 1988). The menin protein is found to be ubiquitously expressed throughout the body in tissues from the endocrine system to nervous, digestive, reproductive, and immune systems in various species including humans, rodents, and zebrafish (Chandrasekharappa et al., 1997; Khodaei et al., 1999; Maruyama et al., 1999).

In endocrine cells, a germline mutation and subsequent loss of heterozygosity of the *MEN1* allele results in lack of menin expression or function, tumourigenesis, and multiple endocrine neoplasia in both mice and humans (Larsson et al., 1988; Yamaguchi et al., 1980). A patient is diagnosed with this autosomal dominant disease if they have two or more tumours that originate from parathyroid, pituitary, or gastro-entero-pancreatic cells or if they present with three of the five main endocrine tumours described by Dreijerink et al in 2006 (Brandi et al., 2001; Larsson et al., 1988; Yamaguchi et al., 1980). A carrier with one or more of the 500+ possible germ line mutations can expect 94-100% penetrance by fifty years of age and more specifically, pancreatic islet tumours have been found in 30-80% of patients (Balogh et al., 2006; Brandi et al., 2001; Chandrasekharappa et al., 1997; Dreijerink et al., 2006a; Fontaniere et al., 2008; Lemos and Thakker, 2008). Islet tumours can be a major cause of death in humans due to malignancy and the major complications associated with this type of tumour (Fontaniere et al., 2008). Types of complications can depend on their location in the pancreas, which cells are affected, and what hormones are being overexpressed.

1.3.2 *MEN1* Characterization & Menin Functionality

From analyzing the *MEN1* gene or the menin protein, studies have found that it has no homology to any known proteins and has few identifiable functional motifs (Biondi et al., 2004; Chandrasekharappa et al., 1997). The *MEN1* gene, found on 11q13 in humans, has been shown to include two independent nuclear localization motifs at the C-terminus, 2 nuclear export signals (NES) found in two leucine zippers, a proline rich C-terminal, and 5 GTP consensus sequences on the N-terminal (Cao et al., 2009; Chandrasekharappa et al., 1997; Guru et al., 1998; Larsson et al., 1988; Yaguchi et al., 2002). Being mainly nuclear, menin may also directly bind double stranded DNA non-specifically through its nuclear localization sequences (NLS) thereby functioning as a tumour suppressor (Guru et al., 1998; La et al., 2004).

To characterize the functionality of menin as a tumour suppressor, researchers have focused on identifying molecules that menin may interact with. A detailed summary of Menin interactions, as mentioned below, is shown in **Figure 1.3**. Studies suggest that menin regulates proliferation and cell death through DNA repair mechanisms, cell cycle progression, chromatin modification, and transcriptional inhibition and activation. In DNA repair, Menin interacts with replication protein A2 (RPA2), a subunit of RPA which binds to ssDNA and is involved in ATR (ataxia telangiectasia and Rad3 related)-mediated sensing of DNA damage. However, how Menin regulates RPA2 is unknown as RPA2 still binds to ssDNA at normal levels (Gallo et al., 2010; Sukhodolets et al., 2003). Menin also binds and promotes FancD2 (fanconi anemia, complementation group D2) function, a protein required in promoting the BRCA1 (breast cancer 1, early onset)-mediated DNA repair pathway (Garcia-Higuera et al., 2001; Jin et al., 2003). Menin itself is also stabilized by phosphorylation during DNA damage but during tumourigenesis (specifically pancreatic ductal adenocarcinoma) menin expression and promoter methylation is reduced (Cavallari et al., 2009; Francis et al., 2011; Shen et al., 2009). In damaged or tumourigenic cells, menin may promote cell death through direct repression of *hTERT* (human telomerase reverse transcriptase) transcription to suppress maintenance of telomeres after cell replication (Blasco, 2005; Lin and Elledge, 2003).

With cell cycle progression, studies show that Menin binds and suppresses transcriptional activation mediated by activator S-phase kinase (ASK), a protein required for S-phase entrance (Kumagai et al., 1999; Schnepp et al., 2004). Menin also recruits MLL (mixed-lineage leukemia) in histone methyl transferase complexes (HMTC) which promotes methylation of H3K4 and transcriptional activation of genes including *p18*, *p27*, and *TFF1* (trefoil factor 1), and regulates homeobox genes (*HOX* genes) either positively or negatively depending on the tissue. Studies also show that Menin directly binds to the promoters of these specific genes (Dreijerink et al., 2006b; Hughes et al., 2004; Milne et al., 2002; Milne et al., 2005; Nakamura et al., 2002; Wu and Hua, 2011; Yokoyama et al., 2004). P27 and p18 are both CDK (cyclin-dependent kinase) inhibitors thereby suppressing G1-phase progression and S-phase entrance (Agarwal et al., 2009; Milne et al., 2005). Menin, within this HMTC complex, also interacts with retinoblastoma binding protein 5 (RbBP5) and the large subunit of RNA polymerase II (POLR2B, polymerase (RNA) II (DNA directed) polypeptide B) promoting HMTC activity (Hughes et al., 2004). Menin levels have been shown to correlate with and control the post-translational processing of the hyperphosphorylated (inactive) form of the Retinoblastoma protein (ppRb), thereby negatively affecting the anti-tumourigenic nature of Rb in cell cycle progression and other Rb controlled processes (Ivo et al., 2011). Within the HMTC, Menin may also bind to estrogen receptor alpha (ERα) in an estradiol (E_2) dependent manor, acting as a coactivator of ERα-mediated transcriptional activity (ie. on the *TFF1* promoter). Menin also binds TFF1 directly and the role of TFF1 is tissue specific but may be involved with cell death, proliferation, and motility (Dreijerink et al., 2006b; Ribieras et al., 1998).

Menin can also directly repress transcriptional activity mediated by an oncogene, JunD, through prevention of phosphorylation and recruitment of mSin3A and histone deacetylase complexes (HDAC), with menin binding to all three components (Agarwal et al., 1999; Agarwal et al., 2003; Gallo et al., 2010; Gobl et al., 1999; Kim et al., 2003). This menin-JunD interaction negates the oncogenic activity of JunD thereby repressing proliferation (Agarwal et al., 2003). Menin can suppress transcriptional activation mediated by NFκB (nuclear factor of kappa light polypeptide gene enhancer in B-cells) through binding to NFκB1, NFκB2, and RelA (v-rel reticuloendotheliosis viral oncogene

Figure 1.3. Menin Interactions Summary

This diagram summarizes the direct interacting partners of Menin and the effect of this interaction on various cellular processes. Although there are other interacting partners of Menin, only the ones discussed in the main text are shown. The thick connecting bars illustrate an interaction whereby Menin positively (green) or negatively (red) affects the activity and/or expression of that specific interacting partner. Thick gray bars indicate that the interacting effect of Menin is unknown. The thin blue bars illustrate the effects of this interaction on downstream cellular processes such that the interaction promotes (arrow), inhibits (blunted line), or its effect on that process is unknown or variable within cell types (line). Connecting adjacent partners indicate an interaction and complex formation; some components may not always be required depending on the cell type or cellular process. Blue shapes not directly connected to Menin (but connected to a Menin interacting partner) are required for Menin's interacting effect on that partner.

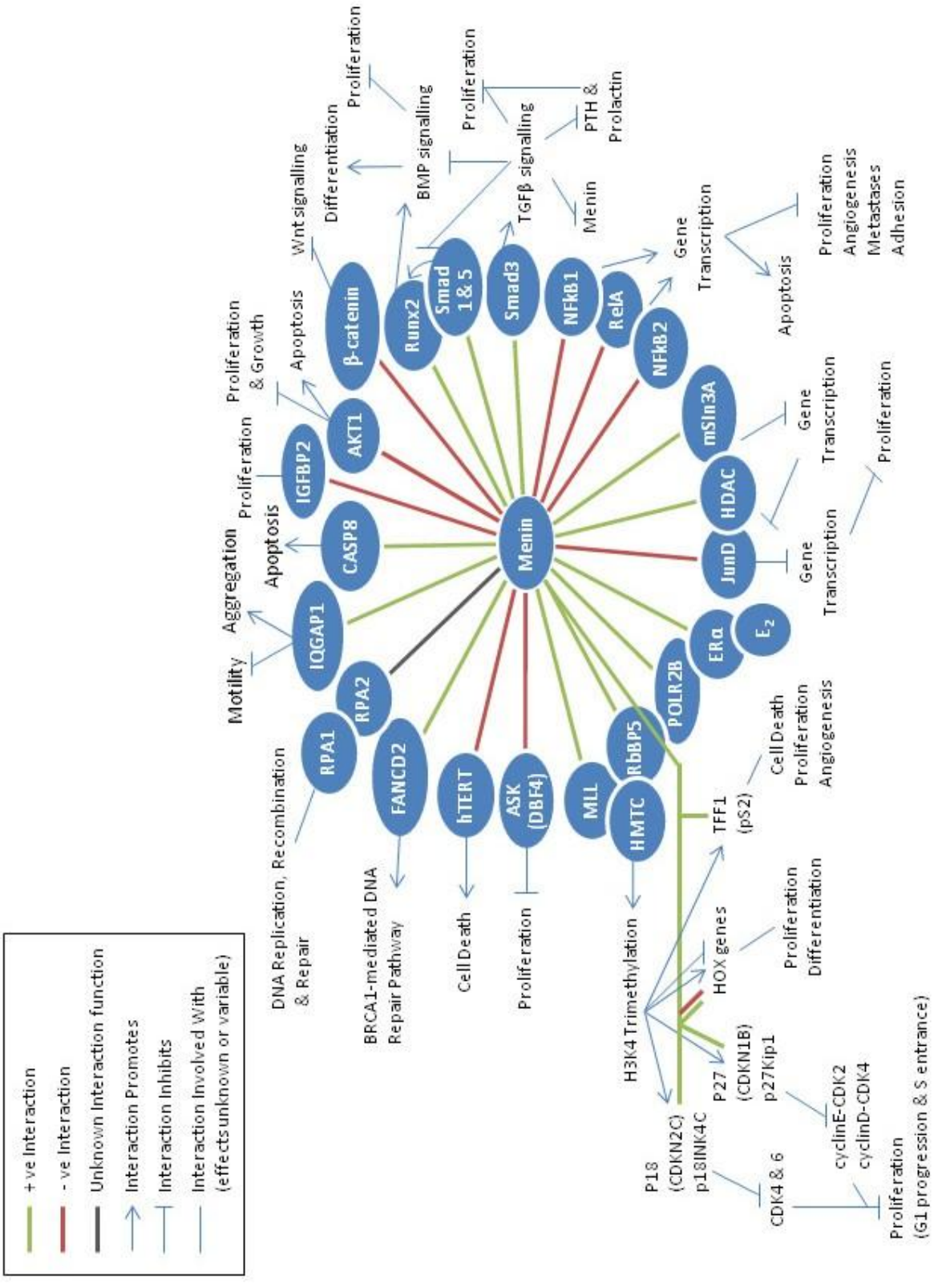
+ ve Interaction
- ve Interaction
Unknown Interaction function
Interaction Promotes
Interaction Inhibits
Interaction Involved With (effects unknown or variable)
Menin
RPA1
RPA2
FANCD2
IOGAP1
CASP8
AKT1
IGFBP2
β-catenin
Runx2
Smad 1&5
Smad3
NFkB1
RelA
NFkB2
mSin3A
HDAC
JunD
ERα
E2
POLR2B
RbBP5
HMTC
MLL
ASK (DBF4)
hTERT
DNA Replication, Recombination & Repair
BRCA1-mediated DNA Repair Pathway
Cell Death
Proliferation
Motility
Aggregation
Apoptosis
Proliferation
Proliferation & Growth
Apoptosis
Wnt signalling
Differentiation
Proliferation
BMP signalling
Proliferation
TGFβ signalling
Menin
PTH & Prolactin
Gene Transcription
Apoptosis
Proliferation
Angiogenesis
Metastases
Adhesion
Gene Transcription
Gene Transcription
Proliferation
Cell Death
Proliferation
Angiogenesis
TFF1 (pS2)
HOX genes
Proliferation
Differentiation
H3K4 Trimethylation
P27 (CDKN1B) p27Kip1
P18 (CDKN2C) p18INK4C
CDK4 & 6
cyclinE-CDK2
cyclinD-CDK4
Proliferation (G1 progression & S entrance)

Figure 1.3.

homolog A) subunits, thereby promoting apoptosis and repressing proliferation, angiogenesis, and metastases (Escarcega et al., 2007; Heppner et al., 2001). Menin also binds and enhances Smad3-mediated transcriptional activation through the TGFβ (transforming growth factor, beta) pathway. This pathway is involved in repressing proliferation, parathyroid hormone (PTH) secretion, prolactin expression, and is able to repress menin as well (Balogh et al., 2010; Hendy et al., 2005; Kaji et al., 2001). Menin can positively bind Smads 1 and 5 along with Runx2 (runt-related transcription factor 2) to promote BMP (bone morphogenetic protein) signalling which enhances differentiation but reduces proliferation (Kaji et al., 2001; Sowa et al., 2004). The Menin-Smad3 interaction is also able to repress the effects of the Menin-Smad1/5 interaction (Sowa et al., 2004).

The canonical Wnt/β-catenin signalling pathway regulates a variety of cellular functions including differentiation, proliferation, and cell adhesion. Within this pathway, the function of menin is variable such that menin is able to repress Wnt (wingless integration 1) signalling by binding and shuttling β-catenin out of the nucleus as well as stabilizing membrane bound E-cadherin (Cao et al., 2009). However, studies show that menin also promotes Wnt signalling by regulating H3K4 trimethylation and thus promotes Wnt target gene, Axin2, expression (Chen et al., 2008). Menin is also involved in the PI3K/AKT pathways by binding to AKT1 and negatively regulating its activity by preventing its translocation from the cytoplasm to the plasma membrane. This AKT1-menin interaction reduces PI3K/AKT pathway signalling thereby leading to an increase in apoptosis and reducing proliferation and cell growth (Wang et al., 2011). Another interacting partner of menin is IGFBP2 (insulin-like growth factor binding protein 2) where menin binds to its promoter, repressing IGFBP2 expression. IGFBP2 is involved in proliferation but its regulatory effect varies between cell types (Yan et al., 2009). Studies show that menin binds and promotes CASP8 (Caspase-8) expression and IQGAP1 (IQ motif containing GTPase activating protein 1) functionality. These interactions promote apoptosis through CASP8, and through IQGAP1 promote aggregation and suppress cell motility (La et al., 2007; Yan et al., 2009). There are still additional partners of menin, however this summary describes the majority of well-known direct interactions and their cellular effects.

In addition, a study of menin function in melanoma tissue demonstrates the indirect ability of menin to repress malignancy through regulating multiple pathways such that tumourigenic cells present with reduced growth factor pleiotrophin, receptor protein tyrosine phosphatase, PI3K (phosphoinositide 3-kinase), phosphorylated FAK (focal adhesion kinase), and phosphorylated ERK 1/2 (extracellular-signal-regulated kinases, also known as MAP kinase) (Gao et al., 2011).

Overall, menin is involved with numerous cellular pathways and interacting partners, all of which act to suppress neoplastic formation, growth, and malignancy.

1.3.3 **Menin in Rodent Development**

Menin is found in a variety of species, all having a very similar homology to the human encoded menin protein. For example, Menin found in mice display a 96.6% homology to that found in humans, rats exhibit 97% homology, and zebrafish are 75% homologous (Biondi et al., 2004; Khodaei et al., 1999; Maruyama et al., 1999). For this reason, the mouse has been a common test model for localization and functional studies of Menin. Stewart and colleagues in 1998 reported that murine *Men1* is found by 7 days of gestation and at embryonic day 13.5 (e13.5) in the forelimb, gut, head, heart, and lung. By e14 *Men1* is highly expressed throughout the developing embryo and later becomes restricted to certain cells within various adult tissues throughout the body (Stewart et al., 1998). Interestingly, homozygous *Men1* null mice show no gross abnormalities at e9.5 but die in utero by e11.5-12.5 which allowed researchers to study which systems and organs have been affected or underdeveloped (Crabtree et al., 2001). Analysis of those studies provided evidence that Menin is required for development of the neural tube (central nervous system), heart (differentiation of certain cardiac cells), liver (differentiation of hepatoblasts), and the endocrine pancreas (Bertolino et al., 2003a; Fontaniere et al., 2008). **Table 1.1** summarizes the Menin knockout mouse and cell culture models. Heterozygous *Men1* mice exhibit similar characteristics of the MEN1 disease but not until 9 months of age (9 m) where they begin to develop hyperplastic pancreatic islets, Insulin-secreting islet tumours (at slightly lower levels per islet), and display increased

vascularization (Crabtree et al., 2001). Studies show that Menin may also be involved in differentiation through the retinoic acid (RA) pathway since RA induces Menin expression and Menin induces RA and RA receptors (Kanungo and Chandrasekharappa, 2012). A study using embryoid bodies (EBs) formed by differentiating wild-type and *Men1*$^{-/-}$ embryonic stem (ES) cells gave further insight into Menin's role in development. Results showed a probable hemoglobinization deficiency with the following RNA alterations at e8: reduced *Runx2, Postn*, and *Msx2* (osteoblast differentiation genes); *KDR* (a VEGF receptor, endothelial cell proliferation and differentiation in the liver); *Hoxa9* (a myeloid and lymphoid development gene); and *Kit1* (a hematopoietic growth factor and an erythrocyte differentiation gene). Genes involved in pancreatic development that were reduced included *Sox4, Foxa1, Btc, Igf2, Nfatc1, Wnt5a, Wisp1*, and cell cycle controls *cyclinG2* and *cdkn1c* (Zhang et al., 2007).

1.3.4 **Menin in Rodent Pancreatic Development & Function**

Looking more closely at the developing rodent pancreas, one can gather some information regarding the function of Menin through development. It has been found to be expressed at each stage e11.5-e18.5 in the entire pancreatic epithelium, and at e16.5 it is found in Insulin^{+}, Glucagon^{+}, and Mucin1^{+} ductal cells (Fontaniere et al., 2008). It is important to note that Menin is not required for pancreatic bud formation. Analysis of the pancreas of homozygous *Men1*$^{-/-}$ mice just before lethality at e12.5 (1st transition, appearance of endocrine progenitors) has revealed a reduced number of Glucagon^{+} cells and an increase in apoptosis (Fontaniere et al., 2008). This suggests that Menin is required to support differentiation or survival (by repressing apoptosis) of Glucagon^{+} cells at this stage, but this requirement is not absolute (Fontaniere et al., 2008). See **Table 1.1** for a detailed list of menin mouse and cell culture models and their corresponding results. Cultured pancreatic cells reminiscent of the 2nd transition of development (e12.5 + 7 days culture) showed a significant decrease in Insulin^{+} cells but no change in exocrine cells. This indicates that Menin is involved in the endocrine but not exocrine development of the pancreas. Cystic structures also formed in the cultured

Table 1.1: Summary of Mouse and Cell Culture Menin Knockout Models

Model	Knockout Conditions	Global Effects	Pancreatic Effects
Men1$^{-/-}$ mice	Global knockout	-die in utero e11.5-e12.5 -neural tube, heart, liver, and pancreas organogenesis	-↓ Glucagon^{+} cells -↑ Apoptosis
Men1$^{-/-}$ culture	Cultured *Men1*$^{-/-}$ mouse pancreatic cells (7 days)	-N/A	-↓ Insulin^{+} cells -↓ Ngn3^{+} cells -exocrine unchanged -cystic structures
Men1$^{-/+}$ mice	Global knockout	-no development effect	-no developmental effect -MEN1 at 9 m (hyperplastic islets, insulinomas, increased vascularization)
Men1$^{-/-}$ EBs	Differentiated ES cell knockout (Cell culture)	-hemoglobinization deficiency -genes relating to development of osteoblasts, endothelial cells (liver), myeloid and lymphoid cells, hematopoietic stem cells and erythrocytes	-*Sox4, Foxa1, Btc, Igf2, Nfatc1, Wnt5a, Wisp1* and cell cycle controls *cyclinG2* and *cdkn1c* -↓ *Nkx2.2* -earlier *Foxa2* and *Sox17* expression (endodermal differentiation markers)
Men1$^{F/F}$-RipCre^{+} mice	Insulin directed beta-cell knockout	-no developmental effect	-no developmental effect -insulinomas by 2 m (MEN1)
Men1$^{F/F}$-Pdx1Cre^{+} mice	Pdx1 directed beta-cell knockout	-no developmental effect	-no developmental effect -insulinomas by 3 m (MEN1)

cells which suggest that Menin prevents abnormal endocrine or ductal differentiation. Also, the number of $Ngn3^{+}$ cells was decreased which could lead to the observed decrease in $endocrine^{+}$ cells. Menin could therefore be regulating Ngn3 expression or the formation of $Ngn3^{+}$ cells which regulates the amount of endocrine cells in the pancreas (Fontaniere et al., 2008). In a beta-cell specific knockdown (*Men1*$^{F/F}$-$RipCre^{+}$) mice, Menin showed consistently reducing expression levels from e11 and mice consequently developed islet tumours by 2 m (*Men1*$^{-/-}$ cells) suggesting a shorter latency period than heterozygous mice (Bertolino et al., 2003b). A Pdx1 directed *Men1* inactivation (*Men1*$^{F/F}$-$Pdx1Cre^{+}$) showed no effect on pancreatic development with low Menin levels (measured at 2 m) and characteristics of insulinoma formation by 3 m, thus confirming the requirement for Menin tumour suppression and suggesting a possible threshold effect of Menin expression during development (Shen et al., 2009). Looking at *Men1* null EBs specifically in pancreatic development, genes *Sox4, Foxa1, Btc,* and *Igf2* were down-regulated (Zhang et al., 2011; Zhang et al., 2007). Results also showed varying transcription factor expression levels from e3-7 and stabilizing by e9 except for a significant reduction in *Nkx2.2* at e9-10 suggesting a possible dedifferentiation process with the lack of *Nkx2.2*. Also, endoderm markers *Foxa2* and *Sox17* showed an earlier expression suggesting that null EBs preferentially initiate differentiation along the endodermal pathway (Zhang et al., 2011). However, overexpression of Menin can also induce endodermal differentiation independent of RA (Kanungo and Chandrasekharappa, 2012).

In the adult pancreas, studies show that menin is not only involved in tumour suppression and proliferation but also in insulin secretion, cell motility, and adhesion (Fontaniere et al., 2008). Within beta-cell compensatory situations such as pregnancy and obesity, menin is repressed to allow for proliferation and the subsequent increase in beta-cell mass (Karnik et al., 2007). This compensatory process of increasing beta-cell mass balances out the increased demand for insulin. In adult rat islets, the presence of Menin inhibits Insulin promoter activity and its ability to respond to Glucose induction, an important feature in development and a model of hypersecretion for insulinomas (Sayo et al., 2002). Insulin and Glucose have both been shown to reduce Menin expression and cytoplasmic localization via the PI3K/AKT/FoxO1 pathway. FoxO1 is able to bind Menin to reduce

its expression but Menin is also able to reduce FoxO1 activity at the same time (Wuescher et al., 2011; Zhang et al., 2012). Another feature of menin includes its ability to interact with IQGAP1 in the adult pancreas, a scaffold protein regulating cell motility and adhesion. This Menin-IQGAP1 interaction is able to promote islet aggregation and may be a crucial component in islet development (Yan et al., 2009).

Overall, Menin seems to have a dual functionality, one to promote endocrine (including progenitor) differentiation and survival and the other in the fully developed pancreas to suppress proliferation and insulin hypersecretion and to promote aggregation (Fontaniere et al., 2008).

1.4 **Project Rationale and Outline**

To date, most human menin research has focused on the clinical neoplastic aspect of menin within the MEN1 disease and knowledge on the functional role of *MEN1*/menin during human fetal pancreatic development is limited. Previous studies have implicated Menin as an essential protein for rodent pancreatic development and have suggested that its action in pancreatic progenitor cells is through Ngn3 regulation. In this study I hope to take the knowledge of its role in proliferation and rodent pancreatic development to determine if this phenomenon is recapitulated in human pancreatic development to further elucidate its functional significance. Understanding how menin interacts with other factors involved in pancreatic development and their functional significance during proliferation and differentiation in the human fetal pancreas, is crucial to the understanding of human pancreatic endocrine development. This novel knowledge will aid in furthering developmental studies and advancing islet generation studies for diabetic cell-based therapies (Gupta V, 2002; Jeon et al., 2009; Kim and Hebrok, 2001).

Objective

To examine the expression pattern and functional roles of menin during human fetal islet development through its association and interaction with other necessary transcription factors.

Hypothesis

Menin is required for islet differentiation by regulating islet progenitor proliferation and the expression of NGN3 and other essential pancreatic transcription factors in the developing human pancreas.

Specific Questions

1. What is the spatial and temporal expression pattern of menin throughout human pancreatic development?
2. What developmental transcription factors are co-localized with menin in the developing human fetal pancreas?
3. What is the relationship between proliferating cells and menin^{+} cells in the developing human fetal pancreas?
4. Does downregulation of *MEN1* in islet-epithelial cell clusters affect endocrine cell proliferation and differentiation?
5. Does overexpression of *MEN1* in islet-epithelial cell clusters affect endocrine cell proliferation and differentiation?

Chapter 2

Research Design and Methods

Chapter 2 – **Research Design and Methods**

2.1 **Pancreatic Tissue Collection**

Human fetal pancreata were collected from 8 to 21 weeks of fetal age in accordance with protocols approved by the Human Health Sciences Research Ethics Board at the University of Western Ontario (**Appendix I**) and guidelines from the Canadian Council on Heath Sciences Research Involving Human Subjects. The fetal age is typically two weeks less than the gestational age (based on the menstrual cycle), to account for the two pre-ovulation weeks that precede conception. Pancreatic tissues were dissected and washed with sterile phosphate buffered saline (PBS) and immediately processed for either RNA and/or protein extraction, fixation for immunofluorescence, or for islet-epithelial cell cluster isolation as described below.

2.2 **Immunofluorescence & TUNEL Assay**

To determine menin expression patterns and co-localizations in the developing human pancreas, whole human fetal pancreata were collected at three 3 developmental stages 8-12 weeks (1st trimester), 14-16 weeks (early 2nd trimester), and 18-21 weeks (later 2nd trimester) of fetal age and fixed in 4% paraformaldehyde (PFA) (Fisher Scientific Company; Ottawa, ON, Canada) overnight at 4°C. Samples were washed in 1xPBS and processed using a standard protocol of dehydration and paraffin embedding with an automated tissue processing and embedding machine (Shandon Citadel^{TM} Tissue Processor, Citadel 1000, Thermo Electron Corporation; Waltham, Massachusetts, USA). Pancreatic sections were cut at 4 μm thickness using a microtome (Leica RM2245, Vashaw Scientific Inc.; Norcross, GA, USA) through the entire length of the pancreas. Prior to immunostaining, paraffin sections were deparaffinized in xylene and rehydrated with decreasing ethanol concentrations (100%, 90%, and 70%), rinsed in distilled H_2O (dH_2O) and washed with 1xPBS. Heat-induced antigen retrieval was used on all pancreatic sections by immersing the slides in boiling citrate-based antigen retrieval buffer (pH 6.0) and heating at medium to high power (70%) for 20 minutes using a

microwave (Amana 1000 Watt Commercial microwave). Slides were then cooled to room temperature (approximately 1 hour), rinsed in dH_2O, and washed with 1xPBS. Nonspecific binding was blocked with 10% normal goat serum diluted in blocking buffer at room temperature for 30 minutes in a humidity chamber. Blocking serum was tapped off and slides were incubated with appropriate dilutions of primary antibodies as listed in **Table 2.1** overnight at 4°C in a humidity chamber (Lyttle et al., 2008). The next morning, sections were washed in 1xPBS, and incubated with appropriate dilutions of fluorescein-conjugated secondary antibodies as listed in **Table 2.1** for 1 hour at room temperature. Secondary antibodies were obtained from Jackson Immunoresearch Laboratories (West Grove, PA, USA). Slides were washed in 1xPBS before a nuclei counterstain, 4'-6'-diamidino-2-phenylindol (DAPI) (Sigma; St Louis, MO, USA), was applied to the slides at a 1:2000 dilution in PBS. Negative controls for the anti-menin antibody were performed with the omission of either primary or secondary antibodies as shown in Appendix II: **Supplementary Figure 1**.

Cell death was determined with TUNEL labeling using the In Situ Cell Death Detection Kit by Roche Applied Science (Penzberg, Germany) where the terminal deoxynucleotidyl transferase is conjugated with fluorescein-dUTP at the 3′-end. This kit was used according to the manufacturer's instructions with a 1:20-40 dilution of TUNEL labeling enzyme (Saleem et al., 2009).

2.3 **Morphometric Analysis**

Images of immunostained sections were acquired using a Leica DMIRE2 fluorescence microscope (Leica Microsystems; Bannockburn, Il, USA) and a digital camera (Retiga 1300, High-sensitivity IEEE 1394 FireWire^{TM} digital camera, QIMAGING; Burnaby, British Colombia, Canada) connected to a Macintosh computer. Openlab image software (Improvision; Lexington, MA, USA) was used to capture, store, and export the images. Velocity LE and Velocity Demo imaging software (PerkinElmer, Waltham, MA, USA) were used to store and analyze images.

Table 2.1: List of Antibodies/Antisera for Immunofluorescence and Western-Blot Analyses

Primary antibody	Dilution	Company, Location
mouse monoclonal Amylase	1:50	Santa Cruz Biotech., Santa Cruz, CA, USA
mouse monoclonal Calnexin	1:2000[a]	BD Biosciences, Mississauga, ON, Canada
rabbit polyclonal Caspase-3	1:1000[a]	Cell signaling, Danvers, MA, USA
rabbit polyclonal Cleaved Caspase-3 (Asp175)	1:200	Cell signaling, Danvers, MA, USA
mouse monoclonal Cytokeratin 19	1:50	Dako, Mississauga, ON, Canada
rabbit polyclonal Cytokeratin 19	1:200	Abcam Inc, Cambridge, MA, USA
mouse monoclonal Glucagon	1:2000	Sigma, St. Louis, MO, USA
rabbit polyclonal Glucagon	1:50	Santa Cruz Biotech., Santa Cruz, CA, USA
mouse monoclonal Insulin	1:1000	Sigma, St. Louis, MO, USA
rabbit polyclonal Insulin	1:50	Santa Cruz Biotech., Santa Cruz, CA, USA
mouse monoclonal ISL1	1:200	DSHB, University of Iowa, Iowa city, USA
mouse monoclonal KI67	1:100	BD Biosciences, Mississauga, ON, Canada
rabbit polyclonal KI67	1:200	Abcam Inc, Cambridge, MA, USA
rabbit polyclonal Menin/MEN1	1:300-4000[a]	Bethyl Lab Inc., Montgomery, TX, USA
mouse monoclonal NGN3	1:100	DSHB, University of Iowa, Iowa city, USA
mouse monoclonal NKX 2-2	1:200	Gift-Dr.Wright, University of Vanderbilt, Nashville, TN, USA
mouse monoclonal NKX 6-1	1:100	DSHB, University of Iowa, Iowa city, USA

guinea monoclonal PDX-1	1:1000	Gift-Dr.Wright, University of Vanderbilt, Nashville, TN, USA
rabbit polyclonal Pancreatic Polypeptide	1:50	Zymed, San Francisco, CA, USA
rabbit polyclonal Somatostatin	1:50	Zymed, San Francisco, CA, USA
rat monoclonal Somatostatin	1:50	Abcam Inc, Cambridge, MA, USA
mouse monoclonal Sox9	1:100	Novus Biologicals, LLC Littleton, CO, USA
rabbit polyclonal Sox9	1:50-1000[a]	Santa Cruz Biotech., Santa Cruz, CA, USA
Secondary antibodies		
Goat anti-mouse	1:100	JRL; West Grove, PA, USA
Goat anti-rabbit	1:100	JRL; West Grove, PA, USA
Goat anti-guinea pig	1:100	JRL; West Grove, PA, USA
Goat anti-rat	1:100	JRL; West Grove, PA, USA

[a] dilution factor applied for western blot analysis. DSHB, Developmental Studies Hybridoma Bank; JRL, Jackson Immunoresearch Laboratories

To determine the percentage of cells expressing nuclear menin (nMenin) in the ductal, endocrine, and $PDX1^+$ cell populations at any given time point, double immunofluorescence staining for nMenin with CK19 (ductal), insulin, glucagon, or PDX1 was performed and double positive cells were counted. To determine the co-localization of nMenin in the proliferating cells, double labelled nMenin and KI67 cells were imaged and counted. For cell counting analysis, ten fields from the head to the tail of each pancreas were randomly imaged with a minimum of three pancreata per age group (Al-Masri et al., 2010). At least 1500 cells per ductal region ($CK19^+$), 500 cells per endocrine region ($insulin^+$, $glucagon^+$), and 500 cells for each $PDX1^+$ and $KI67^+$ cell populations were counted per pancreata and the data was expressed as a percentage.

2.4 **Isolation of Islet-Epithelial Cell Clusters**

Human fetal pancreata from ages 15 to 19 weeks of fetal age were selected since this is a period in the second trimester where there is a significant increase in beta-cell differentiation and function. As well, NGN3 expression decreases as development proceeds and so a time period in the middle of development (since earlier 8-12 wks is not possible due to sample availability) is optimal for characterization of the involvement of menin in NGN3 expression and islet differentiation (Lyttle et al., 2008). 15-19 wk pancreata were collected and immediately dissected (as in Section 2.1) from surrounding tissue and digested with a collagenase dissociation buffer (collagenase V, 1 mg/mL [Sigma]; 1xHBSS, 500 mL [Sigma]; HEPES, 25 nM [Sigma]; DNaseI [Roche]) for 30 min in a 37°C water bath. Residual enzyme was removed with wash buffer (1x HBSS) and the remaining cells, termed islet-epithelial cell clusters, were comprised mainly of undifferentiated epithelial cells ($CK19^+$ cells, most of which expressed PDX1), endocrine cells (~7-10%), and exocrine cell markers (~8%) (Li et al., 2006). Cell clusters were immediately plated and cultured as described below.

2.5 Transfection of Islet-Epithelial Cell Clusters with *MEN1* siRNA

Isolated islet-epithelial cell clusters were plated at 1-5x10^4 cells/well in a 12-well plate cultured with 600 uL/well of CMRL 1066 plus 10% fetal bovine serum (FBS, Invitrogen; Burlington, ON, Canada). After a 24 hr recovery and adhesion culture, cells were transiently transfected with 53 nM menin siRNA (human, sc-35922) (*MEN1*-siRNA) or control siRNA (sc-37007, proprietary sequence, Ctrl-siRNA) commercially produced by Santa Cruz Biotechnology Inc. using a siRNA transfection kit (Santa Cruz; CA, USA) according to manufacturer's instructions. A pool of two target-specific sequences for human menin siRNA, as listed in **Table 2.2**, was used with a minimum of 3 to 6 individual pancreata per experimental group. Following a 24, 48, and 72 hr transfection period, islet-epithelial cell clusters were harvested and processed for immunofluorescence, RNA isolation, or protein analysis to determine knockdown efficiency (Al-Masri et al., 2010).

2.6 Transfection of Islet-Epithelial Cell Clusters with *MEN1* Overexpression Vector

Isolated islet-epithelial cell clusters were plated at 1-5x10^4 cells/well in a 12-well plate using 600 uL/well of CMRL 1066 supplemented with 10% FBS. After a 24 hr recovery period, cells were washed with CMRL 1066 supplemented with 1% Bovine Serum Albumin (BSA, Sigma) and fresh CMRL 1066 – 1% BSA was added as per transfection protocol requirements. The cells were then transiently transfected with 1 μg/well of either the pEGFP-N2 vector with a human full-length *MEN1* cDNA insertion (N2-M1) or a control pEGFP vector (Ctrl-EGFP); both gifts from Dr. Xiaoying Li, (Cao et al., 2009). Lipofectamine™ 2000 diluted in CMRL 1066 – 1% BSA was used for transfection according to manufacturer's instructions (Invitrogen). Following a 48 hr transfection period, islet-epithelial cell clusters were harvested and processed for immunofluorescence, RNA and/or protein extraction with at least 5-6 repeats per experimental group.

Table 2.2: Menin siRNA (h) Sequences; A Pool of 2 Different siRNA Duplexes (sc-35922)*

Sequence no.	Sense	Antisense
sc-35922A	CUCUUCAGCUUCAUCACAGtt	CUGUGAUGAAGCUGAAGAGtt
sc-35922B	AGAUGGAGGUGGCGUUCAUtt	AUGAACGCCACCUCCAUCUtt

*Santa Cruz Biotechnology, Santa Cruz, CA, USA

2.7 Immunofluorescence of Islet-Epithelial Cell Clusters

Following transfection, islet-epithelial cell clusters were harvested, washed in 1xPBS, and fixed in 4% PFA overnight at 4°C. The cells were washed in 1xPBS again, embedded in 2% agarose before paraffin embedding (Li et al., 2006), and sectioned as outlined in section 2.2 (Immunofluorescence & Morphometric Analysis). Sections were cut vertically through the pellet until a minimum of 1000 cells were present per section. Staining and analysis were performed as outlined in section 2.2.

2.8 Protein Extraction & Western Blot Analysis

To determine the protein levels of total menin, signalling molecules and transcription factors in the developing human pancreas, and in islet-epithelial cell clusters following various experimental treatments, proteins from human fetal pancreata and cultured cells were extracted by incubation in Nonidet-P40 lysis buffer (Nonidet-40, phenylmethylsulfonyl fluoride, sodium orthovanadate [Sigma]; complete inhibitor cocktail tablet [Roche]) for 20 minutes on ice. Tissue was dispersed by sonication on ice where for whole tissue this was performed 10-20 sec (5-10 times), and for cell clusters the duration was 5 sec (10 times) with a 30 sec cool down in between each sonication time. Cell debris was then separated from the protein by centrifugation at 12,000 rpm for 20 min in the cold room at 4°C and extracted protein (supernatant) was then stored at -80°C for future use (Al-Masri et al., 2010; Li et al., 2006; Saleem et al., 2009). Protein concentration was measured with the Bradford dye assay (BioRad Laboratories; Mississauga, ON, Canada) and analysed with a Multiskan® spectrum spectrophotometer (Thermo Scientific; Vantaa, Finland).

Western blotting was performed by equal loading of lysate protein: pancreata 30 μg and cells 15-25 μg. Protein was separated using 10% (or 12%) sodium dodecyl sulfate-polyacrylamide gel electrophoresis (SDS-PAGE) and transferred to a nitrocellulose membrane (Bio-Rad) by electroelution. Protein was transferred using either the Trans-Blot SD Semi-Dry Transfer Cell at 20 V for 30 minutes or the Transblot Electrophoretic

transfer cell at 250 mA for 2.5 hrs (BioRad). For each transfer, a sandwich (sponge – filter paper – membrane – gel – filter paper – sponge) was assembled. Transferred protein was visualized with 0.2% Ponceau S. Membranes were washed in 1xTBST (Tris-buffered saline with 0.1% Tween 20), and incubated overnight at 4°C in a 5% Non-Fat Dairy Milk blocking solution. Membranes were incubated with appropriate primary antibody dilutions (**Table 2.1**) for 2 hrs at room temperature followed by washing 3x10min with 1xTBST. Appropriate dilutions of corresponding anti-rabbit or anti-mouse conjugated IgG secondary antibodies conjugated to horseradish peroxidise (Cell Signalling, Danvers, MA, USA) were added and incubated for 1 hr at room temperature (Al-Masri et al., 2010; Li et al., 2006; Saleem et al., 2009). Proteins were detected using enhanced chemiluminescent (ECL™-Plus Western blot) detection reagents (Perkin Elmer) and visualized using the Versadoc 5000MP imaging System (Bio-Rad) and Quantity One software (Bio-Rad). Densitometry was performed using Image Lab 3.0 software (Bio-Rad) and normalized to a loading control. A western blotting menin antibody control was performed with the omission of either primary or secondary antibodies as shown in Appendix II: **Supplementary Figure 2.**

2.9 RNA Extraction & Quantitative Real-Time RT-PCR (qRT-PCR) Analysis

Total RNA was extracted from pancreatic tissues using TRIZOL reagent (Invitrogen) (performed by Jinming Li previously in the lab) and from islet-epithelial cell clusters using the RNAqueous-4PCR kit by Ambion (Austin, TX, USA) according the manufacturer's instructions, which also included a DNase I treatment step (Li et al., 2006; Wang et al., 2005). RNA concentration was measured by diluting 1 μL of sample in 250 μL of DEPC (Diethylpyrocarbonate) water in a 96-well plate in duplicate. The Multiskan® spectrum spectrophotometer was used to measure $O.D_{260}$ (total RNA concentration) and the corrected OD ratio of A260/A280 (RNA purity). Electrophoresis with a 1% agarose gel was run to determine RNA quality using ethidium bromide staining (Appendix II: **Supplementary Figure 3**).

Real-time RT-PCR reactions were performed by Jinming Li according to the following protocol. For each RT reaction mixture the following components were added: 2 μg of RNA, 1 μL random hexamers (300 ng/mL), 1 μL Oligo-dT, and DEPC water until a total volume of 10.5 μL was reached. Tubes were then heated in the Chromo4 Real-Time PCR machine (Bio-Rad) for 10 min at 72°C and cooled for 5 min at 4°C (Lyttle et al., 2008; Wang et al., 2005). For each reaction mixture the following master mix was added: 4 μL of buffer, 2 μL of DTT, 2 μL of 10 mM dNTP, and 0.5 μL of Rnasin. Tubes were placed in the PCR machine, when 42°C was reached the machine was opened and 0.8 μL of Gibco BRL Superscript RT enzyme was added to each tube, and the machine was resumed at the following settings: 42°C for 90 min, 94°C for 5 min, and 4°C for 60 min. Samples were then removed and double dH_20 was added for a final concentration of 6 μg/80 μL, then aliquoted into 2 tubes and stored at -20°C. Real-time PCR was performed using the iQ SYBR Green Supermix kit in Chromo4 Real-time PCR (Bio-Rad) with the following mixture: 12.5 μL of iQ SYBR Green Supermix, 2 μL of Primer 1, 2 μL of Primer 2, 2.5 μL of sterile water, and 6 μL of DNA template for a total volume of 25 μL (Lyttle et al., 2008). The PCR primers used are listed in **Table 2.3**. Relative gene expression was calculated using the arithmetic formula "$2^{-\Delta\Delta C}T$" where ^{C}T is the difference between the threshold cycle of a given target cDNA and the internal standard gene 18S rRNA subunit cDNA (Lyttle et al., 2008; Wang et al., 2005). This was performed with at least 5 repeats per experimental group. The melting curves were used to indicate if the qRT-PCR assays had specifically amplified target sequences (Appendix II: **Supplementary Figure 4**). Controls involved omitting reverse transcriptase, cDNA, or DNA polymerase and showed no reaction bands (Wang et al., 2005).

2.10 **Statistical Analysis**

Data was plotted and analysed using GraphPad Prism 5 statistical software (GraphPad Software; La Jolla, CA, USA) which calculated mean, standard error, and statistical analysis. Significant difference was determined using the paired student's t-test or one-

way ANOVA (analysis of variance) followed by the post hoc Bonferoni correction. Data was expressed as means ± SEM and considered statistically significant if $p<0.05$.

2.11 **Collaboration Within This Study**

Within this study, more than 80% of experimental techniques and analyses were performed by myself with the following collaborations. Dr. Rennian Wang performed pancreata collection, qRT-PCR data analysis, and aided with pancreatic dissections. *Ex vivo* pancreatic processing (RNA extraction, protein extraction, and fixation for immunofluorescence (IF)) was performed by Jinming Li along with *ex vivo* tissue section preparation for IF. Jinming Li also designed RNA primers, performed qRT-PCR reactions, and aided with paraffin sectioning, NGN3 IF staining, and TUNEL labelling. For western blotting; protein concentration and gel loading were performed with the aid of Zhi Chao Feng (PhD student).

Please note that *in vitro* islet-epithelial cell cluster *MEN1*-siRNA and N2-M1 experiments were repeated by separate researchers (Dr. Rennian Wang and Jinming Li exclusively) with n=3 for all groups (data not shown). Their results confirmed the data described in this study.

Table 2.3: Sequences of Real-time PCR Primers

Primer Name	Accession Number & Definition	Primer Pair Sequence 5'----3' (*Sense/Antisense*)	Location (*nt*)	Fragment Size (bp)
CDKN1A (p21, Cip1)	NM_000389.4	GGC TCC TTC CCA TCG CTG TCA	991-1011	180
		TCA CCC TGC CCA ACC TTA GAG	1170-1150	
CDKN1B (p27, Kip1)	NM_004064.3	AAG ATG TCA AAC GTG CGA GT	470-489	131
		CGG GTT AAC TCT TCG TGG TC	600-581	
CDKN2C (p18)	NM_001262.2	CGG CGA CTC TCC CTA CTC AG	483-502	248
		GAG TGA TGC GGA AAG CGT CT	731-702	
GCG (Glucagon)	NM_002054.2	CAT TTA CTT TGT GGC TGG AT	108-127	147
		CGC TTG TCC TCG TTC ATC TG	254-235	
HES1	NM_005524.2	GTC AAC ACG ACA CCG GATAAA	297-317	351
		AGT GCG CAC CTC GGT ATT AAC	647-627	
MEN1	NM_000244.2	TGT CAA CCG CGT CAT CCC TA	257-276	138
		GCG GTG AAG CGG GCA TAG AG	394-375	
NGN3	NM_020999.2	AGC CGG CCT AAG AGC GAG TT	363-382	158
		TTG GTG AGC TTC GCG TCG TC	520-501	
NKX2-2	NM_002509.2	CGG GCC GAG AAA GGT ATG GA	916-935	202
		CCG AGC TGT ACT GGG CGT TGT	1117-1097	
NKX6-1	NM_006168.1	AGA CCC ACT TTT TCC GGA CA	724-743	335
		CCG CTG CTG GAC TTG TGC TT	1058-1039	
PDX-1	NM_000209.3	CTC CTA CAG CAC TCC ACC TTG	1262-1282	153
		CCG AGT AAG AAT GGC TTT ATG	1411-1394	
SOX9	NM_000346.2	ACA AGA AGG ACC ACC CGG ATT A	866-887	323
		AGC TCG CCG ATG TCC ACG TCG C	1205-1184	
18S	M11188.1	GTA ACC CGT TGA ACC CCA TTC	1577-1597	153
		CCA TCC AAT CGG TAG TAG CG	1729-1710	

Chapter 3

Project Results

Chapter 3 – **Project Results**

3.1 **Menin Expression Pattern Throughout Human Fetal Pancreatic Development**

To examine the spatial and temporal expression pattern of menin throughout human pancreatic development, pancreata were collected from 8 to 21 weeks of fetal age, and were categorized into three developmental time points. Pancreata from 8-12 wks consist of numerous undifferentiated $PDX1^+$ ductal cells with few scattered single endocrine cells and rare small islet clusters. During the 14-16 wk time point, islet clusters assemble such that pancreata exhibit numerous small vascularized islet clusters, while pancreata from 18-21 wks consist of adult-like islets with a rich vascular network (Lyttle et al., 2008). Using a qRT-PCR approach, we first analyzed the expression of *MEN1* mRNA and demonstrated relative constant expression of *MEN1* through 8-21 weeks of fetal age in the developing human pancreas (**Figure 3.1A**). Western blot analysis revealed no significant changes in total menin protein expression throughout development however a slightly higher expression was noted at 8-12 wks (compared to 14-21 wks) (**Figure 3.1B**).

Since menin can be a nuclear or cytoplasmic protein, our experiments were performed focusing on nuclear menin localization (nMenin) as opposed to cytoplasmic or total menin analysis. This was to focus on the localization where menin is more likely to exert its function, within the nucleus.

nMenin protein localization was analyzed in each pancreatic cell compartment using double immunofluorescence staining at each developmental period from 8-21 wks. The expression of nMenin was found to be highly detectable (>70%) within pancreatic endocrine cells ($insulin^+$ and $glucagon^+$) from the earliest developmental stage studied (8 wks) with no significant changes through the 1^{st} and 2^{nd} gestational trimester (**Figure 3.2**; **Figure 3.3**). Morphometric analysis within the ductal epithelium ($CK19^+$) revealed a high proportion of $nMenin^+$ cells (>70%) in both the 8-12 wk and 18-21 wk developmental periods with a significant reduction during the 14-16 wk developmental stage ($p<0.05$ vs. 8-12 wks, $p=0.06$ vs.

Figure 3.1. Total *MEN1* Gene and Protein Expression During Human Fetal Pancreatic Development.

(A) Real-time RT-PCR analysis of *MEN1* expression in human fetal pancreata during three developmental stages (8-10 wks, 14-16 wks, and 19-21 wks), data are normalized to 8-10 wks (n=5 per age group). **(B)** Western blot analysis of total menin protein abundance (68 kDa) normalized to calnexin (90 kDa, loading control) in the developing human fetal pancreas (n=3 per age group) (Wang et al., 2005). Data are expressed as means ± SEM.

A.

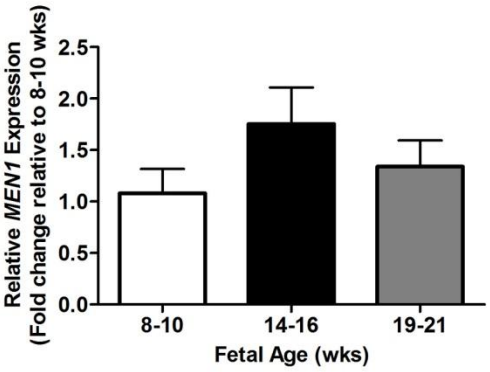
Relative MEN1 Expression
(Fold change relative to 8-10 wks)
2.5
2.0
1.5
1.0
0.5
0.0
8-10
14-16
19-21
Fetal Age (wks)

B.

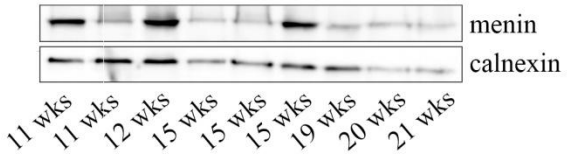
menin
calnexin
11 wks
11 wks
12 wks
15 wks
15 wks
15 wks
19 wks
20 wks
21 wks

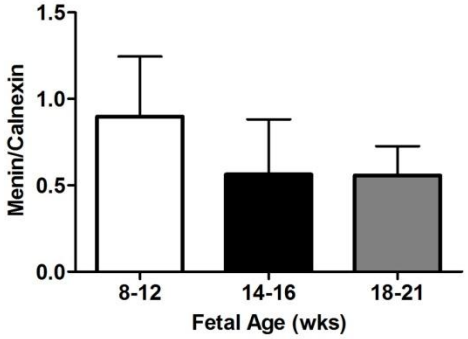
Menin/Calnexin
1.5
1.0
0.5
0.0
8-12
14-16
18-21
Fetal Age (wks)

Figure 3.1.

Figure 3.2. Co-localization of nMenin with Insulin During Human Fetal Pancreatic Development.

Human fetal pancreata sections from three developmental time points (8-12 wks, 14-16 wks, and 18-21 wks) were co-immunolabelled with anti-menin and anti-insulin antibodies, then visualized with Cy2 (green) and Cy3 (red) conjugated secondary antibodies respectively. Nuclei were labelled with DAPI (blue). **(A)** A representative section from 21 wks is shown where the top panel of images display double immunostaining for menin (green), insulin (red), DAPI (blue), and an overlay of the images. Scale bar corresponds to 25 micrometers. The bottom panel shows magnified images corresponding to the boxed section in the above image. Arrows indicate a $nMenin^{+}/insulin^{+}$ cell. **(B)** Quantitative analysis of co-localized $nMenin^{+}/insulin^{+}$ cells relative to the total number of $insulin^{+}$ cells (expressed as a percentage). Data were determined by morphometric analysis and are expressed as means ± SEM (n=4 pancreata per age group).

A.

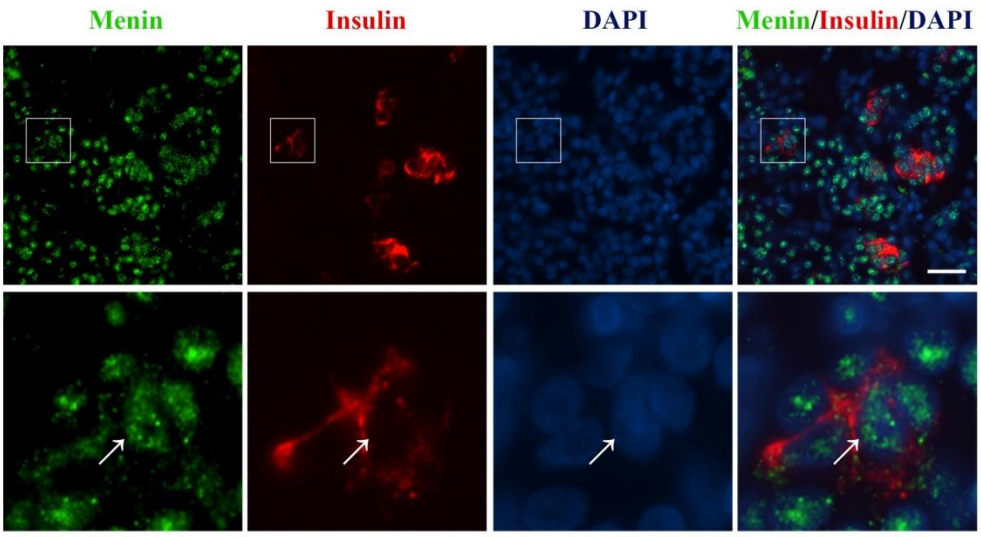
Menin
Insulin
DAPI
Menin/Insulin/DAPI

B.

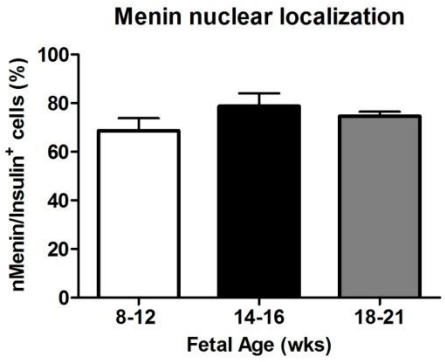
Menin nuclear localization
nMenin/Insulin+ cells (%)
100
80
60
40
20
0
8-12
14-16
18-21
Fetal Age (wks)

Figure 3.2.

Figure 3.3. Co-localization of nMenin with Glucagon During Human Fetal Pancreatic Development.

Human fetal pancreata sections from three developmental time points (8-12 wks, 14-16 wks, and 18-21 wks) were co-immunolabelled with anti-menin and anti-glucagon antibodies then visualized with Cy2 (green) and Cy3 (red) conjugated secondary antibodies respectively. Nuclei were labelled with DAPI (blue). **(A)** A representative section from 20 wks is shown where the top panel of images display double immunostaining for menin (green), glucagon (red), DAPI (blue), and an overlay of the images. Scale bar corresponds to 25 micrometers. The bottom panel shows magnified images corresponding to the boxed section in the above image. Arrows indicate a $nMenin^{+}/glucagon^{+}$ cell. **(B)** Quantitative analysis of co-localized $nMenin^{+}/glucagon^{+}$ cells relative to the total number of $glucagon^{+}$ cells (expressed as a percentage). Data were determined by morphometric analysis and are expressed as means ± SEM (n=3-6 pancreata per age group).

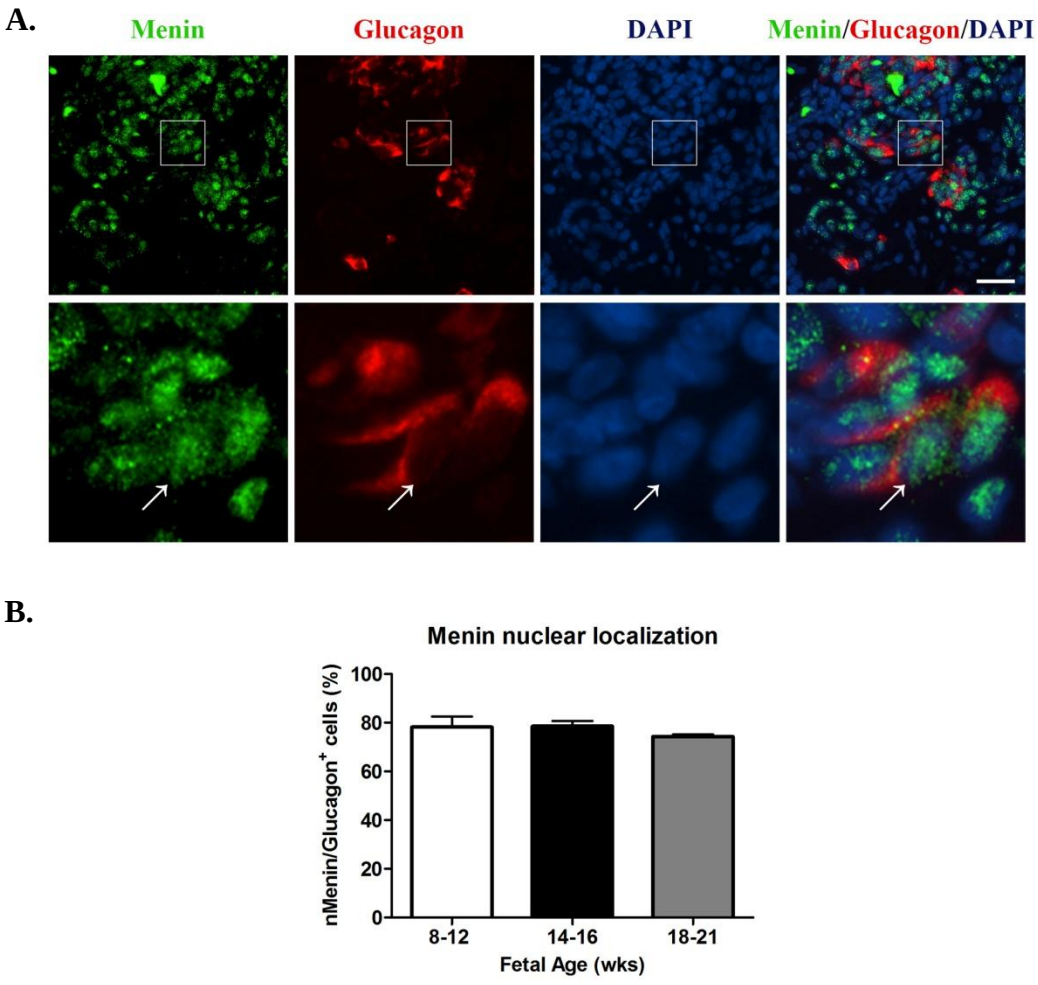
A.
Menin
Glucagon
DAPI
Menin/Glucagon/DAPI
B.
Menin nuclear localization
nMenin/Glucagon+ cells (%)
100
80
60
40
20
0
8-12
14-16
18-21
Fetal Age (wks)

Figure 3.3.

18-21 wks) (**Figure 3.4**). Furthermore, no difference in nMenin expression was observed in somatostatin^{+} cells or in the exocrine (amylase^{+}) compartment of the pancreas throughout development (8-21 wks) (**Figure 3.5**).

3.2 Co-localization of Menin with Transcription Factors Throughout Human Fetal Pancreatic Development

To further refine the expression pattern of menin throughout 8-21 weeks of fetal development, we looked at the co-localization of a variety of transcription factors which have been shown to be critical for human pancreatic development. Using double immunofluorescence and morphometric quantification, PDX1^{+} cells, which indicate undifferentiated pancreatic progenitors and later in development represent mature beta-cells, were first examined (Kim and Hebrok, 2001; Lyttle et al., 2008). Co-localization of nMenin within PDX1^{+} cells was found throughout development with a significant increase in co-localization in the 14-16 wk developmental stage ($p<0.01$ vs. 8-12 wks, $p<0.01$ vs. 18-21 wks) (**Figure 3.6**). Co-localization of nMenin with SOX9 (**Figure 3.7A**), ISL1 (**Figure 3.7B**), NGN3 (**Figure 3.8**), NKX2.2 (**Figure 3.9A**) and NKX6.1 (**Figure 3.9B**) was found throughout development.

3.3 Expression of nMenin in Proliferating (KI67^{+}) Cells in the Developing Human Fetal Pancreas

Menin has been classically characterized as a tumour suppressor, a negative regulator of cellular proliferation, in various endocrine tissues throughout the adult human body (Chandrasekharappa et al., 1997). To examine the abundance of nMenin in proliferating cells in the developing human fetal pancreas, the co-localization between nMenin and proliferating (KI67^{+}) cells was assessed using double immunostaining of whole human fetal pancreata from 8-21 wks of fetal age (**Figure 3.10A**). Morphometric analysis showed that cells expressing nMenin displayed a significant decreasing proliferation capacity (KI67^{+}) as development proceeded ($p<0.05$ 8-12 wks vs. 14-16 wks, $p<0.01$

Figure 3.4. Co-localization of nMenin with CK19 During Human Fetal Pancreatic Development.

Human fetal pancreata sections from three developmental time points (8-12 wks, 14-16 wks, and 18-21 wks) were co-immunolabelled with anti-menin and anti-CK19 antibodies then visualized with Cy2 (green) and Cy3 (red) conjugated secondary antibodies respectively. Nuclei were labelled with DAPI (blue). **(A)** A representative section from 21 wks is shown where the top panel of images display double immunostaining for menin (green), CK19 (red), DAPI (blue), and an overlay of the images. Scale bar corresponds to 25 micrometers. The bottom panel shows magnified images corresponding to the boxed section in the above image. Arrows indicate a $nMenin^{+}/CK19^{+}$ cell. **(B)** Quantitative analysis of co-localized $nMenin^{+}/CK19^{+}$ cells relative to the total number of $CK19^{+}$ cells (expressed as a percentage). Data were determined by morphometric analysis and are expressed as means ± SEM (n=3-6 pancreata per age group). *$p<0.05$.

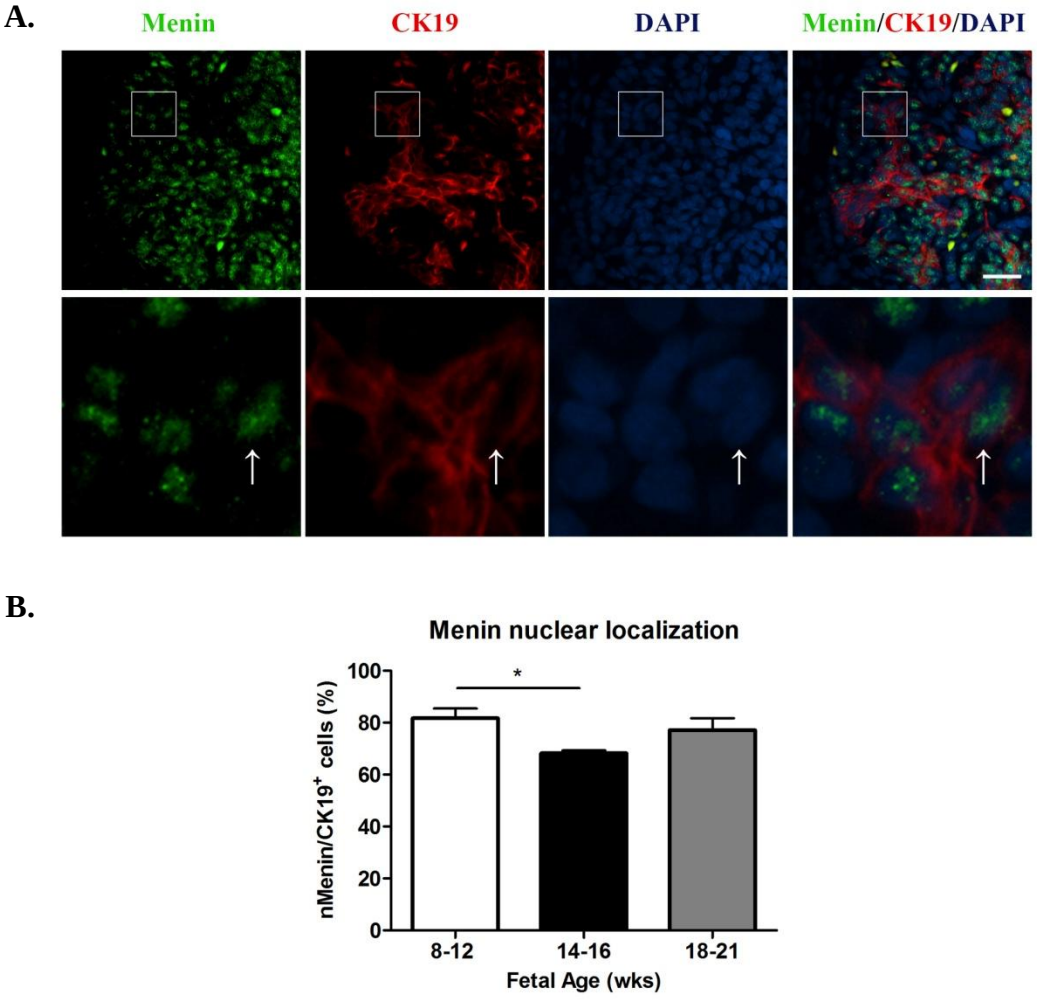
A.
Menin
CK19
DAPI
Menin/CK19/DAPI
B.
Menin nuclear localization
nMenin/CK19+ cells (%)
100
80
60
40
20
0
*
8-12
14-16
18-21
Fetal Age (wks)

Figure 3.4.

Figure 3.5. Co-localization of nMenin with Somatostatin and Amylase During Human Fetal Pancreatic Development.

Human fetal pancreata sections from 8-21 wks of fetal age were co-immunolabelled with anti-menin and anti-somatostatin or anti-amylase bodies then visualized with Cy2 (green) and Cy3 (red) conjugated secondary. Nuclei were labelled with DAPI (blue). Representative pancreatic sections are shown where the top panel of images display double immunostaining for menin (green), **(A)** somatostatin or **(B)** amylase (red), DAPI (blue), and an overlay of the images. Scale bars correspond to 25 micrometers. The bottom panels show magnified images corresponding to the boxed section in the above image. Arrows indicate a **(A)** $nMenin^{+}/somatostatin^{+}$ cell from 18 wk pancreata or a **(B)** $nMenin^{+}/amylase^{+}$ cell from 21 wk pancreata.

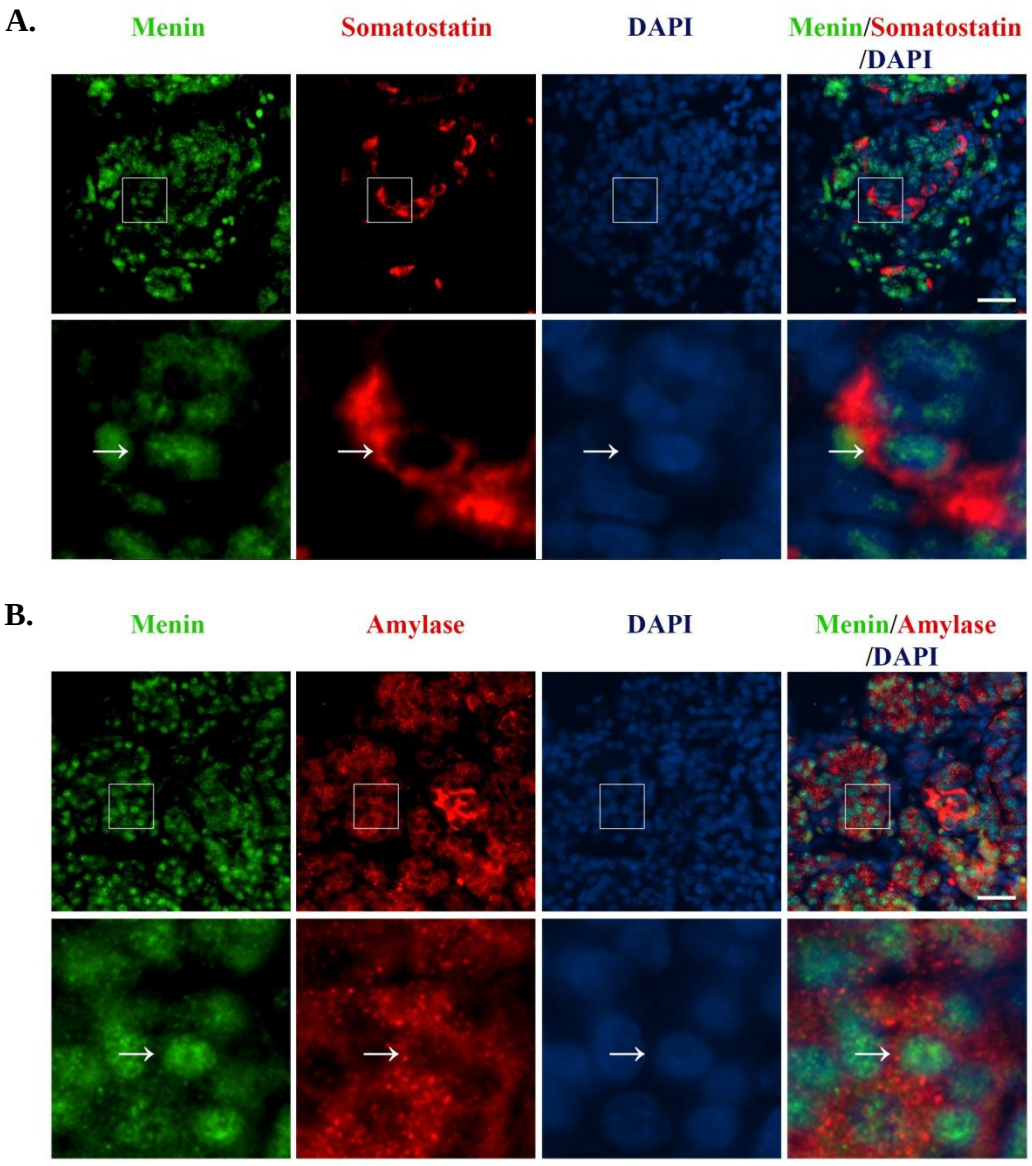
A.
Menin
Somatostatin
DAPI
Menin/Somatostatin
/DAPI
B.
Menin
Amylase
DAPI
Menin/Amylase
/DAPI

Figure 3.5.

Figure 3.6. Co-localization of nMenin with PDX1 During Human Fetal Pancreatic Development.

Human fetal pancreata sections from three developmental time points (8-12 wks, 14-16 wks, and 18-21 wks) were co-immunolabelled with anti-menin and anti-PDX1 antibodies then visualized with Cy2 (green) and Cy3 (red) conjugated secondary antibodies respectively. Nuclei were labelled with DAPI (blue). **(A)** A representative section from 21 wks is shown where the top panel of images display double immunostaining for menin (green), PDX1 (red), DAPI (blue), and an overlay of the images. Scale bar corresponds to 25 micrometers. The bottom panel shows magnified images corresponding to the boxed section in the above image. Arrows indicate a $nMenin^{+}/PDX1^{+}$ cell. **(B)** Quantitative analysis of co-localized $nMenin^{+}/PDX1^{+}$ cells relative to the total number of $PDX1^{+}$ cells (expressed as a percentage). Data were determined by morphometric analysis and are expressed as means ± SEM (n=3-6 pancreata per age group). $^{**}p<0.01$.

A.

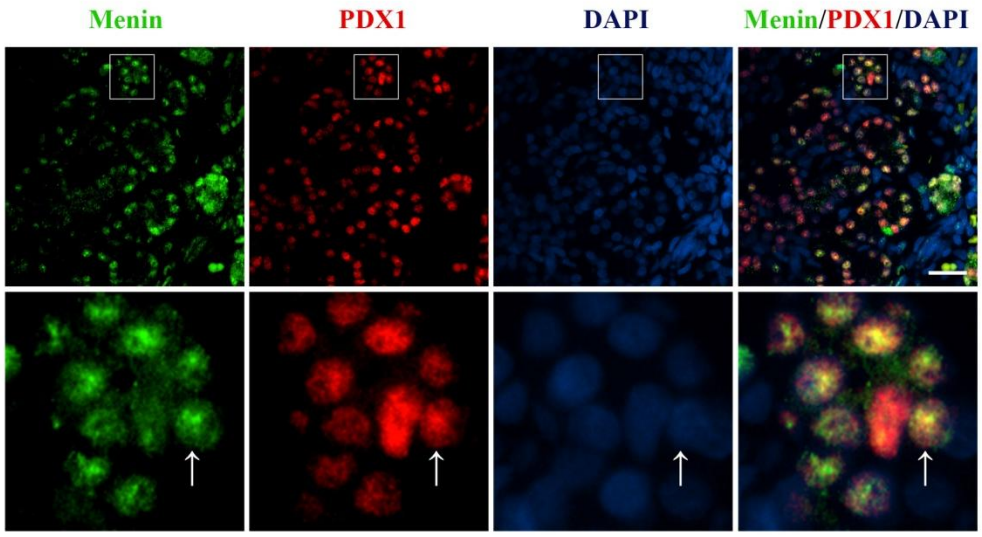
Menin
PDX1
DAPI
Menin/PDX1/DAPI

B.

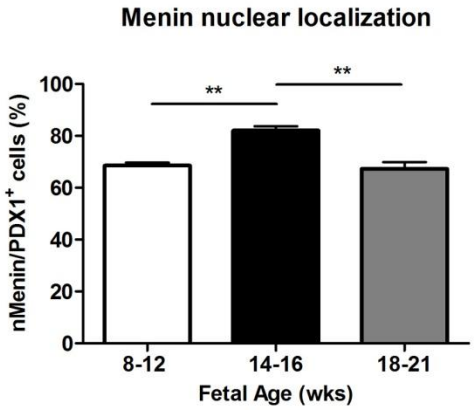
Menin nuclear localization
nMenin/PDX1+ cells (%)
100
80
60
40
20
0
**
**
8-12
14-16
18-21
Fetal Age (wks)

Figure 3.6.

Figure 3.7. Co-localization of nMenin with SOX9 and ISL1 During Human Fetal Pancreatic Development.

Human fetal pancreata sections from 8-21 wks were co-immunolabelled with anti-menin and anti-SOX9 or anti-ISL1 antibodies then visualized with Cy2 (green) and Cy3 (red) conjugated secondary antibodies. Nuclei were labelled with DAPI (blue). Representative pancreatic sections are shown where the top panel of images display double immunostaining for menin (green), **(A)** SOX9 or **(B)** ISL1 (red), DAPI (blue), and an overlay of the images. Scale bars correspond to 25 micrometers. The bottom panels show magnified images corresponding to the boxed section in the above image. Arrows indicate a **(A)** $nMenin^{+}/SOX9^{+}$ cell from 21 wk pancreata or a **(B)** $nMenin^{+}/ISL1^{+}$ cell from 22 wk pancreata.

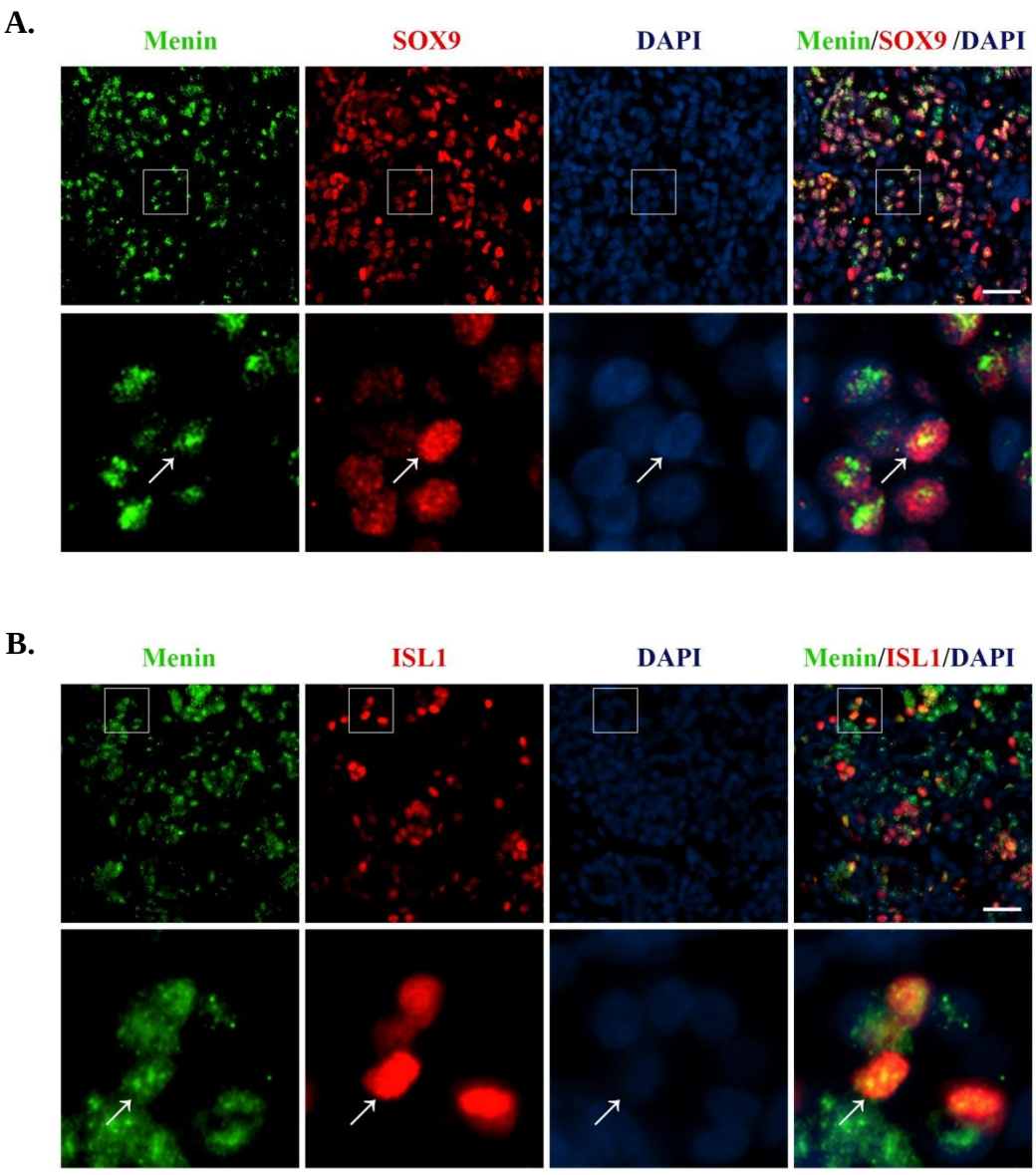
A.
Menin
SOX9
DAPI
Menin/SOX9 /DAPI
B.
Menin
ISL1
DAPI
Menin/ISL1/DAPI

Figure 3.7.

Figure 3.8. Co-localization of nMenin with NGN3 During Human Fetal Pancreatic Development.

Human fetal pancreata sections from 8-21 wks were co-immunolabelled with anti-menin and anti-NGN3 antibodies then visualized with Cy2 (green) and Cy3 (red) conjugated secondary antibodies respectively. Nuclei were labelled with DAPI (blue). A representative section from 21 wks is shown where the top panel of images display double immunostaining for menin (green), NGN3 (red), DAPI (blue), and an overlay of the images. Scale bar corresponds to 25 micrometers. The bottom panel shows magnified images corresponding to the boxed section in the above image. Arrows indicate a $nMenin^{+}/NGN3^{+}$ cell.

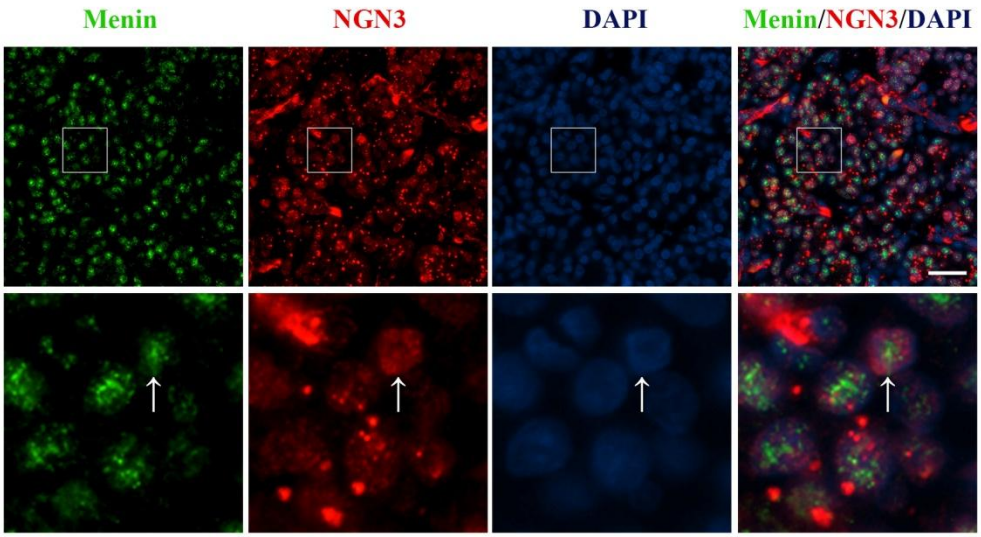

Figure 3.8.

Figure 3.9. Co-localization of nMenin with NKX2.2 and NKX6.1 During Human Fetal Pancreatic Development.

Human fetal pancreata sections from 8-21 wks were co-immunolabelled with anti-menin and anti-NKX2.2 or anti-NKX6.1 antibodies then visualized with Cy2 (green) and Cy3 (red) conjugated secondary antibodies. Nuclei were labelled with DAPI (blue). Representative pancreatic sections are shown where the top panel of images display double immunostaining for menin (green), **(A)** NKX2.2 or **(B)** NKX6.1 (red), DAPI (blue), and an overlay of the images. Scale bars correspond to 25 micrometers. The bottom panels show magnified images corresponding to the boxed section in the above image. Arrows indicate a **(A)** $nMenin^{+}/NKX2.2^{+}$ cell from 20 wk pancreata or a **(B)** $nMenin^{+}/NKX6.1^{+}$ cell from 21 wk pancreata.

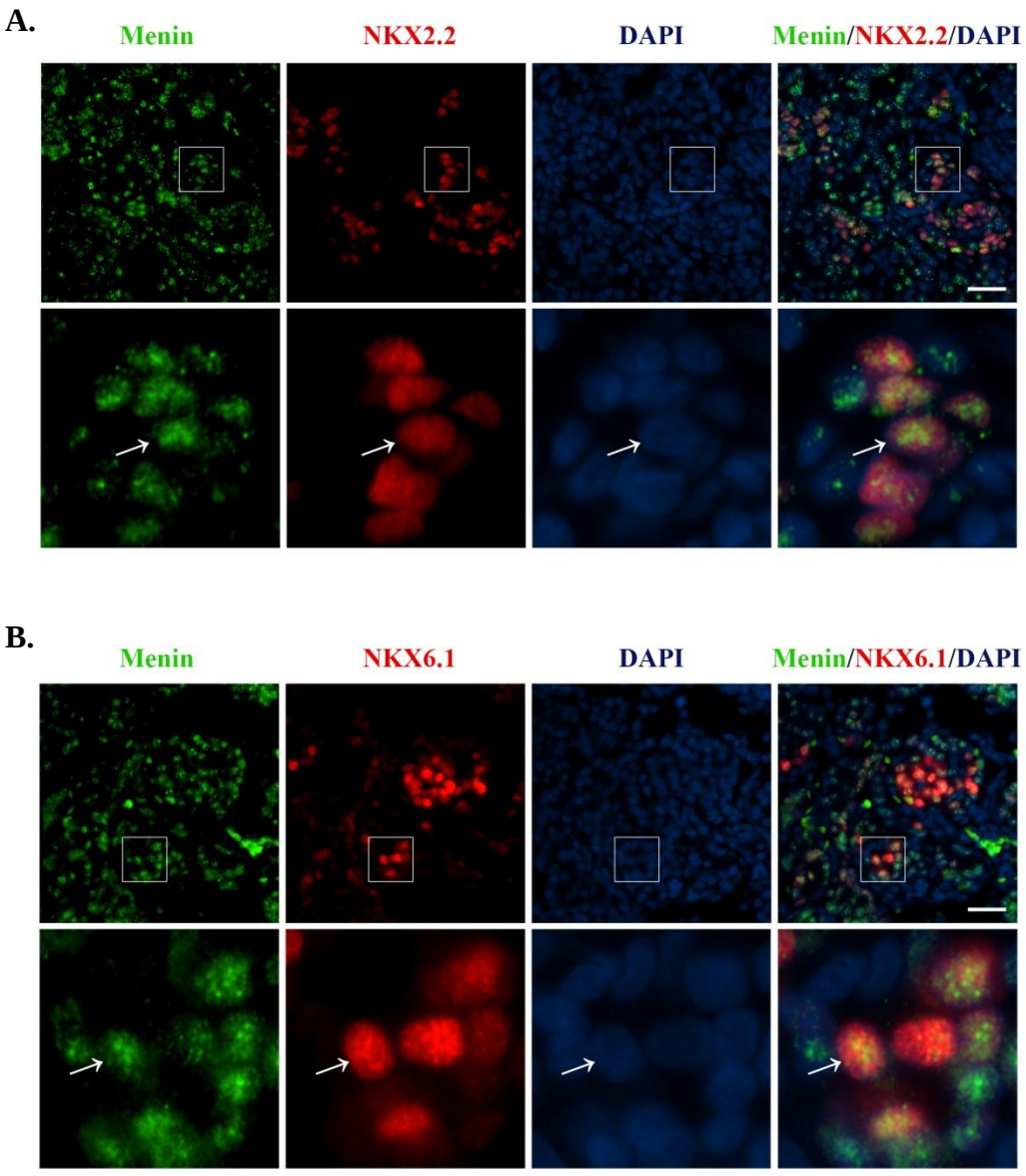
A.
Menin
NKX2.2
DAPI
Menin/NKX2.2/DAPI
B.
Menin
NKX6.1
DAPI
Menin/NKX6.1/DAPI

Figure 3.9.

8-12 wks vs. 18-21 wks) (**Figure 3.10B**). Interestingly, 75-80% of proliferating KI67^{+} cells were positive with nMenin at 8-16 wks, but decreased significantly at 18-21 wks ($p<0.01$ 8-12 wks vs. 18-21 wks, $p<0.01$ 14-16 wks vs. 18-21 wks). This indicates that menin may play a role in proliferation during fetal pancreatic development where a possible change of function may occur between 14-16 and 18-21 wks, as pancreatic cells differentiate and mature (**Figure 3.10C**).

3.4 **Downregulation of *MEN1* Reduces Proliferation with No Effect on Endocrine Population Levels**

To examine the effects of *MEN1* knockdown on human fetal pancreatic development, islet-epithelial cell clusters were isolated from fetal pancreata aged 15-19 wks and treated with control siRNA (Ctrl-siRNA) or *MEN1*-siRNA. This developmental period was chosen due to sample availability and to optimize NGN3 expression, as this window of development includes a major wave of endocrine development (Lyttle et al., 2008). Knockdown efficiency was determined with siRNA transfection times of 24, 48, and 72 hrs using both qRT-PCR and double immunostaining approaches in order to reveal an optimal knockdown time point (**Figure 3.11**). Real-time RT-PCR analysis showed a significant reduction of *MEN1* mRNA at 48 hrs ($p<0.05$ vs. 48 hr Ctrl-siRNA) with no change at 24 and 72 hrs (**Figure 3.11A**). The percentage of total nMenin^{+} cells was also significantly reduced at 48 hrs post transfection ($p<0.01$ vs. 48 hr Ctrl-siRNA) (**Figure 3.11B**). A representative image illustrating the differences in nMenin staining between control siRNA and *MEN1*-siRNA knockdown treatments at 48 hrs can be found in **Figure 3.12** where menin nuclear-stained cells are fewer and the reduction in intensity of nuclear staining is apparent. The 48 hr time point was then chosen exclusively for functional *MEN1* knockdown analysis.

In adult endocrine cells throughout the body, including adult islets, menin has been classically characterized as a negative regulator of proliferation (Chandrasekharappa et al., 1997). To examine whether downregulation of *MEN1* expression has an effect on the proliferative capacity in the developing human fetal pancreas, proliferation of islet-

Figure 3.10. Co-localization of nMenin with KI67$^+$ Proliferating Cells.

Human fetal pancreata sections from three developmental time points (8-12 wks, 14-16 wks, and 18-21 wks) were co-immunolabelled with anti-menin and anti-KI67 antibodies then visualized with Cy2 (green) and Cy3 (red) conjugated secondary antibodies respectively. Nuclei were labelled with DAPI (blue). **(A)** A representative section from 20 wks is shown where the top panel of images display double immunostaining for menin (green), KI67 (red), DAPI (blue), and an overlay of the images. Scale bar corresponds to 25 micrometers. The bottom panel shows magnified images corresponding to the boxed section in the above image. Arrows indicate a nMenin$^+$/KI67$^+$ cell and arrow heads indicate a KI67$^+$ cell. **(B)** Quantitative analysis of co-localized KI67$^+$/nMenin$^+$ cells relative to the total number of nMenin$^+$ cells (expressed as a percentage). **(C)** Quantitative analysis of co-localized nMenin$^+$/KI67$^+$ cells relative to the total number of KI67$^+$ cells (expressed as a percentage). Data were determined by morphometric analysis and are expressed as means ± SEM (n=3-6 pancreata per age group). *$p<0.05$, **$p<0.01$.

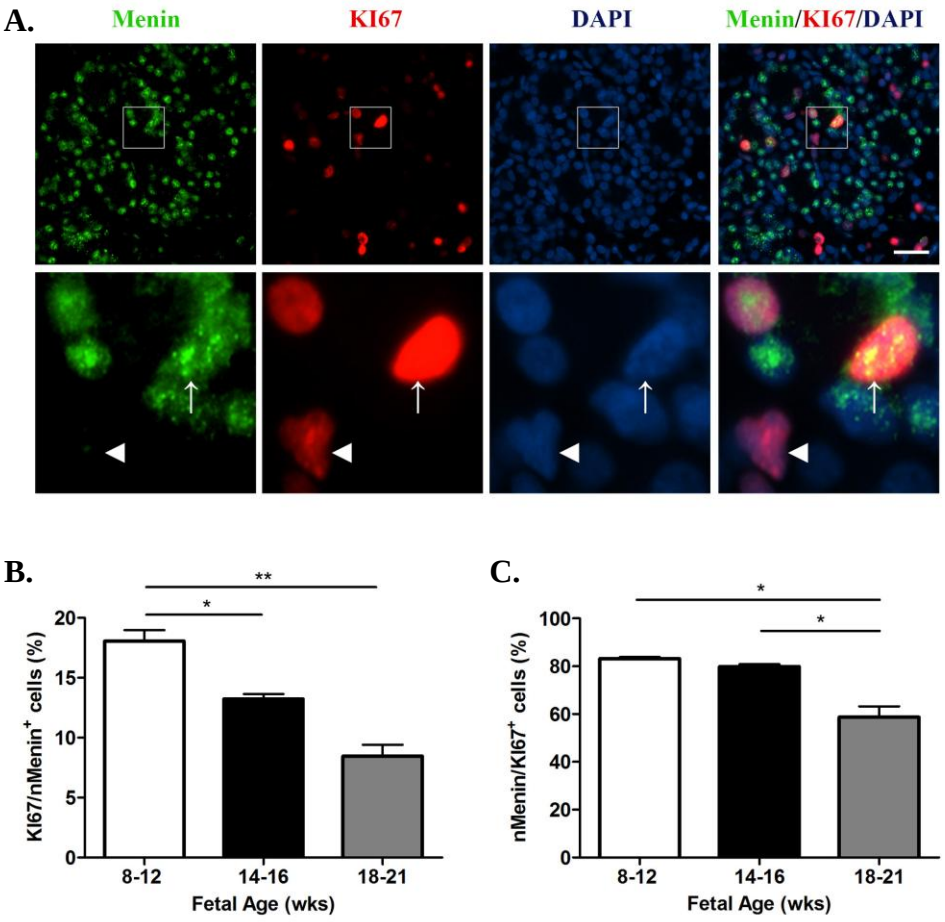
A.
Menin
KI67
DAPI
Menin/KI67/DAPI
B.
KI67/nMenin+ cells (%)
20
15
10
5
0
**
*
8-12
14-16
18-21
Fetal Age (wks)
C.
nMenin/KI67+ cells (%)
100
80
60
40
20
0
*
*
8-12
14-16
18-21
Fetal Age (wks)

Figure 3.10.

Figure 3.11. Time Dependent Effect of *MEN1* siRNA on *MEN1* mRNA and nMenin Expression in Islet-Epithelial Cell Clusters.

Islet-epithelial cell clusters, isolated from human fetal pancreata 15 to 19 wks, were transfected with either control (Ctrl) or *MEN1* siRNA and cultured for 24, 48, or 72 hrs. **(A)** qRT-PCR analysis of total *MEN1* mRNA levels at each transfection period for control and *MEN1* siRNA treatments. Data were normalized to 18S rRNA and are expressed as means ± SEM where n=4-6 per experimental group. **(B)** Quantitative analysis of the total number of $nMenin^+$ cells in the islet-epithelial cell clusters of control and *MEN1* siRNA groups. Data were determined by morphometric analysis and are expressed as means ± SEM where n=3-4 for each experimental group. *$p<0.05$, **$p<0.01$ vs. corresponding control siRNA treatment.

A.

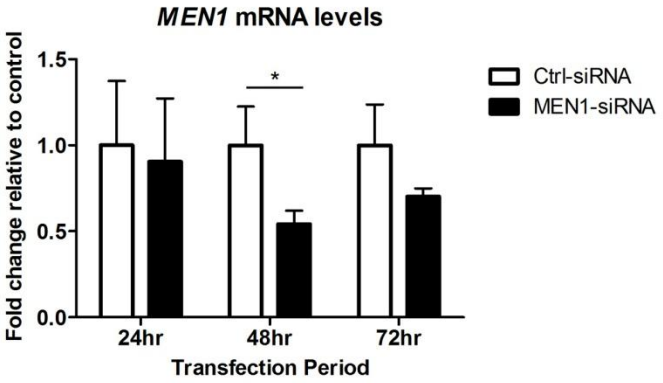

B.

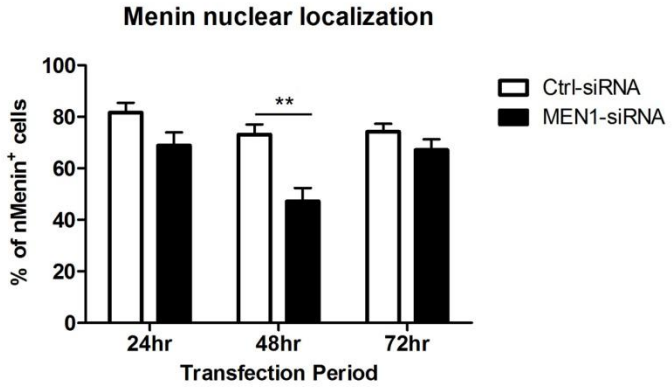

Figure 3.11.

Figure 3.12. Effect of *MEN1* siRNA on nMenin Expression in Islet-Epithelial Cell Clusters.

Representative images of islet-epithelial cell clusters isolated from human fetal pancreata 15 to 19 wks which were transfected with **(A)** control (Ctrl) siRNA or **(B)** *MEN1* siRNA at 48 hrs post treatment. Cells were harvested, paraffin-embedded, and sections were immunolabelled with an anti-menin antibody visualized with a Cy2 (green) conjugated secondary antibody. Nuclei were labelled with DAPI (blue). For each set, the top panel of images shows staining for menin (green), DAPI (blue), and an overlay of images. Scale bars correspond to 25 micrometers. The bottom panels show an enlargement of the boxed section from the above image. Arrows indicate **(A)** a nuclear menin positive or **(B)** a nuclear menin negative cell.

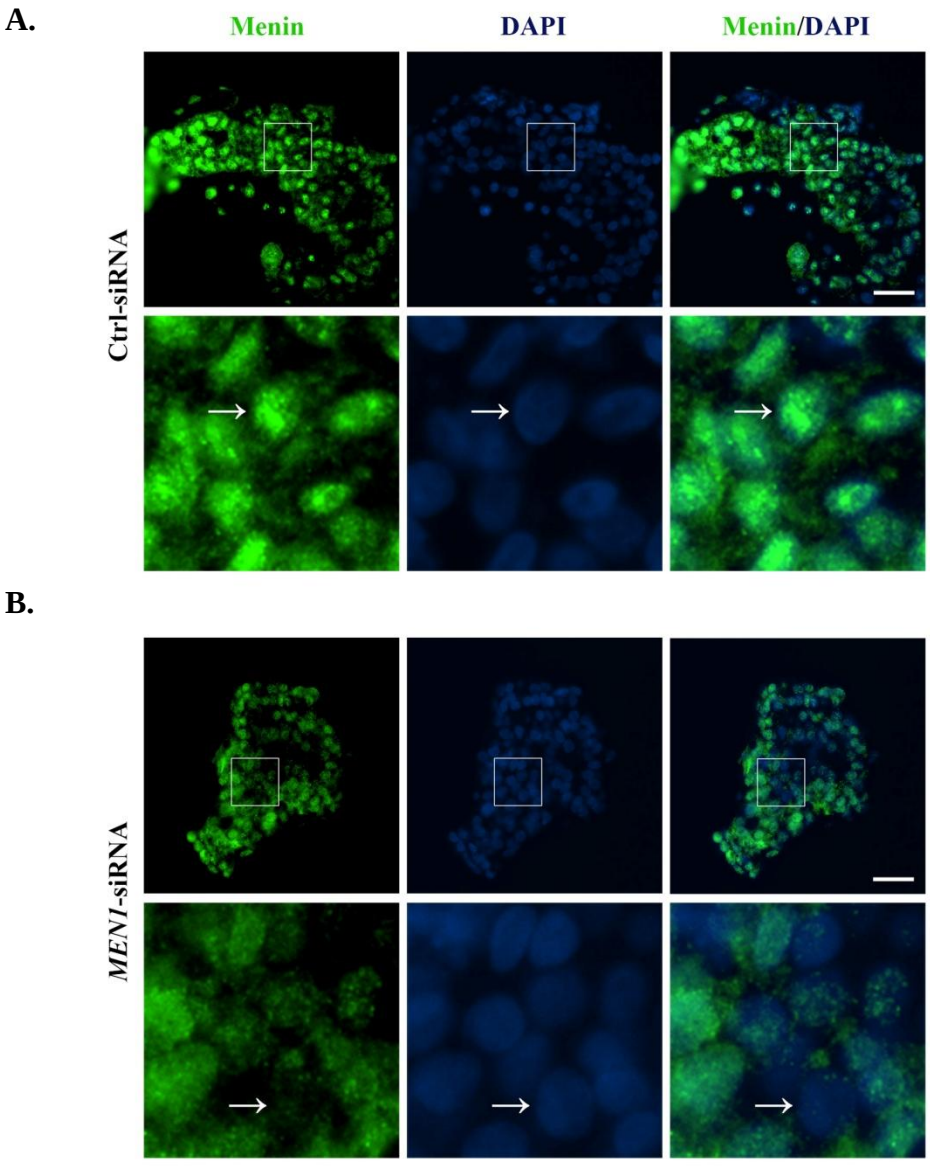

Figure 3.12.

epithelial cells (KI67 labelling index) was assessed in our *MEN1*-siRNA study using immunofluorescence staining techniques. Morphological analysis revealed significantly reduced total proliferation levels ($KI67^+$ cells) in the *MEN1*-siRNA treated group ($p<0.05$ vs. Ctrl-siRNA) (**Figure 3.13**).

It was noted that there was no significant change in the proliferation of $insulin^+$ cells, but the proliferation capacity of $glucagon^+$ cells was significantly reduced with *MEN1* knockdown ($p<0.05$ vs. Ctrl-siRNA) (**Figure 3.14A, D**). However, there was no effect on insulin and glucagon mRNA expression (**Figure 3.14B, E**) or the population levels of $insulin^+$ and $glucagon^+$ cells (**Figure 3.14C, F**) with *MEN1* and control siRNA treatments. Somatostatin- and pancreatic polypeptide-expressing endocrine cells were co-stained with KI67 as well and no observable difference was found in the proliferation capacity of these cell types or the total quantity of either somatostatin- (**Figure 3.15A, B**) or PP-cell (**Figure 3.15C, D**) population.

To elucidate by what means *MEN1* knockdown reduces cellular proliferation, we analyzed the effect of *MEN1* siRNA on cell cycle regulators and the activation of the PI3K/AKT and Wnt/β-catenin pathways. The cell cycle regulators analyzed were p18, p21, and p27, which are cell cycle inhibitors, and cyclinD1 which promotes cell cycle progression (Wu and Hua, 2011). In adult tissues, Menin has been shown to regulate the expression of all four of these cell cycle regulators either directly or indirectly to reduce proliferation (Wu and Hua, 2011). In this study, analysis of *p18*, *p21*, *p27*, and *cyclinD1* mRNA showed no significant change with *MEN1* downregulation (Appendix II: **Supplementary Figure 5A**). Menin has also been shown to negatively regulate both the PI3K/AKT and Wnt/β-catenin pathways to reduce proliferation in adults (Cao et al., 2009; Wang et al., 2011). Here we show that with *MEN1* knockdown, pAKT (indicative of an activated pathway) and pβ-catenin (pSer675, indicative of an active Wnt pathway) protein levels were similar between Ctrl-siRNA and *MEN1*-siRNA treatment groups (Appendix II: **Supplementary Figure 6**).

Figure 3.13. Effect of *MEN1* siRNA on Islet-Epithelial Cell Cluster Proliferation.

Islet-epithelial cell clusters isolated from human fetal pancreata 15 to 19 wks were transfected with either control siRNA or *MEN1* siRNA for a 48 hr treatment. Cells were harvested, paraffin-embedded, and sections were immunolabelled with an anti-KI67 antibody visualized with a Cy3 (red) conjugated secondary antibody. Nuclei were labelled with DAPI (blue). **(A)** Quantitative analysis of the total number of $KI67^+$ cells relative to the total amount of cells present ($KI67^+$/DAPI, expressed as a percentage) for control and *MEN1* siRNA treatments. Data were determined by morphometric analysis and are expressed as means ± SEM where n=4-5 for each experimental group. *$p<0.05$ vs. control siRNA treatment. **(B, C)** Representative images denoting proliferation ($KI67^+$) for **(B)** control siRNA and **(C)** *MEN1* siRNA treatment groups. For each set, the top panel of images shows staining for KI67 (red), DAPI (blue), and an overlay of images. Scale bars correspond to 25 micrometers. The bottom panels show magnified images corresponding to the boxed section in the above image. Arrows indicate a KI67 positive cell.

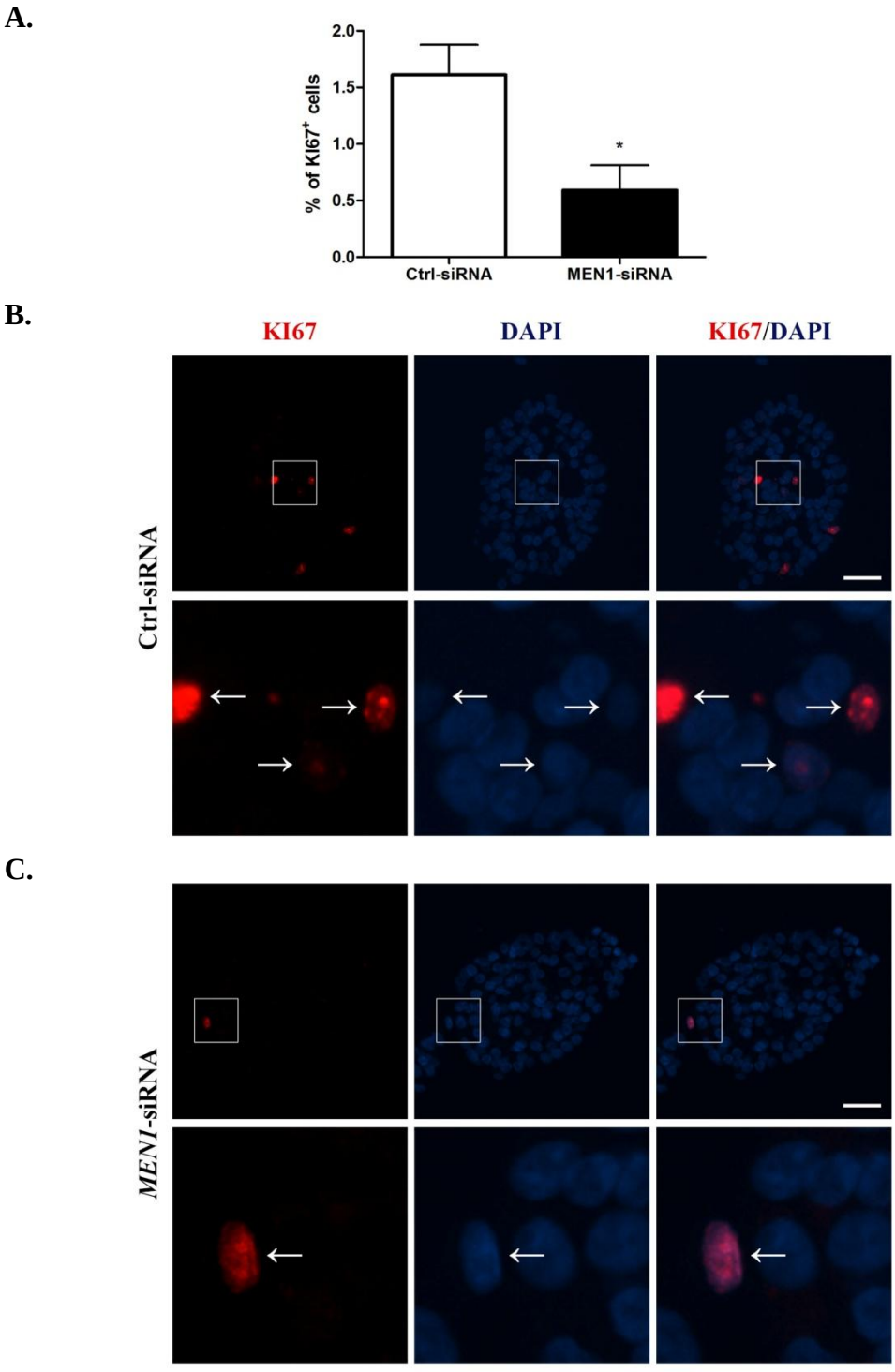
A.
2.0
1.5
1.0
0.5
0.0
% of KI67+ cells
*
Ctrl-siRNA
MEN1-siRNA
B.
KI67
DAPI
KI67/DAPI
Ctrl-siRNA
C.
MEN1-siRNA

Figure 3.13.

Figure 3.14. Effect of *MEN1* siRNA on Endocrine Cell Proliferation and Differentiation in Islet-Epithelial Cell Clusters.

Islet-epithelial cell clusters isolated from human fetal pancreata 15 to 19 wks were transfected with either control siRNA or *MEN1* siRNA and cultured for 48 hrs. **(A-C)** Analysis of the insulin population where **(D-F)** describe analysis of the glucagon population of endocrine cells. Quantitative analysis of the proliferation capacity between control and *MEN1* siRNA groups in the **(A)** insulin$^+$ or **(D)** glucagon$^+$ cell populations, expressed as a percentage relative to the control treatment for each sample, where proliferation capacity is the amount of KI67$^+$ cells relative to a certain cell population. Data were determined by morphometric analysis and are expressed as means ± SEM where n=3-4 for each treatment. qRT-PCR analysis of **(B)** insulin and **(E)** glucagon gene expression for control and *MEN1* siRNA treatments. Data were normalized to 18S rRNA and are expressed as means ± SEM where n=4-6 per experimental group. Quantitative analysis of **(C)** insulin$^+$ and **(F)** glucagon$^+$ cell populations expressed as a percentage (total insulin$^+$ or glucagon$^+$ cells relative to the total amount of cells present, DAPI stained nuclei) for control and *MEN1* siRNA treatments. Data were determined by morphometric analysis and are expressed as means ± SEM where n=3-4 for each treatment. *$p<0.05$ vs. control siRNA treatment.

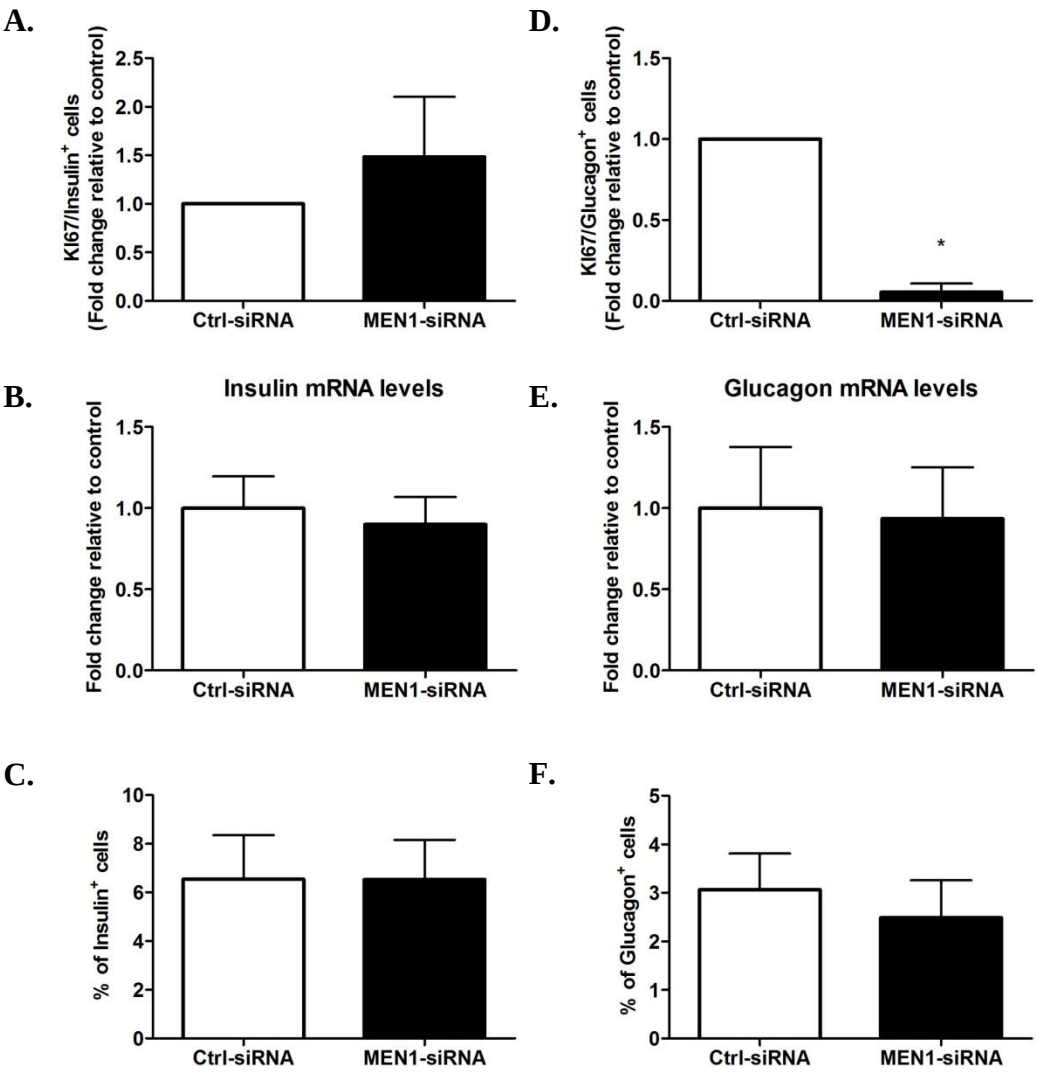
A.
Ki67/Insulin+ cells
(Fold change relative to control)
2.5
2.0
1.5
1.0
0.5
0.0
Ctrl-siRNA
MEN1-siRNA
D.
Ki67/Glucagon+ cells
(Fold change relative to control)
1.5
1.0
0.5
0.0
*
Ctrl-siRNA
MEN1-siRNA
B.
Insulin mRNA levels
Fold change relative to control
1.5
1.0
0.5
0.0
Ctrl-siRNA
MEN1-siRNA
E.
Glucagon mRNA levels
Fold change relative to control
1.5
1.0
0.5
0.0
Ctrl-siRNA
MEN1-siRNA
C.
% of Insulin+ cells
10
8
6
4
2
0
Ctrl-siRNA
MEN1-siRNA
F.
% of Glucagon+ cells
5
4
3
2
1
0
Ctrl-siRNA
MEN1-siRNA

Figure 3.14.

Figure 3.15. Effect of *MEN1* siRNA on Somatostatin and Pancreatic Polypeptide Expression.

Islet-epithelial cell clusters isolated from human fetal pancreata 15 to 19 wks were transfected with either control siRNA or *MEN1* siRNA for a 48 hr treatment. Cells were harvested, paraffin-embedded, and sections were co-immunolabelled with an **(A, B)** anti-somatostatin antibody or **(C, D)** anti-pancreatic polypeptide (PP) antibody along with an anti-KI67 antibody which were visualized with a Cy2 (green) and Cy3 (red) conjugated secondary antibody. Nuclei were labelled with DAPI (blue). **(A, B)** Representative images for somatostatin^{+} and KI67^{+} cells for **(A)** control siRNA and **(B)** *MEN1* siRNA treatment groups. **(C, D)** Representative images for PP^{+} and KI67^{+} cells for **(C)** control siRNA and **(D)** *MEN1*-siRNA treatment groups. For each set, the top panel of images shows staining for somatostatin or PP (green), KI67 (red), DAPI (blue), and an overlay of images. The bottom panels show magnified images corresponding to the boxed section in the above image. Scale bars correspond to 25 micrometers. Arrows indicate somatostatin^{+} or PP^{+} cells. Arrowheads indicate KI67^{+} cells.

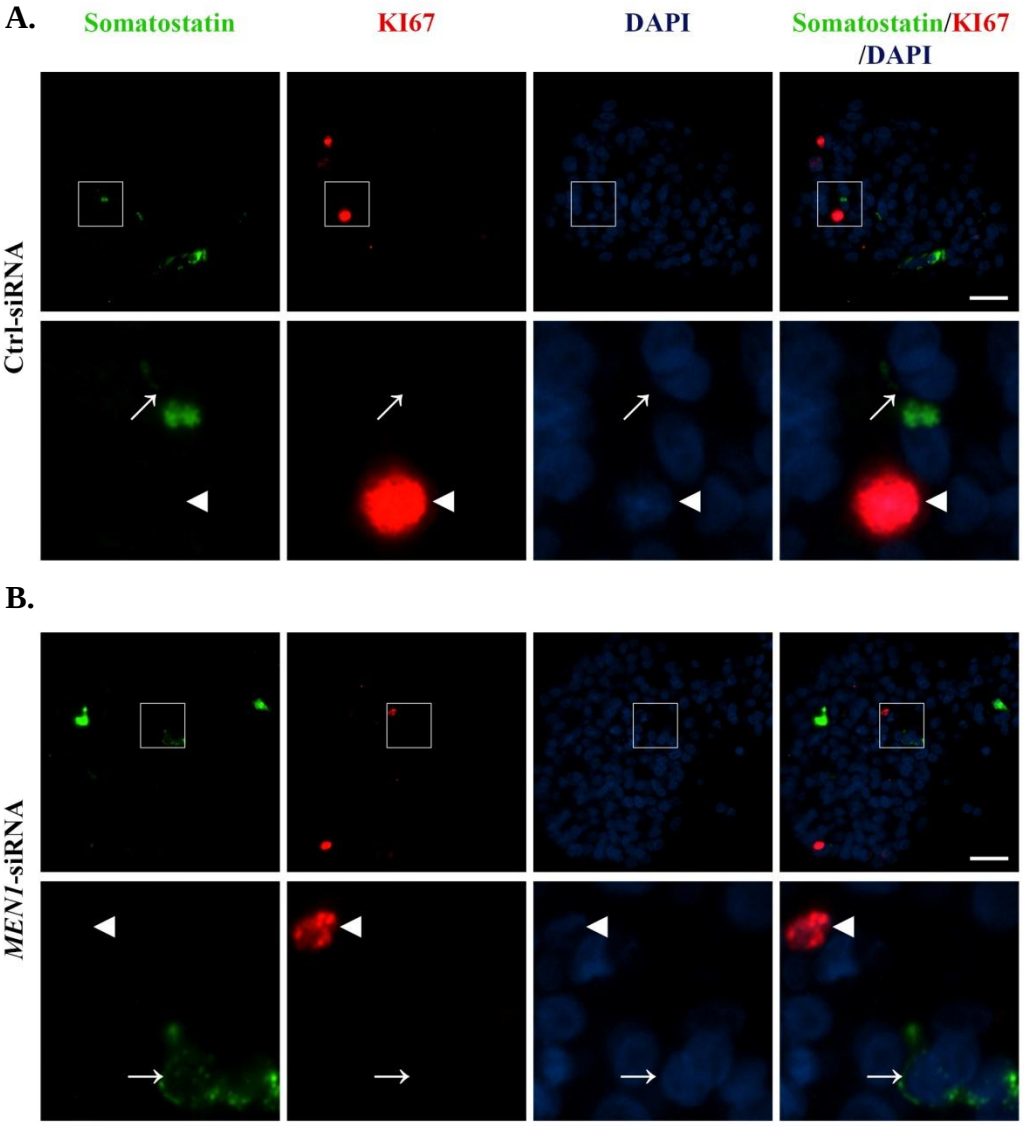
A.
Somatostatin
KI67
DAPI
Somatostatin/KI67
/DAPI
Ctrl-siRNA
B.
MEN1-siRNA

Figure 3.15.

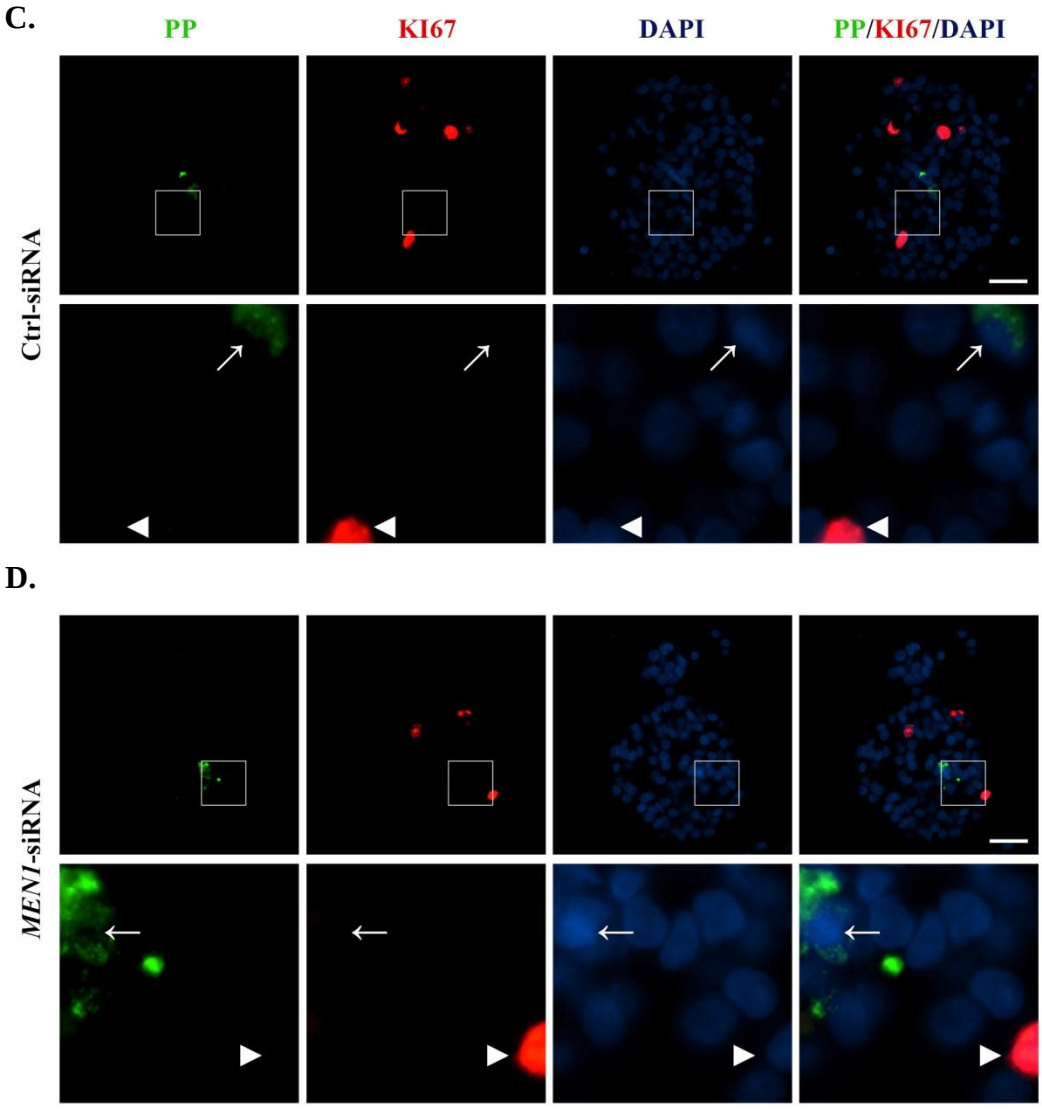

Figure 3.15.

3.5 **Downregulation of *MEN1* Effects the Expression of Transcription Factors**

To explore the impact of *MEN1* knockdown on islet development, the levels of various transcription factors that are critical for human fetal islet development were analyzed using qRT-PCR, immunofluorescence staining, and western blotting techniques following a 48 hr *MEN1* and control siRNA transfection period. Analysis of PDX1 expression following transfection showed a slight reduction in *PDX1* mRNA and the number of $PDX1^+$ cells, however no statistical significance was found (**Figure 3.16A, B**). When looking at the progenitor pool marker SOX9, there was a significant reduction in *SOX9* mRNA with *MEN1* downregulation ($p<0.05$ vs. Ctrl-siRNA), however the SOX9 protein level was unchanged (**Figure 3.16C, D**). Analysis of NGN3 demonstrated stable expression between treatment groups for both mRNA expression and the population of $NGN3^+$ expressing islet-epithelial cell clusters (**Figure 3.16E, F**). Interestingly, *MEN1* knockdown did have a significant effect on NGN3 downstream transcription factors NKX2.2 and NKX6.1 (**Figure 3.17A-C**). A significant decrease in *NKX2.2* and *NKX6.1* mRNA levels was observed with *MEN1* downregulation compared with Ctrl-siRNA treatment (**Figure 3.17A, C**) with no quantifiable change in the total number of $NKX2.2^+$ cells (**Figure 3.17B**). Exocrine levels, assessed by the transcription factor HES1, showed no change in *HES1* mRNA levels with *MEN1* downregulation (**Figure 3.17D**).

3.6 **Downregulation of *MEN1* Reduces Cell Survival Capabilities**

Previous studies have demonstrated that menin functions as a tumour suppressor through various pathways including an involvement in cell survival by promoting DNA repair and genome stability, but also through promoting apoptotic pathways (Garcia-Higuera et al., 2001; Gustavson et al., 1983; La et al., 2007). Cell survival and cell death were investigated between control and *MEN1* siRNA groups using immunofluorescence analysis of TUNEL labelling and western blot analysis of the total content of the cleaved Caspase-3 protein (**Figure 3.18**). Morphological analysis of $TUNEL^+$ cells revealed a significant increase in apoptotic ($TUNEL^+$) cells with *MEN1* knockdown ($p<0.01$ vs.

Figure 3.16. Effect of *MEN1* siRNA on PDX1, SOX9, and NGN3 Expression.

Islet-epithelial cell clusters, isolated from human fetal pancreata 15 to 19 wks, were transfected with either control siRNA or *MEN1* siRNA for a 48 hr treatment. **(A)** Analysis of *PDX1* mRNA expression by qRT-PCR for control and *MEN1* siRNA treatments. **(B)** Quantitative analysis of the $PDX1^{+}$ cell population relative to the total amount of cells present (DAPI stained nuclei, expressed as a percentage) for control and *MEN1* siRNA groups. **(C)** Analysis of *SOX9* mRNA expression by qRT-PCR for both treatment groups. **(D)** Western blot analysis of total SOX9 protein expression (65 kDa) normalized to calnexin expression (90 kDa) for both treatment groups, n=3 per treatment group. **(E)** Analysis of *NGN3* mRNA expression by qRT-PCR for both treatment groups. **(F)** Quantitative analysis of the $NGN3^{+}$ cell population relative to the amount of cells present (DAPI stained nuclei, expressed as a percentage) for both treatment groups. **(A, C, E)** Data were normalized to 18S rRNA where n=4-6 per experimental group. **(B, F)** Data were determined by morphometric analysis where n=3-4 for each treatment. Data were expressed as means ± SEM, *$p<0.05$ vs. control siRNA treatment.

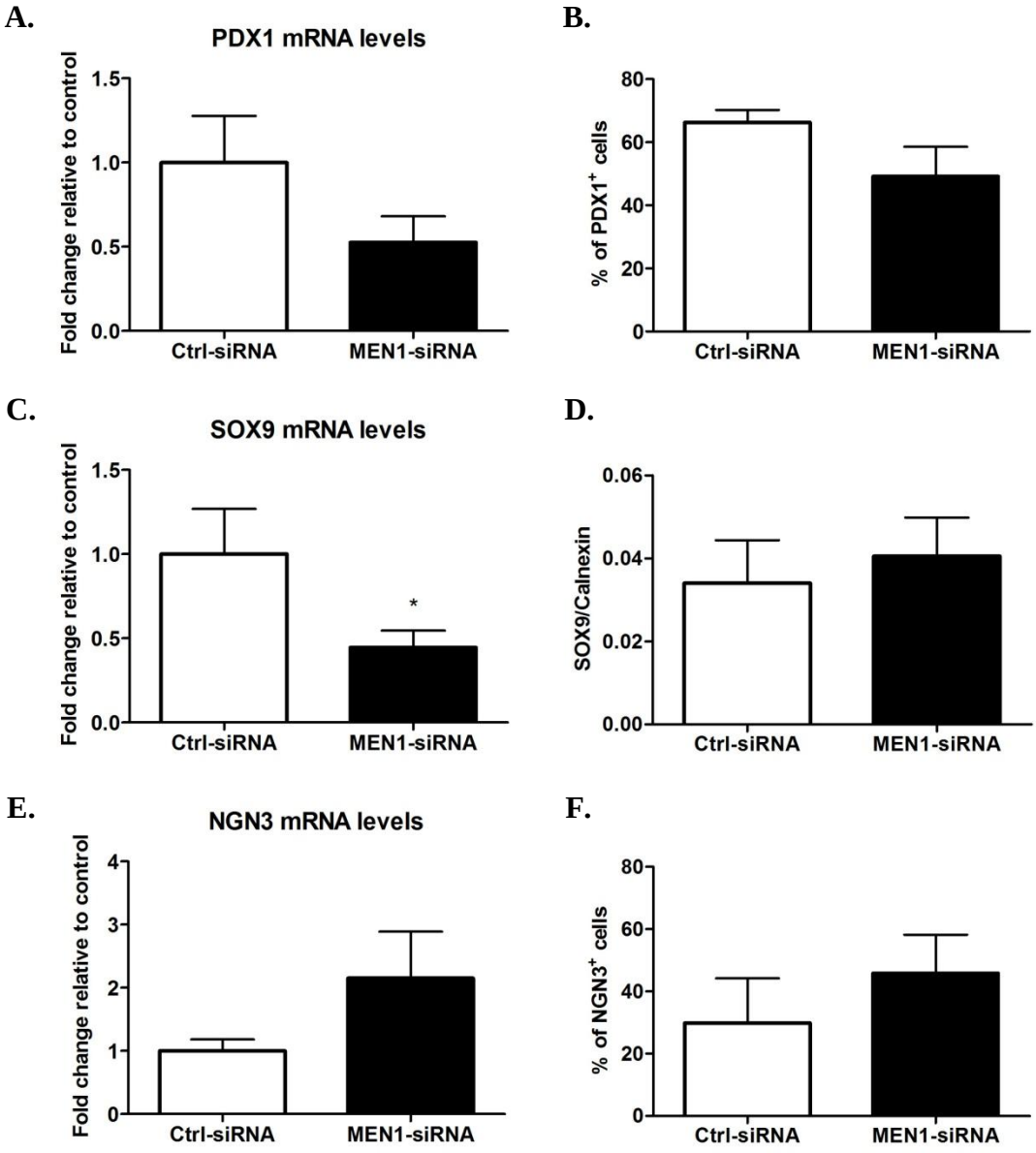
A.
PDX1 mRNA levels
Fold change relative to control
1.5
1.0
0.5
0.0
Ctrl-siRNA
MEN1-siRNA
B.
% of PDX1+ cells
80
60
40
20
0
Ctrl-siRNA
MEN1-siRNA
C.
SOX9 mRNA levels
Fold change relative to control
1.5
1.0
0.5
0.0
*
Ctrl-siRNA
MEN1-siRNA
D.
SOX9/Calnexin
0.06
0.04
0.02
0.00
Ctrl-siRNA
MEN1-siRNA
E.
NGN3 mRNA levels
Fold change relative to control
4
3
2
1
0
Ctrl-siRNA
MEN1-siRNA
F.
% of NGN3+ cells
80
60
40
20
0
Ctrl-siRNA
MEN1-siRNA

Figure 3.16.

Figure 3.17. Effect of *MEN1* siRNA on NKX2.2, NKX6.1, and HES1 Expression.

Islet-epithelial cell clusters, isolated from human fetal pancreata 15 to 19 wks, were transfected with either control siRNA or *MEN1* siRNA for a 48 hr treatment period. qRT-PCR analysis of total **(A)** *NKX2.2*, **(C)** *NKX6.1*, or **(D)** *HES1* gene expression for control and *MEN1* siRNA treatments. Data were normalized to 18S rRNA and are expressed as means ± SEM where n=4-6 per experimental group. **(B)** Quantitative analysis of the total $NKX2.2^{+}$ cell population relative to the total amount of cells present (DAPI stained nuclei, expressed as a percentage) for control and *MEN1* siRNA treatments. Data was determined by morphometric analysis and are expressed as means ± SEM where n=3-4 for each treatment. *$p<0.05$ vs. control siRNA treatment.

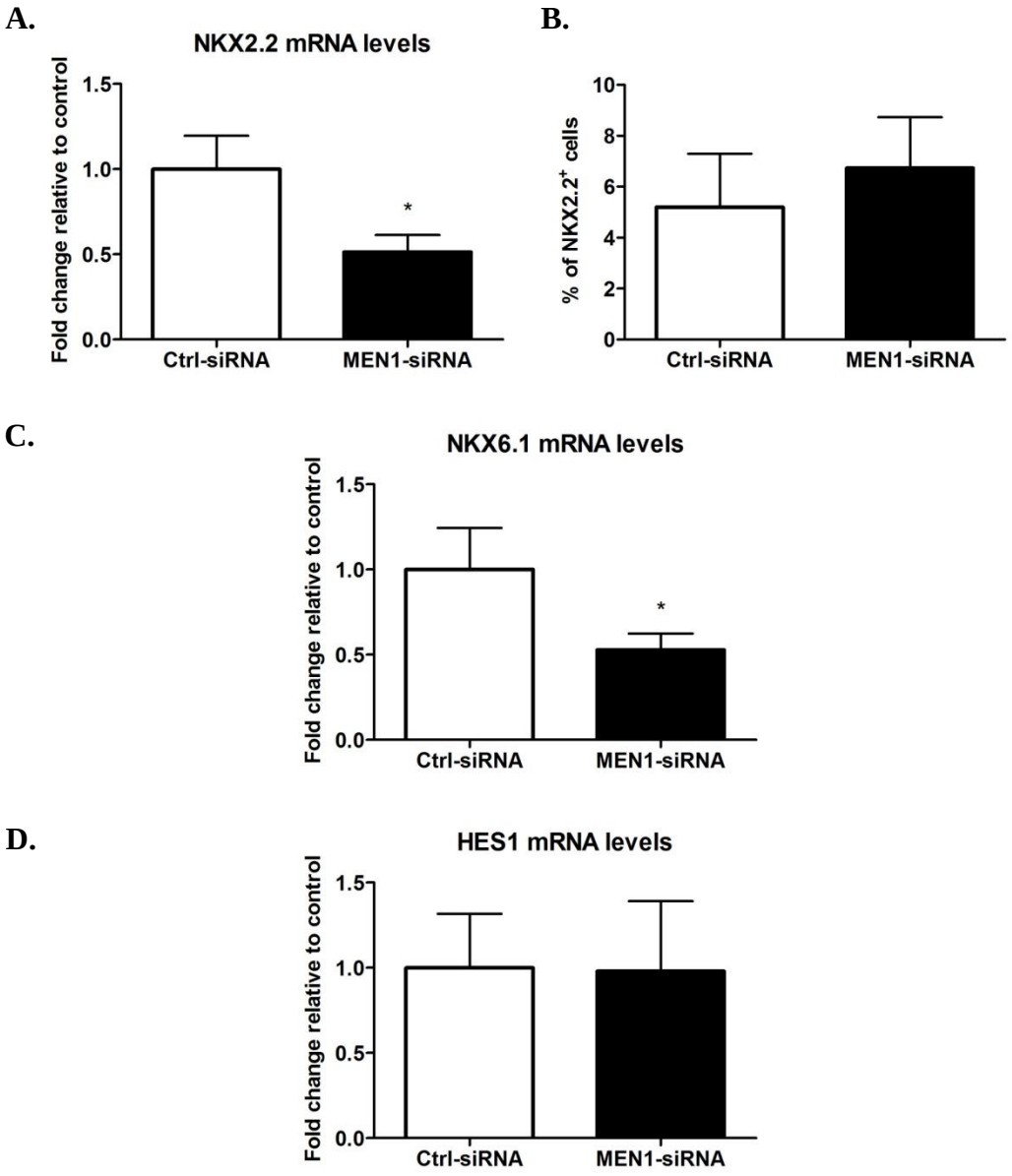
A.
NKX2.2 mRNA levels
Fold change relative to control
1.5
1.0
0.5
0.0
*
Ctrl-siRNA
MEN1-siRNA
B.
% of NKX2.2+ cells
10
8
6
4
2
0
Ctrl-siRNA
MEN1-siRNA
C.
NKX6.1 mRNA levels
Fold change relative to control
1.5
1.0
0.5
0.0
*
Ctrl-siRNA
MEN1-siRNA
D.
HES1 mRNA levels
Fold change relative to control
1.5
1.0
0.5
0.0
Ctrl-siRNA
MEN1-siRNA

Figure 3.17.

Ctrl-siRNA) (**Figure 3.18A**). Quantification of cleaved Caspase-3 protein level in the *MEN1* siRNA group displayed an increasing trend of cleaved Caspase-3 signals where p=0.08 (**Figure 3.18B**), indicating a confirmation of morphological assessment and an increase in cell death, or a reduction in cell survival with a decrease in menin. Studies have shown that the PI3K/AKT and Wnt/β-catenin pathways are both involved in apoptotic regulation along with proliferation, another reason why the effect of menin knockdown on these pathways was studied (see section 3.4) (Chen et al., 2008; Wang et al., 2011).

3.7 Overexpression of *MEN1* Promotes Proliferation and Effects Islet Development

The effects of *MEN1* overexpression in islet-epithelial cell clusters was explored using cultured islets isolated from human fetal pancreata 15-19 wks which were transfected with either a control pEGFP vector (Ctrl-EGFP) or a pEGFP-N2 vector with a human full-length *MEN1* cDNA insertion (N2-M1). After a 48 hr transfection, qRT-PCR analysis showed a significant two fold increase of *MEN1* mRNA levels with N2-M1 transfection ($p<0.05$ vs. Ctrl-EGFP) (**Figure 3.19A**). Morphological analysis of islet-epithelial cell cluster sections stained with an anti-menin antibody 48 hrs post-transfection also indicated a significant increase of $nMenin^+$ cells (from approximately 75% to 90%) with N2-M1 treatment ($p<0.05$ vs. Ctrl-EGFP) (**Figure 3.19B**). **Figure 3.19C, D** show representative images illustrating menin overexpression within islet-epithelial cell clusters.

The functional role of menin in regulating proliferation during human fetal pancreatic development was investigated with increasing menin expression (N2-M1 transfection). Quantification of the proliferative cell population displayed a significant increase in $KI67^+$ cells with menin overexpression ($p<0.05$ vs. Ctrl-EGFP) (**Figure 3.20**). These results correspond with and confirm those found in **Figure 3.13** with a knockdown of menin expression. Our next step was to determine if this increase in proliferation affected a specific endocrine population. Examination of insulin (**Figure 3.21A**) and

Figure 3.18. Effect of *MEN1* siRNA on Cell Death in Islet-Epithelial Cell Clusters.

Islet-epithelial cell clusters, isolated from human fetal pancreata 15 to 19 wks, were transfected with either control siRNA or *MEN1* siRNA for a 48 hr treatment period. **(A)** Quantitative analysis of the total amount of $TUNEL^+$ cells relative to the total amount of cells present (DAPI stained nuclei, expressed as a percentage) for both control and *MEN1* siRNA treatment groups. Data were determined by morphometric analysis. **(B)** Western blot analysis of cleaved Caspase-3 (cCaspase-3) protein expression (17, 19 kDa) relative to total Caspase-3 (tCaspase-3) protein expression (35 kDa) for both treatment groups, normalized to control. Representative images of TUNEL labelling for **(C)** control or **(D)** *MEN1* siRNA treatment groups. Cells were harvested, paraffin-embedded, sections were TUNEL labelled (green) as in Section 2.2, and the nuclei were labelled with DAPI (blue). For each set, the top panel of images shows staining for TUNEL (green), DAPI (blue), and an overlay of images. Scale bars correspond to 25 micrometers. The bottom panels show magnified images corresponding to the boxed section in the above image. Arrows indicate a TUNEL positive cell. Data are expressed as means ± SEM. n=3. $^{**}p<0.01$ vs. control siRNA treatment.

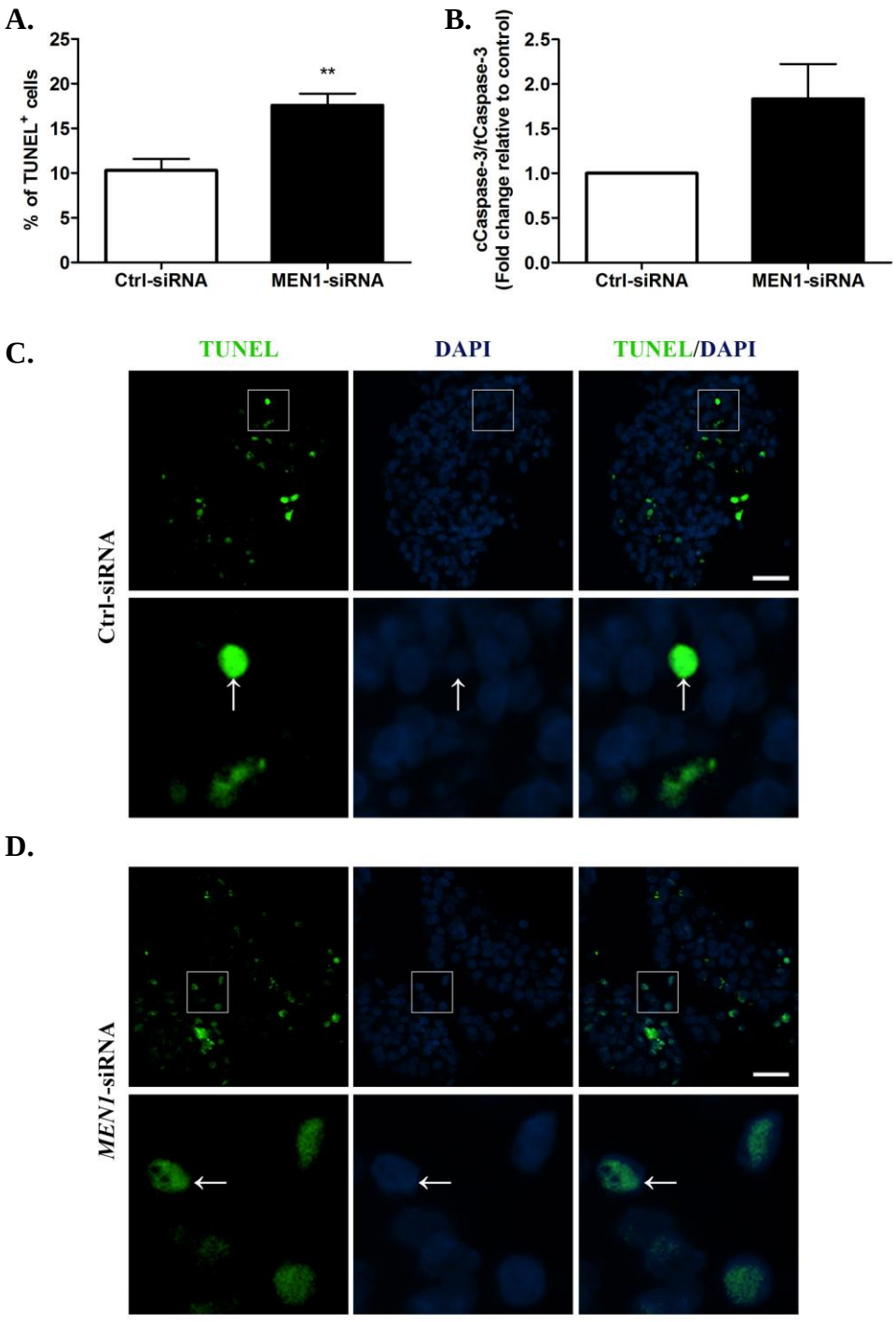
A.
% of TUNEL+ cells
25
20
15
10
5
0
**
Ctrl-siRNA
MEN1-siRNA
B.
cCaspase-3/tCaspase-3
(Fold change relative to control)
2.5
2.0
1.5
1.0
0.5
0.0
Ctrl-siRNA
MEN1-siRNA
C.
TUNEL
DAPI
TUNEL/DAPI
Ctrl-siRNA
D.
MEN1-siRNA

Figure 3.18.

Figure 3.19. Effect of *MEN1* Overexpression on *MEN1* mRNA and nMenin in Islet-Epithelial Cell Clusters.

Islet-epithelial cell clusters, isolated from human fetal pancreata 15 to 19 wks, were transfected with either a control (Ctrl-EGFP) or a *MEN1* (N2-M1) vector and cultured for 48 hrs. **(A)** qRT-PCR analysis of total *MEN1* mRNA levels for control and N2-M1 treatments. Data were normalized to 18S rRNA and are expressed as means ± SEM where n=6 per experimental group. **(B)** Quantitative analysis of the total number of $nMenin^+$ cells relative to the total amount of cells present ($nMenin^+$/DAPI, expressed as a percentage) of both control and N2-M1 groups. Data are expressed as means ± SEM where n=3-4 for each experimental group. *$p<0.05$ vs. Ctrl-EGFP treatment. **(C, D)** Representative images of islet-epithelial cell clusters for **(C)** control or **(D)** N2-M1 treatment groups. Cells were harvested, paraffin-embedded, and sections were immunolabelled with an anti-menin antibody visualized with a Cy2 (green) conjugated secondary antibody. Nuclei were labelled with DAPI (blue). For each set, the top panel of images shows staining for menin (green), DAPI (blue), and an overlay of images. Scale bars correspond to 25 micrometers. The bottom panels show magnified images corresponding to the boxed section in the above image. Arrows indicate a nuclear menin positive cell.

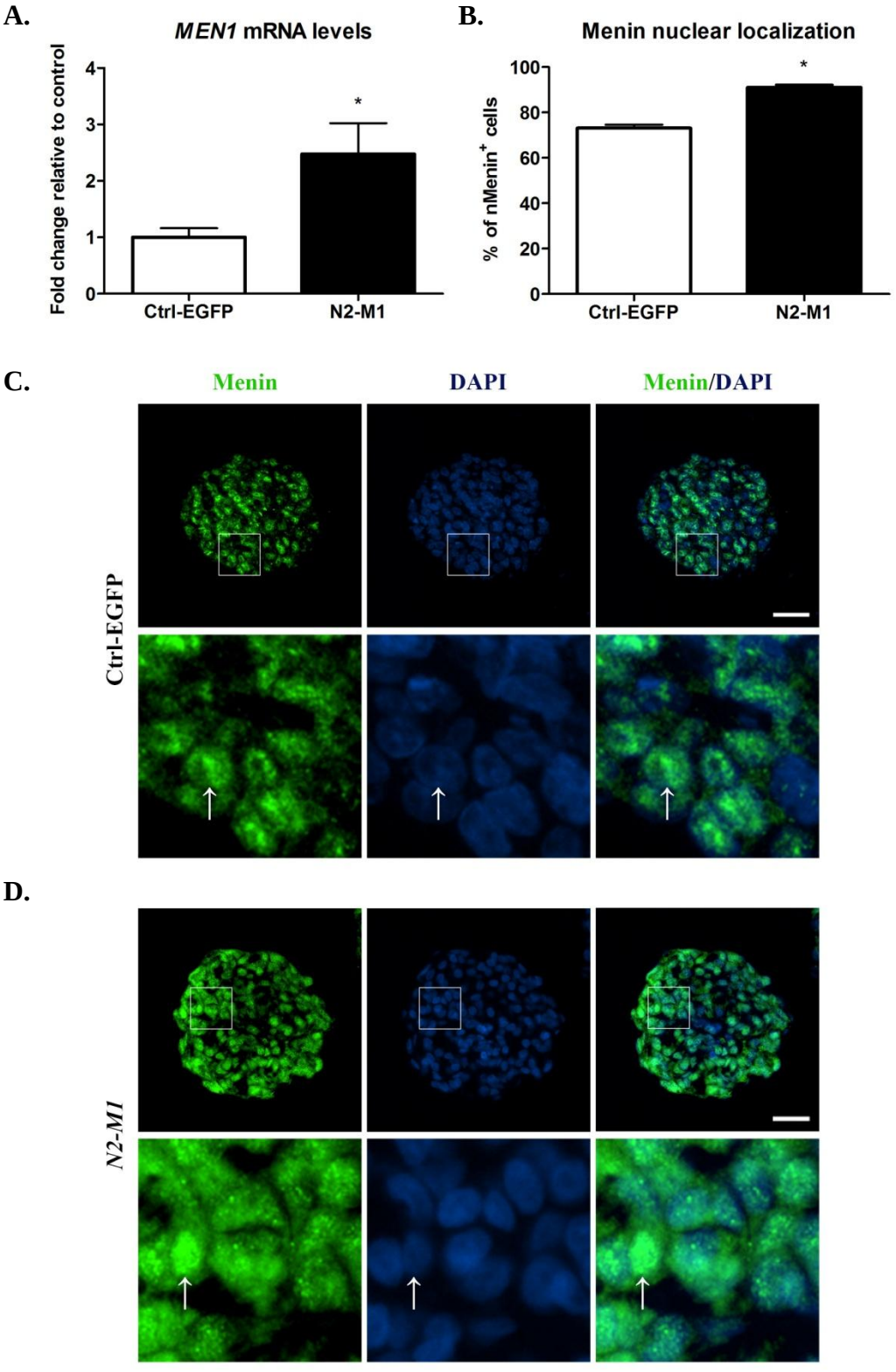
A.
MEN1 mRNA levels
Fold change relative to control
0
1
2
3
4
*
Ctrl-EGFP
N2-M1
B.
Menin nuclear localization
% of nMenin+ cells
0
20
40
60
80
100
*
Ctrl-EGFP
N2-M1
C.
Menin
DAPI
Menin/DAPI
Ctrl-EGFP
D.
N2-M1

Figure 3.19.

Figure 3.20. Effect of *MEN1* Overexpression on Islet-Epithelial Cell Cluster Proliferation.

Islet-epithelial cell clusters, isolated from human fetal pancreata 15 to 19 wks, were transfected with either a control (Ctrl-EGFP) or a *MEN1* (N2-M1) vector and cultured for 48 hrs. Cells were harvested, paraffin-embedded, and sections were immunolabelled with an anti-KI67 antibody visualized with a Cy3 (red) conjugated secondary antibody. Nuclei were labelled with DAPI (blue). **(A)** Quantitative analysis of the total number of $KI67^+$ cells relative to the total amount of cells present ($KI67^+$/DAPI, expressed as a percentage) for control and N2-M1 treatments. Data are expressed as means ± SEM where n=3 for each experimental group. *$p<0.05$ vs. control-EGFP treatment. **(B, C)** Representative images denoting proliferation ($KI67^+$) for **(B)** control and **(C)** N2-M1 treatment groups. For each set, the top panel of images shows staining for KI67 (red), DAPI (blue), and an overlay of images. Scale bars correspond to 25 micrometers. The bottom panels show magnified images corresponding to the boxed section in the above image. Arrows indicate a KI67 positive cell.

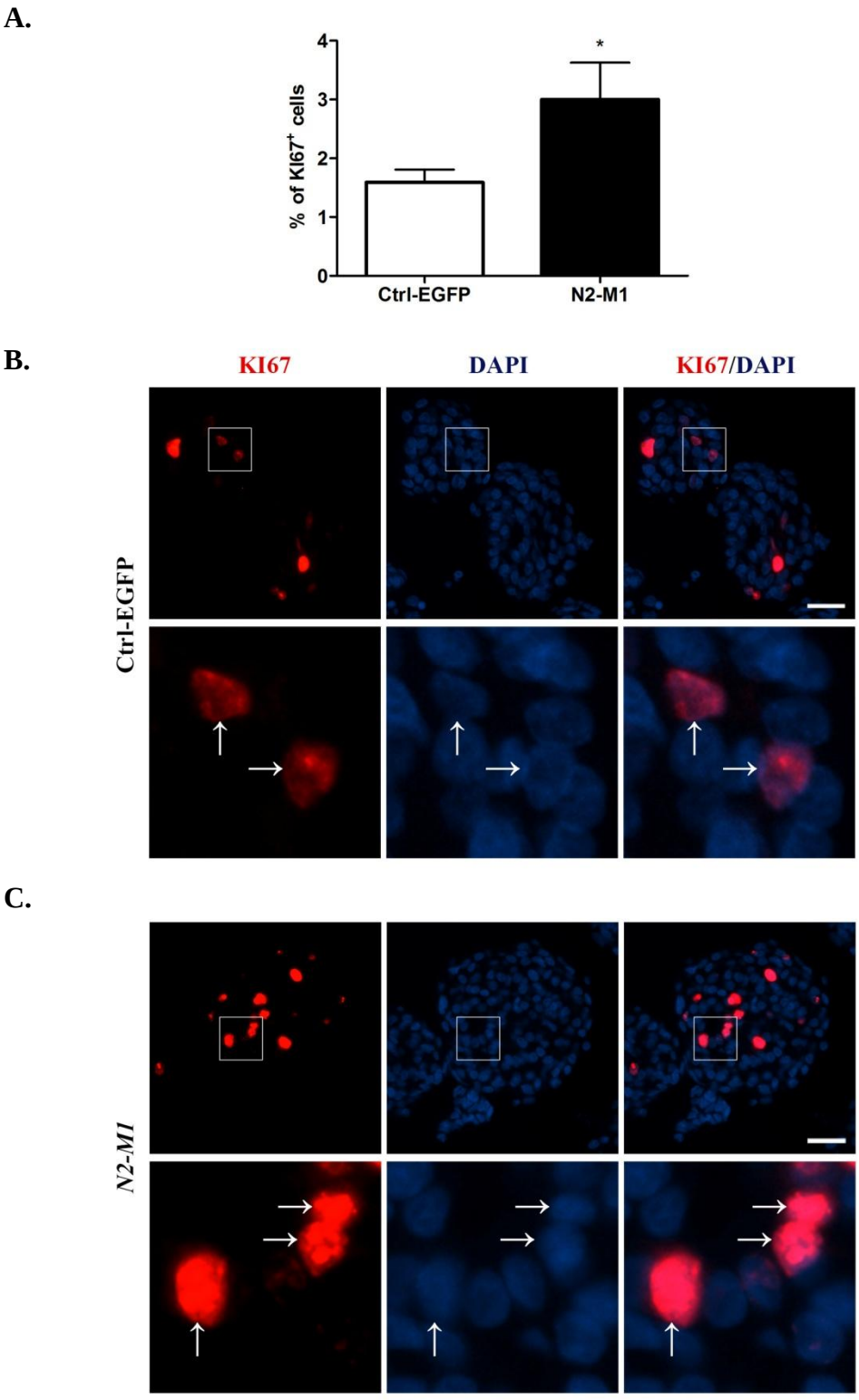
A.
% of KI67+ cells
4
3
2
1
0
*
Ctrl-EGFP
N2-M1
B.
KI67
DAPI
KI67/DAPI
Ctrl-EGFP
C.
N2-M1

Figure 3.20.

glucagon (**Figure 3.22A**) mRNA with qRT-PCR showed no changes in the N2-M1 treatment group when compared to the control group. Immunofluorescence staining techniques were employed for insulin (**Figure 3.21B, C**), glucagon (**Figure 3.22B, C**), somatostatin (**Figure 3.23A, B**), and pancreatic polypeptide (**Figure 3.23C, D**) expressing endocrine cells, all of which exhibited similar populations with menin overexpression compared to the control groups.

To elucidate by what means *MEN1* overexpression increases cellular proliferation, we analyzed the effect of N2-M1 transfection on cell cycle regulators similar to section 3.4. In this study, analysis of *p18*, *p21*, and *p27* mRNA showed no significant change with *MEN1* overexpression (**Supplementary Figure 5B**).

To further explore a function of menin within islet cell development and differentiation, various transcription factors which are critical for endocrine development were chosen and analyzed by qRT-PCR using *PDX1*, *SOX9*, *NGN3*, *NKX2.2*, and *NKX6.1* probes (**Figure 3.24**). Analysis of these results indicated consistent mRNA levels for *PDX1* and *NGN3*. Examination of *SOX9* revealed a significant 4.5 fold increase in *SOX9* mRNA expression with overexpression of menin. *NKX2.2* analysis displayed an increasing trend with N2-M1 transfection where p=0.0527 and *NKX6.1* mRNA expression also displayed an increasing trend but was highly variable.

3.8 **Menin Overexpression Improves Cell Survival Capabilities**

As previously mentioned, menin is involved in cell survival in many ways, two of which include roles in DNA repair and apoptosis. This functionality of menin was studied in islet-epithelial cells transfected with either a control-EGFP vector or a menin overexpression vector (N2-M1). Treated cells were exposed to a TUNEL labelling assay which displayed a significant reduction in the number of apoptotic labelled cells with N2-M1 treatment ($p<0.01$ vs. Ctrl-EGFP) (**Figure 3.25A**). This result was further verified by cleaved Caspase-3 analysis where immunofluorescence examination indicated a significant reduction in apoptosis (cleaved Caspase-3^+ cells) with N2-M1 transfection

($p<0.05$ vs. Ctrl-EGFP) (**Figure 3.25B**), validating the TUNEL results and demonstrating an improved cell survival with menin overexpression.

Figure 3.21. Effect of *MEN1* Overexpression on Insulin Expression.

Islet-epithelial cell clusters, isolated from human fetal pancreata 15 to 19 wks, were transfected with either a control (Ctrl-EGFP) or a *MEN1* (N2-M1) vector and cultured for 48 hrs. **(A)** qRT-PCR analysis of total insulin mRNA levels for control and N2-M1 treatments. Data were normalized to 18S rRNA and are expressed as means ± SEM where n=6 per experimental group. **(B, C)** Representative images of islet-epithelial cell clusters for **(B)** control or **(C)** N2-M1 treatment groups. Cells were harvested, paraffin-embedded, sectioned, and immunolabelled with an anti-insulin antibody visualized with a Cy3 (red) conjugated secondary antibody. Nuclei were labelled with DAPI (blue). For each set, the top panel of images shows staining for insulin (red), DAPI (blue), and an overlay of images. The bottom panels show magnified images corresponding to the boxed section in the above image. Scale bars correspond to 25 micrometers. Arrows indicate an insulin positive cell.

A.

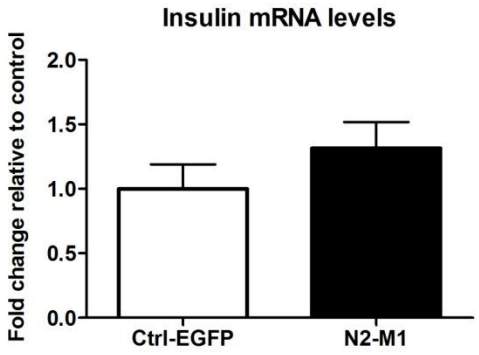

B.

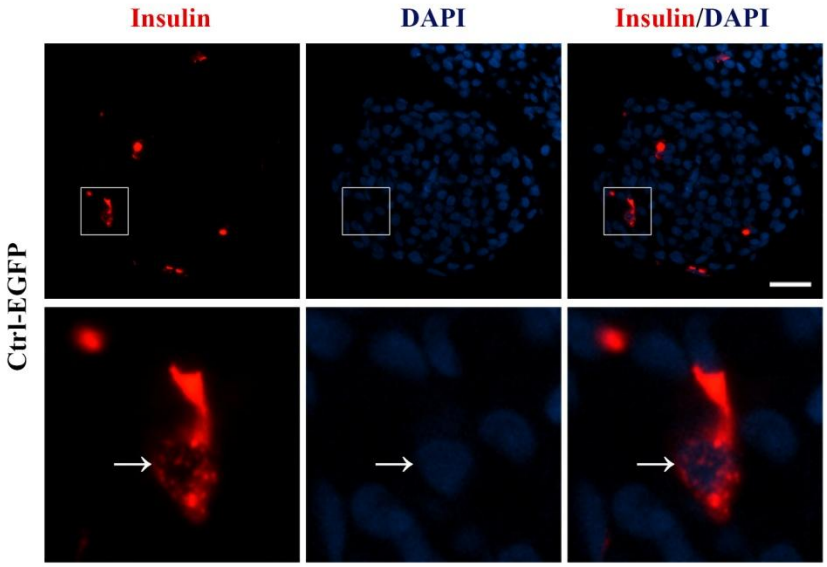

C.

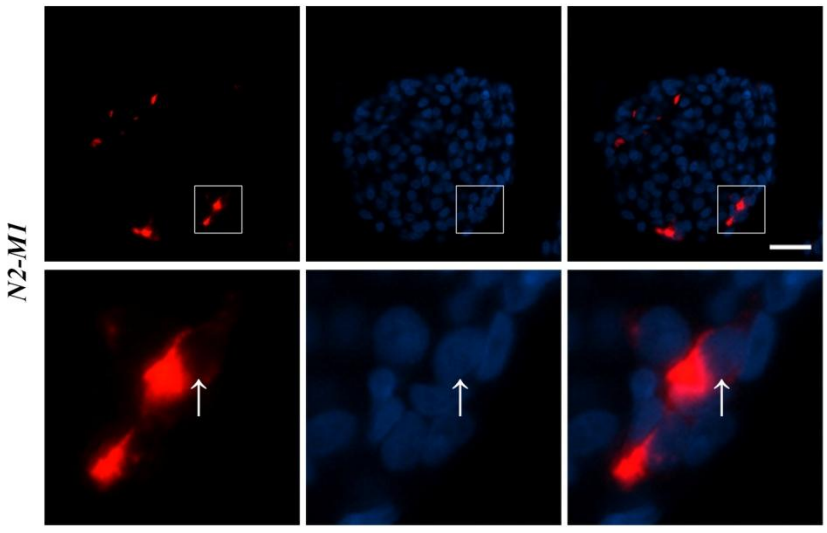

Figure 3.21.

Figure 3.22. Effect of *MEN1* Overexpression on Glucagon Expression.

Islet-epithelial cell clusters, isolated from human fetal pancreata 15 to 19 wks, were transfected with either a control (Ctrl-EGFP) or a *MEN1* (N2-M1) vector and cultured for 48 hrs. **(A)** qRT-PCR analysis of total glucagon mRNA levels for control and N2-M1 treatments. Data were normalized to 18S rRNA and are expressed as means ± SEM where n=6 per experimental group. **(B, C)** Representative images of islet-epithelial cell clusters for **(B)** control or **(C)** N2-M1 treatment groups. Cells were harvested, paraffin-embedded, sectioned, and immunolabelled with an anti-glucagon antibody visualized with a Cy3 (red) conjugated secondary antibody. Nuclei were labelled with DAPI (blue). For each set, the top panel of images shows staining for glucagon (red), DAPI (blue), and an overlay of images. The bottom panels show magnified images corresponding to the boxed section in the above image. Scale bars correspond to 25 micrometers. Arrows indicate a glucagon positive cell.

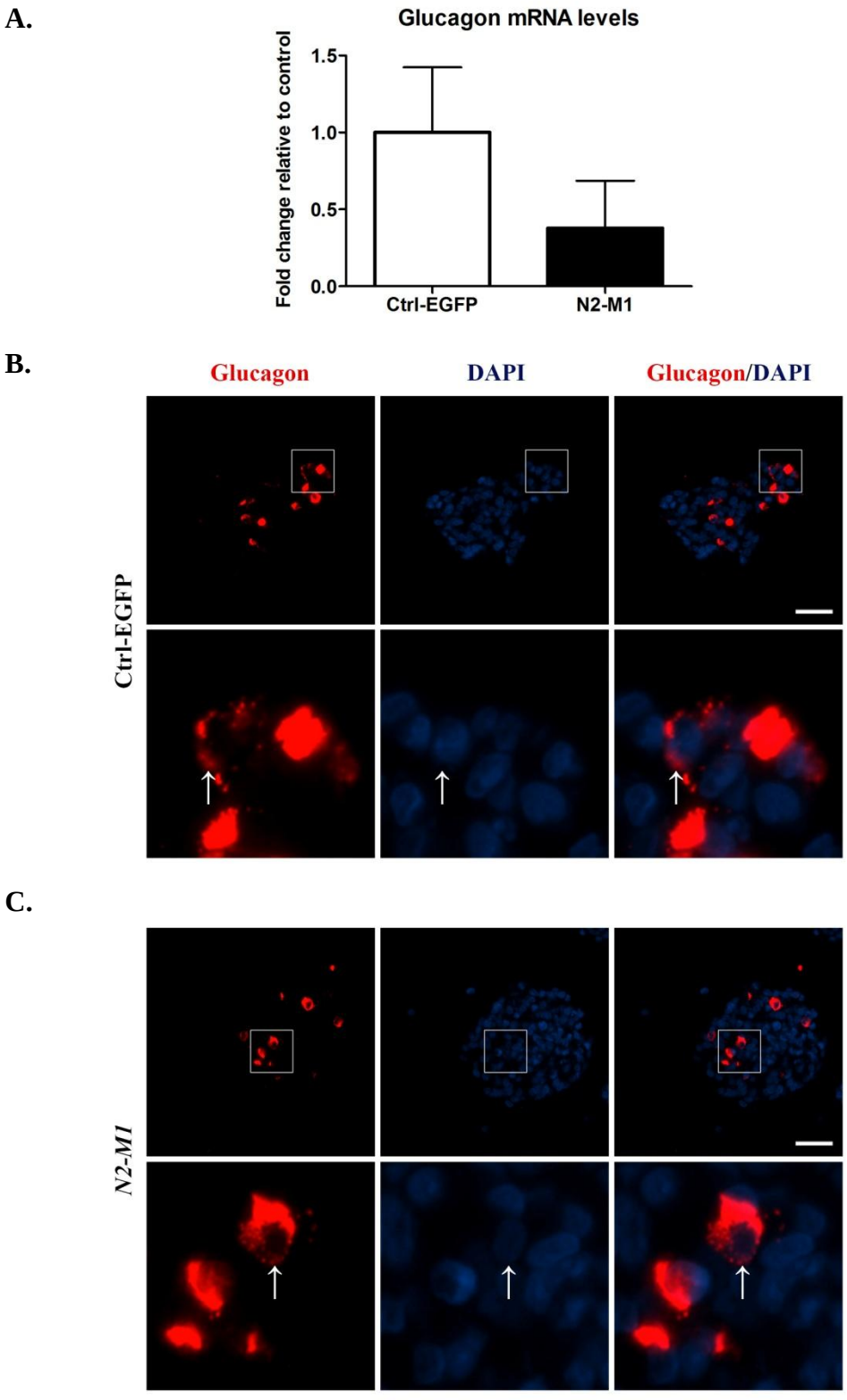
A.
Glucagon mRNA levels
Fold change relative to control
1.5
1.0
0.5
0.0
Ctrl-EGFP
N2-M1
B.
Glucagon
DAPI
Glucagon/DAPI
Ctrl-EGFP
C.
N2-M1

Figure 3.22.

Figure 3.23. Effect of *MEN1* Overexpression on Somatostatin and Pancreatic Polypeptide Expression.

Islet-epithelial cell clusters isolated from human fetal pancreata 15 to 19 wks were transfected with either a control (Ctrl-EGFP) or a *MEN1* (N2-M1) vector for a 48 hr treatment. Cells were harvested, paraffin-embedded, and sections were immunolabelled with an **(A, B)** anti-somatostatin antibody or **(C, D)** anti-pancreatic polypeptide (PP) antibody which were visualized with a Cy2 (red) conjugated secondary antibody. Nuclei were labelled with DAPI (blue). **(A, B)** Representative images of somatostatin^{+} cells for **(A)** control and **(B)** N2-M1 treatment groups. **(C, D)** Representative images of PP^{+} cells for **(C)** control and **(D)** N2-M1 treatment groups. For each set, the top panel of images shows staining for somatostatin or PP (red), DAPI (blue), and an overlay of images. The bottom panels show magnified images corresponding to the boxed section in the above image. Scale bars correspond to 25 micrometers. Arrows indicate a somatostatin^{+} or PP^{+} cell.

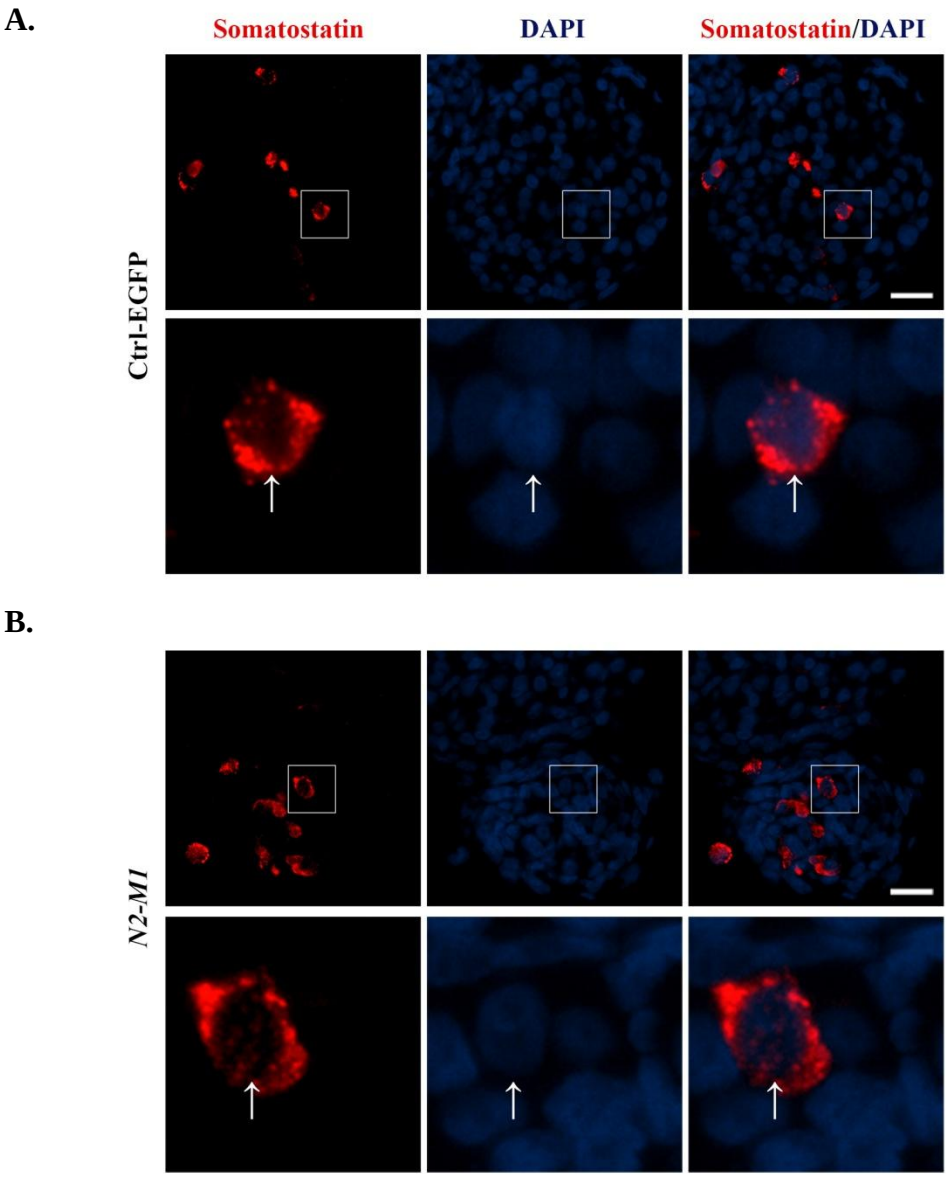

Figure 3.23.

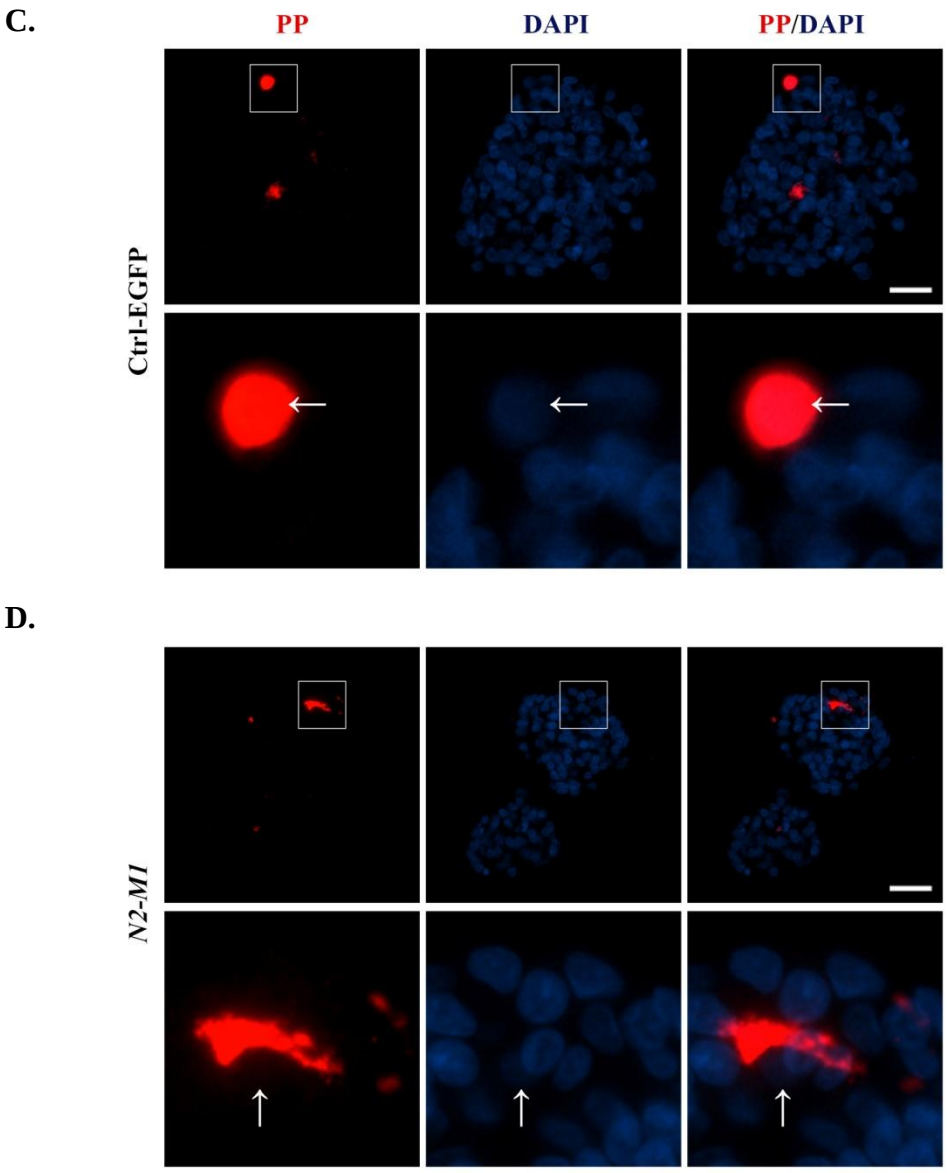

Figure 3.23.

Figure 3.24. Effect of *MEN1* Overexpression on Transcription Factors Essential for Endocrine Differentiation.

Islet-epithelial cell clusters, isolated from human fetal pancreata 15 to 19 wks, were transfected with either a control (Ctrl-EGFP) or a *MEN1* (N2-M1) vector and cultured for 48 hrs. For control (transparent bars) and N2-M1 (black bars) treatment groups, qRT-PCR analysis for *PDX1*, *SOX9*, *NGN3*, *NKX2.2*, and *NKX6.1* mRNA. Data were normalized to 18S rRNA and are expressed as means ± SEM where n=4-6 per experimental group, *$p<0.05$ vs. Ctrl-EGFP.

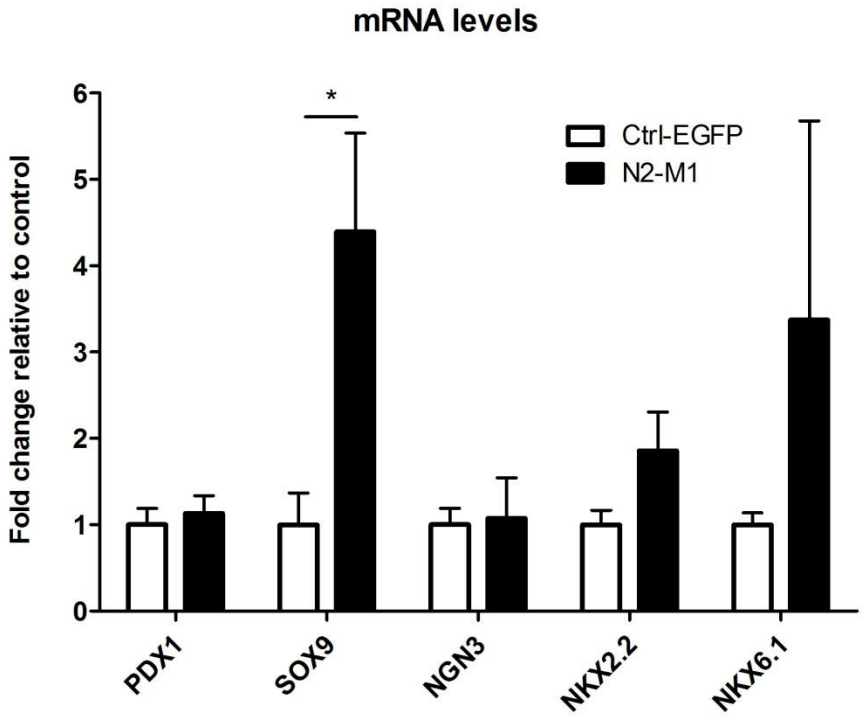
mRNA levels
Fold change relative to control
6
5
4
3
2
1
0
*
Ctrl-EGFP
N2-M1
PDX1
SOX9
NGN3
NKX2.2
NKX6.1

Figure 3.24.

Figure 3.25. Effect of *MEN1* Overexpression on Cell Death in Islet-Epithelial Cell Clusters.

Islet-epithelial cell clusters, isolated from human fetal pancreata 15 to 19 wks, were transfected with either a control (Ctrl-EGFP) or a *MEN1* (N2-M1) vector and cultured for 48 hrs. Cells were harvested, paraffin-embedded, and sections were immunolabelled with an anti-cleaved Caspase-3 antibody visualized with a Cy2 (green) conjugated secondary antibody or sections were TUNEL labelled (green). Nuclei were labelled with DAPI (blue). Quantitative analysis of the total number of **(A)** $TUNEL^{+}$ cells and **(B)** cleaved Caspase-3 $(cCaspase\text{-}3)^{+}$ cells relative to the total amount of cells present (TUNEL or cCaspase-3/DAPI, expressed as a percentage) for control and N2-M1 treatments. Data are expressed as means ± SEM. n=3. *$p<0.05$, **$p<0.01$ vs. Ctrl-EGFP treatment. Representative images denoting TUNEL labelling for **(C)** control and **(D)** N2-M1 treatment groups. For each set, the top panel of images shows staining for TUNEL (green), DAPI (blue), and an overlay of images. Scale bars correspond to 25 micrometers. The bottom panels show magnified images corresponding to the boxed section in the above image. Arrows indicate a TUNEL positive cell.

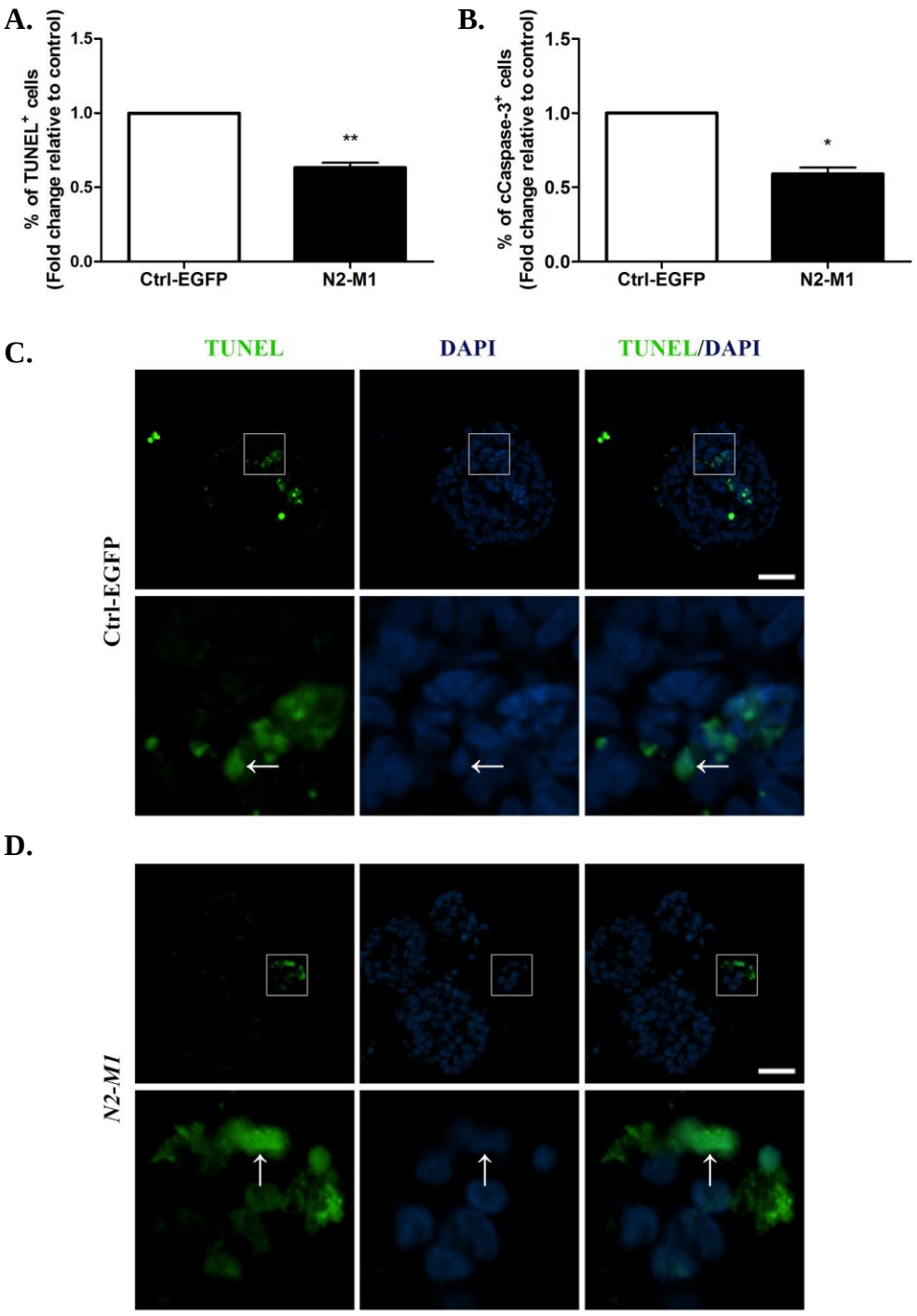
A.
% of TUNEL+ cells
(Fold change relative to control)
1.5
1.0
0.5
0.0
**
Ctrl-EGFP
N2-M1
B.
% of cCaspase-3+ cells
(Fold change relative to control)
1.5
1.0
0.5
0.0
*
Ctrl-EGFP
N2-M1
C.
TUNEL
DAPI
TUNEL/DAPI
Ctrl-EGFP
D.
N2-M1

Figure 3.25.

Chapter 4

Discussion

Chapter 4 – **Discussion**

The objective of this study was to examine the expression pattern and functional roles of menin during human fetal islet development through its association and interaction with other necessary transcription factors. Previous studies have shown Menin to be essential during murine pancreatic development, however little information is known regarding the expression of menin or its function during human fetal pancreatic development. From our knowledge within the murine species, I have hypothesized that menin is required for islet differentiation by regulating islet progenitor proliferation and the expression of NGN3 and other essential pancreatic transcription factors in the developing human pancreas. The expression pattern of menin and its function was elucidated by examining five questions using *ex vivo* and *in vitro* experimental techniques (see section 1.4 for a complete list of these 5 questions as described below). Initially, e*x vivo* techniques were employed using the whole human fetal pancreas revealing a consistent menin expression pattern within various cell types, and its co-localization with multiple transcription factors that are critical for pancreatic development. The developmental time period analyzed was from 8-21 wks of fetal age, a period characterized by major morphological changes of pancreatic and islet architecture (Lyttle et al., 2008). *In vivo* siRNA and overexpression studies were utilized to explore the function of menin, demonstrating roles for menin in maintenance of proliferation, transcription factor expression, and cell survival during human pancreatic development.

4.1 **What is the Spatial and Temporal Expression Pattern of Menin Throughout Human Pancreatic Development?**

By understanding the spatio-temporal distribution pattern of menin at differing stages in the development of the human pancreas, this allowed us to further deduce the role menin may be playing during islet cell development. To address the temporal expression of the *MEN1* gene, this study employed both mRNA and protein analysis techniques using pancreata collected during the 1st and 2nd trimester of pregnancy. Previously in our laboratory, microarray investigation of 8-21 wk human fetal pancreata revealed that

MEN1 is highly expressed relative to adult pancreatic islets and qRT-PCR experimental results have shown that *MEN1* is expressed consistently during human pancreatic development. Quantitative analysis of protein collected from whole fetal pancreata during this study showed that menin was indeed expressed at all time points from the 1st through the 2nd trimester at a relatively consistent amount. Expression studies of Menin within the developing mouse have reported that Menin expression begins at e7 (prior to pancreatic bud formation) within the majority of tissues and is expressed in the pancreas at e11.5 through e18.5 and into adulthood (Chandrasekharappa et al., 1997; Fontaniere et al., 2008; Stewart et al., 1998). This period from e11.5-e18.5 in the mouse is similar to the developmental window in our study as it describes a time from which the ductal tree is forming, with pancreatic buds predominately consisting of undifferentiated ductal epithelium and few single endocrine cells present, through to an almost fully formed pancreas with endocrine cells condensed into islet cell clusters (Habener et al., 2005). Therefore our temporal expression pattern of menin corresponds with the presence of menin described by Fontaniere and colleagues in 2008 from e11.5-e18.5. However, they did not perform quantification studies as we have provided in this study. To perform menin expression analysis we used mRNA and total protein collected from whole fetal human pancreata consisting of both cytoplasmic and nuclear fractions such that our results here were unable to reflect any such changes in the sub-cellular localization of menin throughout pancreatic development. To determine menin sub-cellular fluctuations, nuclear/cytoplasmic extraction techniques are needed. Nuclear menin expression was however present at all developmental stages studied because all localization studies and islet cell quantifications were performed using immunofluorescence techniques which focused on nMenin localization. This is because the nuclear fraction represents the active form of menin (Guru et al., 1998).

To determine the spatial distribution of menin expression throughout development, immunofluorescence co-localization was performed from 8-21 wks of fetal age. Results revealed expression within endocrine cells (insulin^{+}, glucagon^{+}, somatostatin^{+} cells), ductal cells (CK19^{+}), and in the exocrine (amylase^{+}) compartment at all time points studied. Morphometric analysis focused on quantifying the localization of menin throughout development within alpha, beta, and ductal cells. Ductal cells were analyzed

as they are the location of pancreatic progenitors, endocrine progenitors, and fully differentiated endocrine cells (before they migrate out into surrounding tissue) (Bouwens et al., 1997). Insulin^{+} and glucagon^{+} cells both showed a consistent high level of menin expression throughout development, and menin co-localization was significantly reduced within ductal cells during 14-16 wks compared to 8-12 wks. This may suggest that there is a change of requirement or function for menin at 14-16 wks, a period of increased differentiation and reduced proliferation. At 14-16 wks all epithelial cells, including endocrine cells, are CK19^{+}, and since there is no change in menin localization within endocrine cells, this ductal localization reduction may not be due to endocrine differentiation. The co-localization studies of menin with various transcription factors as well as functional knockdown and overexpression studies (which are discussed in the following sections) gives us more insight into the role of menin and its presence during endocrine differentiation. Cytoplasmic assessment as well as menin protein abundance within each cellular compartment was not taken into consideration in the current study. Future analysis such as cell sorting in combination with nuclear/cytoplasmic extraction techniques will allow for precise analysis of menin protein abundance and distribution within purified cell populations, and also within separate cellular compartments. Overall, these localization results show the expression of menin in all compartments of the pancreas during development and correspond with various studies during murine pancreatic development (at e16, e18) and within the fully developed adult pancreas of both humans and rodents (Cavallari et al., 2009; Fontaniere et al., 2008; Karges et al., 1999; Thakker, 1998). This cell type-independent menin expression leads us to postulate that menin may be involved in a global cellular function or pathway which is common to most cell types in the pancreas.

Our results outline the spatio-temporal distribution pattern of menin within the developmental window of 8-21 wks of fetal age. Due to ethical guidelines we were unable to confirm the expression of menin and its stability both within the pancreas as a whole and within pancreatic compartments prior to 8 wks during bud and initial endocrine progenitor development and following 21 wks during maturation up until birth. Studies using human stem cells differentiated into pancreatic endocrine cell lineages could give us more insight into the involvement of menin prior to 8 wks in the pancreas,

similar to the study performed by Zhang and colleagues using mouse embryonic stem cells (Zhang et al., 2011). Cell cultures could also be employed for studies post 21 wks, however this may prove difficult as we demonstrate the involvement of menin in apoptotic regulation (see sections 4.4 and 4.5).

4.2 What Developmental Transcription Factors are Co-localized with Menin in the Developing Human Fetal Pancreas?

To further elucidate at which stage of endocrine differentiation nuclear menin may be present and performing its function, we studied the co-expression of menin with various transcription factors that are critical throughout pancreatic development. Our results show co-localization with all transcription factors studied from 8-21 wks; PDX1, SOX9, ISL1, NGN3, NKX2.2, and NKX6.1. This suggests that menin is found within cells at each stage of the endocrine differentiation process, from pancreatic progenitors at 8 wks until the fully differentiated mature islets at 21 wks. During the period from 14-16 wks we observed an increase in nMenin/PDX1$^+$ co-localization within PDX1$^+$ cells. At this time point, PDX1$^+$ cells can be found within the ductal cell population as well as within newly-formed insulin$^+$ cells, such that PDX1 regulates insulin gene expression in this period where there is a significant increase in endocrine differentiation and pancreatic insulin content and secretion (Lyttle et al., 2008). Since PDX1 expression is consistent throughout development, the increase in nMenin within the 14-16 wk time point may not be involved in regulating PDX1, but may work in tandem with PDX1 and be involved in regulating endocrine initiating pathways within PDX1$^+$ cells at this time point. Previous studies have shown that Menin is present throughout the pancreatic epithelium from e11.5-e18.5 (a period similar to our time point 8-21 wks), specifically in Insulin, Glucagon, and ductal cells, suggesting that any transcription factor which localizes to these compartments, for example NGN3, must also express Menin. Also, studies using Pdx1-directed Cre knockdown of Menin confirm a co-localization, however most research focuses on the levels of transcription factor expression post Menin knockdown,

and thus the co-localization of menin with transcription factors have not been specifically addressed during fetal development (Shen et al., 2009).

Although immunofluorescence co-staining allows us to analyze the sub-cellular localization of each transcription factor with menin, our results focused on nuclear co-localization of menin with various nuclear transcription factors. Most transcription factors however (ie. NGN3), are also cytoplasmic (similar to menin) and so our results could not take into account a possible change in sub-cellular localization throughout development (Lejonklou et al., 2009). Some transcription factors (ie. PDX1 and SOX9) are also expressed in multiple cellular populations such that some populations express a higher or lower expression level of that specific transcription factor (Lyttle et al., 2008). For example SOX9 is highly expressed in pancreatic progenitors and its expression decreases as endocrine cells mature such that during our analysis there were SOX9 high- and SOX9 low-expressing cells (McDonald et al., 2012). Immunofluorescence techniques were held stable with consistent analysis parameters to account for any discrepancy in sub-cellular localization or alterations in expression intensity, however techniques involving cell sorting and nuclear/cytoplasmic extraction could provide more accurate and detailed co-localization and quantification results.

4.3 **What is the Relationship Between Proliferating Cells and Menin$^+$ Cells in the Developing Human Fetal Pancreas?**

The relationship of menin and proliferating (KI67$^+$) cells was initially assessed throughout development using double-immunofluorescence staining of *ex vivo* pancreatic sections from 8-21 wks of fetal age. Our results showed that the proliferation capacity of nMenin$^+$ cells decreased as development progressed. This result was not unexpected as Bouwens et al., 1997, noted an overall pancreatic decrease in KI67$^+$ labelling index from 8-41 wks. Specifically, they demonstrated a decrease in proliferation of ductal, insulin, glucagon, and synaptophysin (a non-specific endocrine marker) positive cells (Bouwens et al., 1997). We also showed that approximately 80% of all proliferating cells in the pancreas also express nMenin and that this is significantly reduced at 18-21 wks. This

data suggests that menin may not be functioning as a tumour suppressor from 8-16 wks of fetal age since proliferation of pancreatic cells is optimal early in development (Bouwens et al., 1997). A reduction in co-localization at 18-21 wks may indicate that the role of menin in proliferation may change between the 14-16 wks and 18-21 wk time points as islets develop the adult-like phenotype. In the adult pancreas, menin functions as a tumour suppressor such that a knockdown of menin produces endocrine and ductal cell tumours, as well as an increase in beta-cell mass during compensatory situations such as obesity and pregnancy (Cavallari et al., 2009; Chandrasekharappa et al., 1997; Karnik et al., 2007). Therefore as beta-cells become adult-like and their proliferation decreases, menin may be involved in repressing proliferation after the phase of endocrine differentiation in mature islets (Bouwens et al., 1997; Lyttle et al., 2008). A difference of function for menin between fetal development and adulthood has been suggested for osteoblast differentiation, as well as during development of the heart, CNS, liver, and pancreas (Bertolino et al., 2003a; Fontaniere et al., 2008; Sowa et al., 2004). A study involving cells, possibly cell cultures, prior to 8 wks and post 21 wks could confirm this hypothesis, as ethical reasons halted us from obtaining primary cells at these time points. Also, our results were only able to indicate the presence of menin in the overall proliferation pool during development. Cell sorting techniques isolating certain cell populations (i.e. GLUT1 surface marker for beta-cells) and subsequent immunofluorescence staining could indicate if there may be any change in the expression of menin within proliferating cells of a certain cell population throughout development, as well as detecting any change between cell populations.

4.4 **Does Downregulation of *MEN1* in Islet-Epithelial Cell Clusters Affect Endocrine Cell Proliferation and Differentiation?**

To analyze the function of menin during endocrine differentiation, *MEN1* knockdown was performed using *MEN1* siRNA transfection in islet-epithelial cell clusters 15-19 wks of fetal age. With time-dependent trials, we determined that a 48 hr siRNA incubation

was the optimal time for *MEN1* and nMenin knockdown, therefore subsequent functional analysis trials were performed at this time point.

Since mutation in the *MEN1* gene results in the multiple endocrine neoplasia type 1 disease, menin has been characterized as a tumour suppressor where its main function is to suppress proliferation in adult endocrine tissues. Using a knockdown strategy we sought to determine if menin still functions as a tumour suppressor during endocrine differentiation in the human fetal pancreas. Our *ex vivo* results of menin co-localization within $KI67^+$ cells (as discussed in section 4.3) indicate that menin may not function to suppress proliferation during endocrine differentiation (14-16 wks) and that this function may change as endocrine cells mature. *MEN1*-siRNA-mediated knockdown results revealed a significant decrease in proliferation levels of islet-epithelial cell clusters at 15-19 wks (compared to control siRNA). These results coincide with our *ex vivo* results but are in sharp contrast to the function of menin within the adult pancreas. This change in function between development and adulthood would not be out of the ordinary as other proteins such as tumour suppressor, Rb, have been shown to be required during normal retinal development (Fontaniere et al., 2008). Our next step was to determine which endocrine cell populations were experiencing a reduction in proliferation after menin silencing and how this affected their overall total cell population. Our results indicated that menin had no effect on the proliferation capacity of $insulin^+$ cells, the expression of insulin mRNA, or the total number of $insulin^+$ cells. Our results also indicated that a reduction in menin resulted in a significant decline in the proliferation capacity of $glucagon^+$ cells. Data published by Lyttle et al in 2008 demonstrated that alpha-cell (not beta-cell) proliferation was significantly increased during the 2^{nd} trimester. This may explain why menin affected glucagon-cell proliferation only, the specificity to alpha-cells is because the increase in beta-cell mass at this stage of development is mostly due to differentiation from endocrine precursors. Although our results showed a reduction in alpha-cell proliferation, there were no changes in glucagon mRNA expression or the number of $glucagon^+$ cells. It may be possible that a reduction in proliferation results in an increase in differentiation (from pancreatic or endocrine precursor cells) as a compensatory mechanism to maintain normal alpha-cell numbers. Menin may therefore be functioning to regulate the transition from proliferation to differentiation. Many

studies have implicated menin-interacting partners and menin-regulatory proteins in the regulation of the proliferation to differentiation transition in a variety of tissues. Examples of these proteins are p27, CDK 4 and 6, JunD, members of Wnt/β-catenin, ERK1/2, and NFκB pathways (via RunX2) (Andreu-Perez et al., 2011; Hara et al., 2011; Kaji et al., 2009; Lim and Kaldis, 2012; Naito et al., 2005; Wei et al., 2011). Menin may thus be involved in regulating alpha-cell proliferation and differentiation exclusively.

To determine the mechanism by which menin represses proliferation, we analyzed the expression of cell-cycle regulators, p18, p21, and p27, as well as members of both the Wnt/β-catenin and the PI3K/AKT pathways. None of these were altered with *MEN1* knockdown, therefore menin must be regulating proliferation through alternative pathways. A microarray of *MEN1* knockdown cells with various essential pancreatic differentiation probes could be an alternative to determine multiple gene expression changes associated with a reduction of menin. Although immunofluorescence staining was also performed for somatostatin$^+$ and PP$^+$ endocrine cells, quantification of proliferation capacity and the total cell population count was not analyzed. Due to the low percentage of somatostatin- and PP-cells within the pancreas itself, the number of these cells within islet-cell clusters was minimal, and so a representative quantification would not be possible. However, upon observation there were no obvious changes in somatostatin- or PP-cell populations with *MEN1* knockdown. One could combine samples such that one would have a representative number of somatostatin- and PP-cells to overcome this barrier, however due to restrictions on sample availability we were unable to do this therefore no results were obtained and we decided to focus on the alpha- and beta-cell differentiation process from progenitor cells.

To confirm if menin is involved in differentiation and to determine where menin may be functioning within the transcription factor network, we analyzed factors critical in progenitor pool maintenance and endocrine differentiation. There was a slight decrease but no significant change in the levels of *PDX1* mRNA or the PDX1$^+$ cell population. This suggests that menin may act downstream of PDX1. Interestingly, *SOX9* mRNA level was significantly decreased with *MEN1* knockdown, but the overall level of SOX9 protein expression was unaltered. It is possible that a reduction in mRNA has not yet

affected the protein level, and a longer period of siRNA treatment might be necessary for *SOX9* mRNA reduction and for reduction of overall protein expression. NGN3, the major regulator of endocrine differentiation for all endocrine cell lines, was analyzed and there may be a slight increase but no significant change in *NGN3* mRNA or the number of $NGN3^{+}$ expressing cells with menin knockdown (Lyttle et al., 2008). Two downstream genes of NGN3 were significantly reduced with *MEN1* knockdown. These were *NKX2.2* and *NKX6.1*, genes critical for alpha- and beta-cell differentiation (Lyttle et al., 2008). *HES1*, a gene expressed during exocrine pancreas development was also analyzed showing no alteration in mRNA expression. This was expected as previous research in cultured *Men1* null cells showed that menin, although present in exocrine cells, was not involved in exocrine pancreas development (Fontaniere et al., 2008). Overall, our analyses of critical transcription factors reveal that menin promotes *SOX9*, *NKX2.2*, and *NKX6.1* expression, but does not affect *PDX1*, *NGN3*, and *HES1* expression. These results suggest that menin is involved in preserving the progenitor pool and promoting normal expression of endocrine differentiation markers.

Another function of menin during adulthood is regulation of apoptosis. Within adult tissues menin has been shown to regulate apoptosis in a variety of ways through promoting DNA repair and chromosome stability pathways, but also by promoting cell death through the Caspase-8 cascade (Gallo et al., 2010; La et al., 2007). In human fetal development we have shown that a knockdown of menin increases overall cell death and the cleaved Caspase-3 cascade. These results indicate that during development menin is functioning to suppress apoptosis. The method through which menin is promoting cell survival in fetal tissues has yet to be determined, but we can conclude that it may not be functioning to promote the caspase cascade as in adult pancreatic tissues. These results correspond with *Men1* null pancreata which show an increase in apoptosis with menin knockdown at e12.5, suggesting that menin promotes cell survival of endocrine progenitors (Fontaniere et al., 2008).

Our results correspond with some studies, though there are also some differences. *Men1* global knockout mice die in utero suggesting a requirement of menin in differentiation, specifically the differentiation of early pancreatic endocrine cells. Cultured *Men1* null

pancreatic cells also suggest that menin is required during the major wave of endocrine differentiation, and that this function may be through NGN3 regulation. We did not see an overall decrease in insulin or glucagon cells as the null mouse pancreata indicates, but our results confirm that menin is required for normal endocrine differentiation. Our *MEN1* knockdown cultures did not display any significant alterations in *NGN3* mRNA or the number of NGN3 producing cells, but one cannot dismiss the fact that there may have been an overall change in NGN3 protein expression within each cell. Nuclear/cytoplasmic extraction techniques with subsequent western blotting would be able to quantify and determine the nuclear expression of NGN3. We did see aberrant transcription factor expression with menin knockdown and the precise effect of this has yet to be determined. There may be a reduction in other endocrine cells that we are not able to quantify due to sample quantity limitations or an alteration in the functionality of differentiated endocrine cells. For example, *Nkx2.2* knockout mice display aberrant endocrine differentiation with an increasing production of Ghrelin-producing endocrine cells to compensate for the lack of beta-cells (Prado et al., 2004). As well, studies show lack of Nkx2.2 expression in mature endocrine cells results in reduced insulin expression, pancreatic insulin content, and insulin secretion (Doyle and Sussel, 2007). Our results do not show a change in insulin expression, however should these cells be allowed to propagate further with a reduction in menin, one might observe this result. Further propagation could be achieved if menin did not have such an effect on apoptosis and would also require sustained menin reduction, obtained by using shRNA constructs instead of siRNA–mediated transient knockdown. Also, no change in insulin mRNA or the number of insulin$^+$ cells does not necessarily mean there may not be a change in the insulin content and density of the insulin granules in the cells. One could quantify this by determining the total insulin intensity in sections from immunofluorescence staining and comparing knockdown and control treatment groups. Differentiated *Men1* null embryonic stem cells into EBs did show some additional similarities to our results. This EB study, by Zhang and colleagues in 2011, indicated that menin knockdown may preferentially initiate differentiation at an earlier time point along the endodermal pathway and reduce Nkx2.2 expression. Our results showing reduction in glucagon proliferation, with a normal quantification of the glucagon$^+$ cell population in *MEN1*-

siRNA-treated cells, suggest that similar to null EBs, menin promotes proliferation and represses differentiation (Zhang et al., 2011). This hypothesis came from the fact that when proliferation is reduced in stem cells, they transition to differentiation. For example, this transition is seen within neural stem cells with *CDK2* and *CDK4* knocked out but not within differentiated MEFs (mouse embryonic fibroblasts) (Lim and Kaldis, 2012). Our results with partially-differentiated pancreatic cells may not show this effective transition to differentiation with a reduction in proliferation. Our transcription factor study suggests that menin may be promoting differentiation by promoting the expression of *SOX9, NKX2.2,* and *NKX6.1*. Thus, the involvement of menin in promoting glucagon$^+$ cell proliferation may be a separate function from differentiation within the partially-differentiated pancreatic epithelium at 15-19 wks.

The effect of SOX9 repression could account for some of the alterations that we see in our *MEN1* knockdown cell cultures. Pancreatic specific *Sox9*-inactivated mouse embryos showed a reduction in progenitor pool proliferation and cell survival; a phenomenon seen within our results indicating that the reduction in proliferation and cell survival may be within the progenitor pool (Seymour et al., 2007). Subsequent studies could determine the proliferation capacity of SOX9$^+$ cells with menin knockdown and which cell type are representative of the increase in cell death. SOX9 has been shown in the murine and human fetal pancreas to be required in proliferation, and during endocrine neogensis SOX9 promotes differentiation by binding to and regulating the NGN3 promoter and regulation of downstream transcription factors (ie. NKX6.1) (McDonald et al., 2012; Seymour et al., 2008). Within our results the knockdown in *SOX9* may also be responsible for the reduction in differentiation markers *NKX2.2* and *NKX6.1,* although we did not see a reduction in *NGN3* mRNA or the number of NGN3$^+$ cells. However as stated previously, the protein expression within each cell may be altered, or the *NGN3* promoter may be regulated by other proteins such that this SOX9-induced repression is masked by some other compensatory mechanism. SOX9 is also involved in a variety of other processes during human fetal development, such that haploinsufficiency of SOX9 (beginning at 14 weeks of gestation) results in campomelic dysplasia. Patients with this disorder at birth display less densely-packed epithelial cells within the mesenchymal stroma along with islets that are less clearly formed with variable expression of hormone

and beta-cell markers. We did not see an observable difference in islet packing density (with DAPI florescence staining), but we did see variable beta-cell markers with *MEN1* knockdown. Overall, SOX9 is a key player in all of our results showing changes in proliferation, cell survival, and the transcription factor cascade.

A knockdown of *Nkx6.1* in murine pancreata results in reduced beta-cell differentiation with normal development of other endocrine cell fates, and no difference in exocrine development such that Nkx6.1 may function downstream of NKX2.2 to affect only beta-cells (Sander et al., 2000). In the human fetal pancreas NKX6.1 is highly expressed in beta-cells only, with only a very low expression density within ductal cells, suggesting that NKX6.1 is required in beta-cell differentiation exclusively (Lyttle et al., 2008). We did see a reduction in *NKX6.1* during menin knockdown but no effects were seen on beta-cell quantification. Another function of NKX6.1 includes its involvement in suppressing the alpha- to beta-cell transition as well as islet proliferation and glucose-stimulated insulin secretion in the mature adult pancreas. Further studies could be performed to see how *MEN1* knockdown affects other aspects of NKX6.1 function, such as a possible alpha- to beta-cell transition within development and an effect on insulin secretion as beta-cells become mature and fully differentiated.

The presence of MEN1 disease characteristics and the lack of developmental defect in Menin heterozygous mice and beta-cell specific Menin knockout mice may be due to a threshold effect of Menin expression. Within our results we obtained about a 40-50% knockdown of menin compared to control siRNA treated islet-epithelial cell clusters and so we observed a developmental effect and requirement for menin in human fetal pancreatic development. Heterozygous *Men1* mice displayed normal menin expression within islets and it was hypothesized that the reduction in menin expression by 50% at 9 months of age was the cause of increasing islet hyperplasia, a resulting menin dosage effect (Crabtree et al., 2001). Beta-cell-specific menin knockdown mice were the result of Insulin- and Pdx1-directed Cre recombination and presented with MEN1 disease characteristics at 2 and 3 months respectively with no change in pancreatic development (Bertolino et al., 2003b; Shen et al., 2009). In the Insulin-directed Cre model, menin was excised beginning at e11 but no data demonstrated menin protein depletion until

hyperplastic islets were analyzed at 2 m. Only 3 out of 11 beta-cell knockout mice displayed menin depletion and hyperplasia at 2 months of age (Bertolino et al., 2003b). This indicates that there must be a dosage response to menin expression or that there may have been Cre-mediated gene disruptions among targeted cells during embryonic development for both Insulin- and Pdx1-directed Cre recombination (Fontaniere et al., 2008). Together, our results confirm a dose dependence threshold effect for the effect of menin on pancreatic development.

In summary, menin knockdown results indicate that menin is required in the developing human fetal pancreas where it functions to promote pancreatic proliferation, differentiation of endocrine cells (or promote alterations in the cascade of endocrine differentiation), and promotes cell survival. Menin would thus exhibit its function within the pancreatic progenitor pool ($SOX9^+$ cells) and also within endocrine progenitors downstream of NGN3 (but upstream of NKX2.2 and NKX6.1). This is a different function of menin compared to its anti-tumourigenic role in the fully development endocrine pancreas. The requirement of menin has been implicated in a number of murine developmental studies (not just pancreatic development) and we believe this is the first time menin has been shown to be a requirement for normal human fetal endocrine development.

4.5 **Does Overexpression of *MEN1* in Islet-Epithelial Cell Clusters Affect Endocrine Cell Proliferation and Differentiation?**

To confirm our results found with *MEN1* knockdown, we took a complementary approach in which we overexpressed *MEN1* within islet-epithelial cell clusters of the same time point, 15-19 wks, derived from isolated human fetal pancreata. Experimental analysis of *MEN1* overexpression (termed N2-M1 treatment) on the proliferation capacity of islet-cell clusters revealed that menin promoted islet proliferation. qRT-PCR techniques showed that there was no change in insulin or glucagon expression, and upon observation only there were no apparent changes in endocrine (insulin, glucagon, somatostatin, or PP) cell population levels. However a more in-depth study and

quantification of each cell population level, as well as their proliferation capacity, could be performed in future studies. Cell sorting techniques as well as nuclear/cytoplasmic extractions could give a more precise measurement of their proliferation capacity, gene and hormone expression levels. The mRNA levels of cell cycle regulators, *p18*, *p21*, and *p27*, showed no change with N2-M1 treatment; thus along with the *MEN1* knockdown studies, one can conclude that menin may not elicit its pancreatic functions by regulating these cell cycle genes. Analysis of transcription factors which are critical for endocrine differentiation revealed similar implications for menin as in our *MEN1* knockdown experiments. There was no change in the levels of *PDX1* or *NGN3* mRNA, but there was a significant increase in *SOX9* mRNA, an increase in NKX2.2 ($p=0.527$), and an increasing trend of NKX6.1, although this marker was highly variable. These results indicate an inherent requirement for menin during development for normal endocrine differentiation. Overexpression of *MEN1* also showed an improvement in cell survival capabilities of islet-epithelial cell clusters with reduced TUNEL labelling and reduced cleaved Caspase-3. No study to our knowledge has been done to up-regulate menin within pancreatic development, although numerous studies of menin within adult tissues have been performed to elucidate its function within adult tissues. As it has been discussed in section 4.4, our results indicate that menin is required during fetal endocrine development and its function differs from its anti-tumourigenic properties within the mature adult pancreas. Overall, these results confirm the requirement of menin during human fetal pancreatic development whereby menin functions to promote endocrine progenitor proliferation, differentiation and cell survival.

4.6 **Conclusion and Future Direction**

In summary, this study uses two complementary methods of *MEN1* knockdown and *MEN1* overexpression to provide evidence suggesting that menin is required for normal endocrine differentiation within the human fetal pancreas. Our results indicate that menin positively regulates pancreatic proliferation, cell survival, and normal islet differentiation. Menin is therefore important within the islet progenitor pool, and also

elicits its function in differentiation post-NGN3 expression, but before NKX2.2 and NKX6.1 expression. Some potential future studies have been addressed earlier within the discussion and alternative future studies may include determining which cell population is apoptotic, examining where exactly menin exerts its role in differentiation within the transcription factor cascade, and looking at which interacting partners or pathways menin performs its functions in proliferation, cell survival, and differentiation.

References

Chapter 5 – **References**

Agarwal, S.K., Guru, S.C., Heppner, C., Erdos, M.R., Collins, R.M., Park, S.Y., Saggar, S., Chandrasekharappa, S.C., Collins, F.S., Spiegel, A.M., *et al.* (1999). Menin interacts with the AP1 transcription factor JunD and represses JunD-activated transcription. Cell *96*, 143-152.

Agarwal, S.K., Mateo, C.M., and Marx, S.J. (2009). Rare germline mutations in cyclin-dependent kinase inhibitor genes in multiple endocrine neoplasia type 1 and related states. J Clin Endocrinol Metab *94*, 1826-1834.

Agarwal, S.K., Novotny, E.A., Crabtree, J.S., Weitzman, J.B., Yaniv, M., Burns, A.L., Chandrasekharappa, S.C., Collins, F.S., Spiegel, A.M., and Marx, S.J. (2003). Transcription factor JunD, deprived of menin, switches from growth suppressor to growth promoter. Proc Natl Acad Sci U S A *100*, 10770-10775.

Al-Masri, M., Krishnamurthy, M., Li, J., Fellows, G.F., Dong, H.H., Goodyer, C.G., and Wang, R. (2010). Effect of forkhead box O1 (FOXO1) on beta cell development in the human fetal pancreas. Diabetologia *53*, 699-711.

Anderson, K.R., White, P., Kaestner, K.H., and Sussel, L. (2009). Identification of known and novel pancreas genes expressed downstream of Nkx2.2 during development. BMC Dev Biol *9*, 65.

Andreu-Perez, P., Esteve-Puig, R., de Torre-Minguela, C., Lopez-Fauqued, M., Bech-Serra, J.J., Tenbaum, S., Garcia-Trevijano, E.R., Canals, F., Merlino, G., Avila, M.A., *et al.* (2011). Protein arginine methyltransferase 5 regulates ERK1/2 signal transduction amplitude and cell fate through CRAF. Sci Signal *4*, ra58.

Balogh, K., Patocs, A., Hunyady, L., and Racz, K. (2010). Menin dynamics and functional insight: take your partners. Mol Cell Endocrinol *326*, 80-84.

Balogh, K., Racz, K., Patocs, A., and Hunyady, L. (2006). Menin and its interacting proteins: elucidation of menin function. Trends Endocrinol Metab *17*, 357-364.

Bertolino, P., Radovanovic, I., Casse, H., Aguzzi, A., Wang, Z.Q., and Zhang, C.X. (2003a). Genetic ablation of the tumor suppressor menin causes lethality at mid-gestation with defects in multiple organs. Mech Dev *120*, 549-560.

Bertolino, P., Tong, W.M., Herrera, P.L., Casse, H., Zhang, C.X., and Wang, Z.Q. (2003b). Pancreatic beta-cell-specific ablation of the multiple endocrine neoplasia type 1 (MEN1) gene causes full penetrance of insulinoma development in mice. Cancer Res *63*, 4836-4841.

Biondi, C.A., Gartside, M.G., Waring, P., Loffler, K.A., Stark, M.S., Magnuson, M.A., Kay, G.F., and Hayward, N.K. (2004). Conditional inactivation of the MEN1 gene leads to pancreatic and pituitary tumorigenesis but does not affect normal development of these tissues. Mol Cell Biol *24*, 3125-3131.

Blasco, M.A. (2005). Telomeres and human disease: ageing, cancer and beyond. Nat Rev Genet *6*, 611-622.

Bouwens, L., Lu, W.G., and De Krijger, R. (1997). Proliferation and differentiation in the human fetal endocrine pancreas. Diabetologia *40*, 398-404.

Brandi, M.L., Gagel, R.F., Angeli, A., Bilezikian, J.P., Beck-Peccoz, P., Bordi, C., Conte-Devolx, B., Falchetti, A., Gheri, R.G., Libroia, A., *et al.* (2001). Guidelines for diagnosis and therapy of MEN type 1 and type 2. J Clin Endocrinol Metab *86*, 5658-5671.

Cabrera, O., Berman, D.M., Kenyon, N.S., Ricordi, C., Berggren, P.O., and Caicedo, A. (2006). The unique cytoarchitecture of human pancreatic islets has implications for islet cell function. Proc Natl Acad Sci U S A *103*, 2334-2339.

Cao, Y., Liu, R., Jiang, X., Lu, J., Jiang, J., Zhang, C., Li, X., and Ning, G. (2009). Nuclear-cytoplasmic shuttling of menin regulates nuclear translocation of {beta}-catenin. Mol Cell Biol *29*, 5477-5487.

Cavallari, I., Silic-Benussi, M., Rende, F., Martines, A., Fogar, P., Basso, D., Vella, M.D., Pedrazzoli, S., Herman, J.G., Chieco-Bianchi, L., *et al.* (2009). Decreased expression and promoter methylation of the menin tumor suppressor in pancreatic ductal adenocarcinoma. Genes Chromosomes Cancer *48*, 383-396.

Chandrasekharappa, S.C., Guru, S.C., Manickam, P., Olufemi, S.E., Collins, F.S., Emmert-Buck, M.R., Debelenko, L.V., Zhuang, Z., Lubensky, I.A., Liotta, L.A., *et al.* (1997). Positional cloning of the gene for multiple endocrine neoplasia-type 1. Science *276*, 404-407.

Chen, G., A, J., Wang, M., Farley, S., Lee, L.Y., Lee, L.C., and Sawicki, M.P. (2008). Menin promotes the Wnt signaling pathway in pancreatic endocrine cells. Mol Cancer Res *6*, 1894-1907.

Chen, L., Magliano, D.J., and Zimmet, P.Z. (2012). The worldwide epidemiology of type 2 diabetes mellitus--present and future perspectives. Nat Rev Endocrinol *8*, 228-236.

Cleaver, O., MacDonald, R. J. (2010). Developmental Molecular Biology of the Pancreas. In Pancreatic Cancer, J.P. Neoptolemos, Urrutia, R., Abbruzzese, J. L., Bu¨chler, M. W., ed. (Springer Science+Business Media, LLC), pp. 71-117.

Crabtree, J.S., Scacheri, P.C., Ward, J.M., Garrett-Beal, L., Emmert-Buck, M.R., Edgemon, K.A., Lorang, D., Libutti, S.K., Chandrasekharappa, S.C., Marx, S.J., *et al.* (2001). A mouse model of multiple endocrine neoplasia, type 1, develops multiple endocrine tumors. Proc Natl Acad Sci U S A *98*, 1118-1123.

Donath, M.Y., and Halban, P.A. (2004). Decreased beta-cell mass in diabetes: significance, mechanisms and therapeutic implications. Diabetologia *47*, 581-589.

Doyle, M.J., and Sussel, L. (2007). Nkx2.2 regulates beta-cell function in the mature islet. Diabetes *56*, 1999-2007.

Dreijerink, K.M., Hoppener, J.W., Timmers, H.M., and Lips, C.J. (2006a). Mechanisms of disease: multiple endocrine neoplasia type 1-relation to chromatin modifications and transcription regulation. Nat Clin Pract Endocrinol Metab *2*, 562-570.

Dreijerink, K.M., Mulder, K.W., Winkler, G.S., Hoppener, J.W., Lips, C.J., and Timmers, H.T. (2006b). Menin links estrogen receptor activation to histone H3K4 trimethylation. Cancer Res *66*, 4929-4935.

Escarcega, R.O., Fuentes-Alexandro, S., Garcia-Carrasco, M., Gatica, A., and Zamora, A. (2007). The transcription factor nuclear factor-kappa B and cancer. Clin Oncol (R Coll Radiol) *19*, 154-161.

Fontaniere, S., Duvillie, B., Scharfmann, R., Carreira, C., Wang, Z.Q., and Zhang, C.X. (2008). Tumour suppressor menin is essential for development of the pancreatic endocrine cells. J Endocrinol *199*, 287-298.

Francis, J., Lin, W., Rozenblatt-Rosen, O., and Meyerson, M. (2011). The menin tumor suppressor protein is phosphorylated in response to DNA damage. PLoS One *6*, e16119.

Gallo, A., Agnese, S., Esposito, I., Galgani, M., and Avvedimento, V.E. (2010). Menin stimulates homology-directed DNA repair. FEBS Lett *584*, 4531-4536.

Gao, S.B., Feng, Z.J., Xu, B., Chen, Y., Zheng, H.H., Yin, P., Hua, X., and Jin, G.H. (2011). Menin represses malignant phenotypes of melanoma through regulating multiple pathways. J Cell Mol Med *15*, 2353-2363.

Garcia-Higuera, I., Taniguchi, T., Ganesan, S., Meyn, M.S., Timmers, C., Hejna, J., Grompe, M., and D'Andrea, A.D. (2001). Interaction of the Fanconi anemia proteins and BRCA1 in a common pathway. Mol Cell *7*, 249-262.

Gobl, A.E., Berg, M., Lopez-Egido, J.R., Oberg, K., Skogseid, B., and Westin, G. (1999). Menin represses JunD-activated transcription by a histone deacetylase-dependent mechanism. Biochim Biophys Acta *1447*, 51-56.

Gradwohl, G., Dierich, A., LeMeur, M., and Guillemot, F. (2000). neurogenin3 is required for the development of the four endocrine cell lineages of the pancreas. Proc Natl Acad Sci U S A *97*, 1607-1611.

Gupta V, G.K., Rajeha S, Choudhry R, Tuli A (2002). The histogenesis of islets in the human fetal pancreas. J Anat Soc India *51*, 23-26.

Guru, S.C., Goldsmith, P.K., Burns, A.L., Marx, S.J., Spiegel, A.M., Collins, F.S., and Chandrasekharappa, S.C. (1998). Menin, the product of the MEN1 gene, is a nuclear protein. Proc Natl Acad Sci U S A *95*, 1630-1634.

Gustavson, K.H., Jansson, R., and Oberg, K. (1983). Chromosomal breakage in multiple endocrine adenomatosis (types I and II). Clin Genet *23*, 143-149.

Habener, J.F., Kemp, D.M., and Thomas, M.K. (2005). Minireview: transcriptional regulation in pancreatic development. Endocrinology *146*, 1025-1034.

Hara, T., Miyazaki, M., Hakuno, F., Takahashi, S., and Chida, K. (2011). PKCeta promotes a proliferation to differentiation switch in keratinocytes via upregulation of p27Kip1 mRNA through suppression of JNK/c-Jun signaling under stress conditions. Cell Death Dis *2*, e157.

Hendy, G.N., Kaji, H., Sowa, H., Lebrun, J.J., and Canaff, L. (2005). Menin and TGF-beta superfamily member signaling via the Smad pathway in pituitary, parathyroid and osteoblast. Horm Metab Res *37*, 375-379.

Heppner, C., Bilimoria, K.Y., Agarwal, S.K., Kester, M., Whitty, L.J., Guru, S.C., Chandrasekharappa, S.C., Collins, F.S., Spiegel, A.M., Marx, S.J., *et al.* (2001). The tumor suppressor protein menin interacts with NF-kappaB proteins and inhibits NF-kappaB-mediated transactivation. Oncogene *20*, 4917-4925.

Herrera, P.L. (2000). Adult insulin- and glucagon-producing cells differentiate from two independent cell lineages. Development *127*, 2317-2322.

Hughes, C.M., Rozenblatt-Rosen, O., Milne, T.A., Copeland, T.D., Levine, S.S., Lee, J.C., Hayes, D.N., Shanmugam, K.S., Bhattacharjee, A., Biondi, C.A., *et al.* (2004). Menin associates with a trithorax family histone methyltransferase complex and with the hoxc8 locus. Mol Cell *13*, 587-597.

Ivo, D., Corset, L., Desbourdes, L., Gaudray, P., and Weber, G. (2011). Menin controls the concentration of retinoblastoma protein. Cell Cycle *10*, 166-168.

Jensen, J. (2004). Gene regulatory factors in pancreatic development. Dev Dyn *229*, 176-200.

Jeon, J., Correa-Medina, M., Ricordi, C., Edlund, H., and Diez, J.A. (2009). Endocrine cell clustering during human pancreas development. J Histochem Cytochem *57*, 811-824.

Jin, S., Mao, H., Schnepp, R.W., Sykes, S.M., Silva, A.C., D'Andrea, A.D., and Hua, X. (2003). Menin associates with FANCD2, a protein involved in repair of DNA damage. Cancer Res *63*, 4204-4210.

Jorgensen, M.C., Ahnfelt-Ronne, J., Hald, J., Madsen, O.D., Serup, P., and Hecksher-Sorensen, J. (2007). An illustrated review of early pancreas development in the mouse. Endocr Rev *28*, 685-705.

Kaji, H., Canaff, L., and Hendy, G.N. (2009). Role of menin in bone development. Adv Exp Med Biol *668*, 59-67.

Kaji, H., Canaff, L., Lebrun, J.J., Goltzman, D., and Hendy, G.N. (2001). Inactivation of menin, a Smad3-interacting protein, blocks transforming growth factor type beta signaling. Proc Natl Acad Sci U S A *98*, 3837-3842.

Kanungo, J., and Chandrasekharappa, S.C. (2012). Menin induces endodermal differentiation in aggregated P19 stem cells by modulating the retinoic acid receptors. Mol Cell Biochem *359*, 95-104.

Karges, W., Maier, S., Wissmann, A., Dralle, H., Dosch, H.M., and Boehm, B.O. (1999). Primary structure, gene expression and chromosomal mapping of rodent homologs of the MEN1 tumor suppressor gene. Biochim Biophys Acta *1446*, 286-294.

Karnik, S.K., Chen, H., McLean, G.W., Heit, J.J., Gu, X., Zhang, A.Y., Fontaine, M., Yen, M.H., and Kim, S.K. (2007). Menin controls growth of pancreatic beta-cells in pregnant mice and promotes gestational diabetes mellitus. Science *318*, 806-809.

Khodaei, S., O'Brien, K.P., Dumanski, J., Wong, F.K., and Weber, G. (1999). Characterization of the MEN1 ortholog in zebrafish. Biochem Biophys Res Commun *264*, 404-408.

Kim, H., Lee, J.E., Cho, E.J., Liu, J.O., and Youn, H.D. (2003). Menin, a tumor suppressor, represses JunD-mediated transcriptional activity by association with an mSin3A-histone deacetylase complex. Cancer Res *63*, 6135-6139.

Kim, S.K., and Hebrok, M. (2001). Intercellular signals regulating pancreas development and function. Genes Dev *15*, 111-127.

Kumagai, H., Sato, N., Yamada, M., Mahony, D., Seghezzi, W., Lees, E., Arai, K., and Masai, H. (1999). A novel growth- and cell cycle-regulated protein, ASK, activates human Cdc7-related kinase and is essential for G1/S transition in mammalian cells. Mol Cell Biol *19*, 5083-5095.

La, P., Silva, A.C., Hou, Z., Wang, H., Schnepp, R.W., Yan, N., Shi, Y., and Hua, X. (2004). Direct binding of DNA by tumor suppressor menin. J Biol Chem *279*, 49045-49054.

La, P., Yang, Y., Karnik, S.K., Silva, A.C., Schnepp, R.W., Kim, S.K., and Hua, X. (2007). Menin-mediated caspase 8 expression in suppressing multiple endocrine neoplasia type 1. J Biol Chem *282*, 31332-31340.

Larsson, C., Skogseid, B., Oberg, K., Nakamura, Y., and Nordenskjold, M. (1988). Multiple endocrine neoplasia type 1 gene maps to chromosome 11 and is lost in insulinoma. Nature *332*, 85-87.

Lejonklou, M.H., Edfeldt, K., Johansson, T.A., Stalberg, P., and Skogseid, B. (2009). Neurogenin 3 and neurogenic differentiation 1 are retained in the cytoplasm of multiple endocrine neoplasia type 1 islet and pancreatic endocrine tumor cells. Pancreas *38*, 259-266.

Lemos, M.C., and Thakker, R.V. (2008). Multiple endocrine neoplasia type 1 (MEN1): analysis of 1336 mutations reported in the first decade following identification of the gene. Hum Mutat *29*, 22-32.

Li, J., Goodyer, C.G., Fellows, F., and Wang, R. (2006). Stem cell factor/c-Kit interactions regulate human islet-epithelial cluster proliferation and differentiation. Int J Biochem Cell Biol *38*, 961-972.

Lim, S., and Kaldis, P. (2012). Loss of Cdk2 and Cdk4 induces a switch from proliferation to differentiation in neural stem cells. Stem Cells *30*, 1509-1520.

Limbert, C., Path, G., Ebert, R., Rothhammer, V., Kassem, M., Jakob, F., and Seufert, J. (2011). PDX1- and NGN3-mediated in vitro reprogramming of human bone marrow-derived mesenchymal stromal cells into pancreatic endocrine lineages. Cytotherapy *13*, 802-813.

Lin, S.Y., and Elledge, S.J. (2003). Multiple tumor suppressor pathways negatively regulate telomerase. Cell *113*, 881-889.

Lin, T.M., and Chance, R.E. (1974). Candidate hormones of the gut. VI. Bovine pancreatic polypeptide (BPP) and avian pancreatic polypeptide (APP). Gastroenterology *67*, 737-738.

Liu, X., Wang, Y., Li, Y., and Pei, X. (2013). Research status and prospect of stem cells in the treatment of diabetes mellitus. Sci China Life Sci *56*, 306-312.

Lyttle, B.M., Li, J., Krishnamurthy, M., Fellows, F., Wheeler, M.B., Goodyer, C.G., and Wang, R. (2008). Transcription factor expression in the developing human fetal endocrine pancreas. Diabetologia *51*, 1169-1180.

Maruyama, K., Tsukada, T., Hosono, T., Ohkura, N., Kishi, M., Honda, M., Nara-Ashizawa, N., Nagasaki, K., and Yamaguchi, K. (1999). Structure and distribution of rat menin mRNA. Mol Cell Endocrinol *156*, 25-33.

McDonald, E., Li, J., Krishnamurthy, M., Fellows, G.F., Goodyer, C.G., and Wang, R. (2012). SOX9 regulates endocrine cell differentiation during human fetal pancreas development. Int J Biochem Cell Biol *44*, 72-83.

Milne, T.A., Briggs, S.D., Brock, H.W., Martin, M.E., Gibbs, D., Allis, C.D., and Hess, J.L. (2002). MLL targets SET domain methyltransferase activity to Hox gene promoters. Mol Cell *10*, 1107-1117.

Milne, T.A., Hughes, C.M., Lloyd, R., Yang, Z., Rozenblatt-Rosen, O., Dou, Y., Schnepp, R.W., Krankel, C., Livolsi, V.A., Gibbs, D., *et al.* (2005). Menin and MLL cooperatively regulate expression of cyclin-dependent kinase inhibitors. Proc Natl Acad Sci U S A *102*, 749-754.

Naito, J., Kaji, H., Sowa, H., Hendy, G.N., Sugimoto, T., and Chihara, K. (2005). Menin suppresses osteoblast differentiation by antagonizing the AP-1 factor, JunD. J Biol Chem *280*, 4785-4791.

Nakamura, T., Mori, T., Tada, S., Krajewski, W., Rozovskaia, T., Wassell, R., Dubois, G., Mazo, A., Croce, C.M., and Canaani, E. (2002). ALL-1 is a histone methyltransferase

that assembles a supercomplex of proteins involved in transcriptional regulation. Mol Cell *10*, 1119-1128.

Oster, A., Jensen, J., Serup, P., Galante, P., Madsen, O.D., and Larsson, L.I. (1998). Rat endocrine pancreatic development in relation to two homeobox gene products (Pdx-1 and Nkx 6.1). J Histochem Cytochem *46*, 707-715.

Papizan, J.B., Singer, R.A., Tschen, S.I., Dhawan, S., Friel, J.M., Hipkens, S.B., Magnuson, M.A., Bhushan, A., and Sussel, L. (2011). Nkx2.2 repressor complex regulates islet beta-cell specification and prevents beta-to-alpha-cell reprogramming. Genes Dev *25*, 2291-2305.

Piper, K., Ball, S.G., Keeling, J.W., Mansoor, S., Wilson, D.I., and Hanley, N.A. (2002). Novel SOX9 expression during human pancreas development correlates to abnormalities in Campomelic dysplasia. Mech Dev *116*, 223-226.

Piper, K., Brickwood, S., Turnpenny, L.W., Cameron, I.T., Ball, S.G., Wilson, D.I., and Hanley, N.A. (2004). Beta cell differentiation during early human pancreas development. J Endocrinol *181*, 11-23.

Polak, M., Bouchareb-Banaei, L., Scharfmann, R., and Czernichow, P. (2000). Early pattern of differentiation in the human pancreas. Diabetes *49*, 225-232.

Prado, C.L., Pugh-Bernard, A.E., Elghazi, L., Sosa-Pineda, B., and Sussel, L. (2004). Ghrelin cells replace insulin-producing beta cells in two mouse models of pancreas development. Proc Natl Acad Sci U S A *101*, 2924-2929.

Pusztai, P., Sarman, B., Ruzicska, E., Toke, J., Racz, K., Somogyi, A., and Tulassay, Z. (2008). Ghrelin: a new peptide regulating the neurohormonal system, energy homeostasis and glucose metabolism. Diabetes/Metabolism Research and Reviews *24*, 343-352.

Ribieras, S., Tomasetto, C., and Rio, M.C. (1998). The pS2/TFF1 trefoil factor, from basic research to clinical applications. Biochim Biophys Acta *1378*, F61-77.

Riethof, M., Flavin, P., Lindvall, B., Michels, R., O'Connor, P., Redmon, B., Retzer, K., Roberts, J., Smithm, S., and Sperl-Hillen, J. (2012). Diagnosis and Management of Type 2 Diabetes Mellitus in Adults. In ICSI Health Care Guideline (Institute for Clinical Systems Improvement) Available from http://bit.ly/Diabetes0412.

Rovasio, R.A. (2010). Development and Structure of the Pancreas. In Pancreatic Cancer, J.P. Neoptolemos, Urrutia, R., Abbruzzese, J. L., Bu¨chler, M. W., ed. (Springer Science+Business Media, LLC), pp. 27-38.

Rudnick, A., Ling, T.Y., Odagiri, H., Rutter, W.J., and German, M.S. (1994). Pancreatic beta cells express a diverse set of homeobox genes. Proc Natl Acad Sci U S A *91*, 12203-12207.

Rutter, W.J., Kemp, J.D., Bradshaw, W.S., Clark, W.R., Ronzio, R.A., and Sanders, T.G. (1968). Regulation of specific protein synthesis in cytodifferentiation. J Cell Physiol *72*, Suppl 1:1-18.

Saleem, S., Li, J., Yee, S.P., Fellows, G.F., Goodyer, C.G., and Wang, R. (2009). beta1 integrin/FAK/ERK signalling pathway is essential for human fetal islet cell differentiation and survival. J Pathol *219*, 182-192.

Sander, M., and German, M.S. (1997). The beta cell transcription factors and development of the pancreas. J Mol Med *75*, 327-340.

Sander, M., Sussel, L., Conners, J., Scheel, D., Kalamaras, J., Dela Cruz, F., Schwitzgebel, V., Hayes-Jordan, A., and German, M. (2000). Homeobox gene Nkx6.1 lies downstream of Nkx2.2 in the major pathway of beta-cell formation in the pancreas. Development *127*, 5533-5540.

Sayo, Y., Murao, K., Imachi, H., Cao, W.M., Sato, M., Dobashi, H., Wong, N.C., and Ishida, T. (2002). The multiple endocrine neoplasia type 1 gene product, menin, inhibits insulin production in rat insulinoma cells. Endocrinology *143*, 2437-2440.

Schnepp, R.W., Hou, Z., Wang, H., Petersen, C., Silva, A., Masai, H., and Hua, X. (2004). Functional interaction between tumor suppressor menin and activator of S-phase kinase. Cancer Res *64*, 6791-6796.

Senior, P.A., Kin, T., Shapiro, J., and Koh, A. (2012). Islet Transplantation at the University of Alberta: Status Update and Review of Progress over the Last Decade. Canadian Journal of Diabetes *36*, 32-37.

Seymour, P.A., Freude, K.K., Dubois, C.L., Shih, H.P., Patel, N.A., and Sander, M. (2008). A dosage-dependent requirement for Sox9 in pancreatic endocrine cell formation. Dev Biol *323*, 19-30.

Seymour, P.A., Freude, K.K., Tran, M.N., Mayes, E.E., Jensen, J., Kist, R., Scherer, G., and Sander, M. (2007). SOX9 is required for maintenance of the pancreatic progenitor cell pool. Proc Natl Acad Sci U S A *104*, 1865-1870.

Seymour, P.A., and Sander, M. (2011). Historical perspective: beginnings of the beta-cell: current perspectives in beta-cell development. Diabetes *60*, 364-376.

Shen, H.C., He, M., Powell, A., Adem, A., Lorang, D., Heller, C., Grover, A.C., Ylaya, K., Hewitt, S.M., Marx, S.J., *et al.* (2009). Recapitulation of pancreatic neuroendocrine tumors in human multiple endocrine neoplasia type I syndrome via Pdx1-directed inactivation of Men1. Cancer Res *69*, 1858-1866.

Slack, J.M. (1995). Developmental biology of the pancreas. Development *121*, 1569-1580.

Sowa, H., Kaji, H., Hendy, G.N., Canaff, L., Komori, T., Sugimoto, T., and Chihara, K. (2004). Menin is required for bone morphogenetic protein 2- and transforming growth factor beta-regulated osteoblastic differentiation through interaction with Smads and Runx2. J Biol Chem *279*, 40267-40275.

Stewart, C., Parente, F., Piehl, F., Farnebo, F., Quincey, D., Silins, G., Bergman, L., Carle, G.F., Lemmens, I., Grimmond, S., *et al.* (1998). Characterization of the mouse Men1 gene and its expression during development. Oncogene *17*, 2485-2493.

Sukhodolets, K.E., Hickman, A.B., Agarwal, S.K., Sukhodolets, M.V., Obungu, V.H., Novotny, E.A., Crabtree, J.S., Chandrasekharappa, S.C., Collins, F.S., Spiegel, A.M., *et al.* (2003). The 32-kilodalton subunit of replication protein A interacts with menin, the product of the MEN1 tumor suppressor gene. Mol Cell Biol *23*, 493-509.

Sussel, L., Kalamaras, J., Hartigan-O'Connor, D.J., Meneses, J.J., Pedersen, R.A., Rubenstein, J.L., and German, M.S. (1998). Mice lacking the homeodomain transcription factor Nkx2.2 have diabetes due to arrested differentiation of pancreatic beta cells. Development *125*, 2213-2221.

Tan, A.M., Muthusamy, L., Ng, C.C., Phoon, K.Y., Ow, J.H., and Tan, N.C. (2011). Initiation of insulin for type 2 diabetes mellitus patients: what are the issues? A qualitative study. Singapore Med J *52*, 801-809.

Thakker, R.V. (1998). Multiple endocrine neoplasia--syndromes of the twentieth century. J Clin Endocrinol Metab *83*, 2617-2620.

Ueno, N., Inui, A., Iwamoto, M., Kaga, T., Asakawa, A., Okita, M., Fujimiya, M., Nakajima, Y., Ohmoto, Y., Ohnaka, M., *et al.* (1999). Decreased food intake and body weight in pancreatic polypeptide-overexpressing mice. Gastroenterology *117*, 1427-1432.

Wang, R., Li, J., Lyte, K., Yashpal, N.K., Fellows, F., and Goodyer, C.G. (2005). Role for beta1 integrin and its associated alpha3, alpha5, and alpha6 subunits in development of the human fetal pancreas. Diabetes *54*, 2080-2089.

Wang, Y., Ozawa, A., Zaman, S., Prasad, N.B., Chandrasekharappa, S.C., Agarwal, S.K., and Marx, S.J. (2011). The tumor suppressor protein menin inhibits AKT activation by regulating its cellular localization. Cancer Res *71*, 371-382.

Wei, W., Zeve, D., Suh, J.M., Wang, X., Du, Y., Zerwekh, J.E., Dechow, P.C., Graff, J.M., and Wan, Y. (2011). Biphasic and dosage-dependent regulation of osteoclastogenesis by beta-catenin. Mol Cell Biol *31*, 4706-4719.

Wells, J.M. (2003). Genes expressed in the developing endocrine pancreas and their importance for stem cell and diabetes research. Diabetes Metab Res Rev *19*, 191-201.

Wu, T., and Hua, X. (2011). Menin represses tumorigenesis via repressing cell proliferation. Am J Cancer Res *1*, 726-739.

Wuescher, L., Angevine, K., Hinds, T., Ramakrishnan, S., Najjar, S.M., and Mensah-Osman, E.J. (2011). Insulin regulates menin expression, cytoplasmic localization, and interaction with FOXO1. Am J Physiol Endocrinol Metab *301*, E474-483.

Yaguchi, H., Ohkura, N., Tsukada, T., and Yamaguchi, K. (2002). Menin, the multiple endocrine neoplasia type 1 gene product, exhibits GTP-hydrolyzing activity in the presence of the tumor metastasis suppressor nm23. J Biol Chem *277*, 38197-38204.

Yamaguchi, K., Kameya, T., and Abe, K. (1980). Multiple endocrine neoplasia type 1. Clin Endocrinol Metab *9*, 261-284.

Yan, J., Yang, Y., Zhang, H., King, C., Kan, H.M., Cai, Y., Yuan, C.X., Bloom, G.S., and Hua, X. (2009). Menin interacts with IQGAP1 to enhance intercellular adhesion of beta-cells. Oncogene *28*, 973-982.

Yokoyama, A., Wang, Z., Wysocka, J., Sanyal, M., Aufiero, D.J., Kitabayashi, I., Herr, W., and Cleary, M.L. (2004). Leukemia proto-oncoprotein MLL forms a SET1-like histone methyltransferase complex with menin to regulate Hox gene expression. Mol Cell Biol *24*, 5639-5649.

Zhang, H., Li, W., Wang, Q., Wang, X., Li, F., Zhang, C., Wu, L., Long, H., Liu, Y., Li, X., *et al.* (2012). Glucose-mediated repression of menin promotes pancreatic beta-cell proliferation. Endocrinology *153*, 602-611.

Zhang, H.L., Li, W.Y., Zhang, C.P., Zhu, Y.X., Wu, L., Long, H.M., Li, G., and Luo, M. (2011). Differentially expressed genes in Men1 knockout and wildtype embryoid bodies for pancreatic islet development. Mol Med Report *4*, 301-305.

Zhang, H.L., Luo, T.H., Feng, L., Zhao, Y., Li, W.Y., Xu, J., Zhang, Q., Xu, L.H., Zheng, S., Li, G., *et al.* (2007). Microarray analysis of gene expression in Men1 knockout embryoid body reveals genetic events involved in early mouse embryonic development. Biochem Biophys Res Commun *352*, 456-462.

Appendix I

Ethics Approval

Research Western

Use of Human Participants - Ethics Approval Notice

Principal Investigator: Dr. Rennie Wang
Review Number: 10060
Review Level: Delegated
Approved Local Adult Participants: 100
Approved Local Minor Participants: 0
Protocol Title: Development of Human Fetal Pancreas
Department & Institution: Physiology, London Health Sciences Centre
Sponsor: Natural Sciences and Engineering Research Council

Ethics Approval Date: December 22, 2011 **Expiry Date:** April 30, 2016
Documents Reviewed & Approved & Documents Received for Information:

Document Name	Comments	Version Date
Revised Study End Date		
Increase in number of local Participants	Increased from 100 to 200.	

This is to notify you that The University of Western Ontario Research Ethics Board for Health Sciences Research Involving Human Subjects (HSREB) which is organized and operates according to the Tri-Council Policy Statement: Ethical Conduct of Research Involving Humans and the Health Canada/ICH Good Clinical Practice Practices: Consolidated Guidelines; and the applicable laws and regulations of Ontario has reviewed and granted approval to the above referenced revision(s) or amendment(s) on the approval date noted above. The membership of this REB also complies with the membership requirements for REB's as defined in Division 5 of the Food and Drug Regulations.

The ethics approval for this study shall remain valid until the expiry date noted above assuming timely and acceptable responses to the HSREB's periodic requests for surveillance and monitoring information. If you require an updated approval notice prior to that time you must request it using the UWO Updated Approval Request Form.

Members of the HSREB who are named as investigators in research studies, or declare a conflict of interest, do not participate in discussion related to, nor vote on, such studies when they are presented to the HSREB.

The Chair of the HSREB is Dr. Joseph Gilbert. The UWO HSREB is registered with the U.S. Department of Health & Human Services under the IRB registration number IRB 00000940.

Signature

Ethics Officer to Contact for Further Information

Janice Sutherland (jsutherl@uwo.ca)	Grace Kelly (grace.kelly@uwo.ca)	Shantel Walcott (swalcot@uwo.ca)

This is an official document. Please retain the original in your files.

Appendix II

Supplementary Material

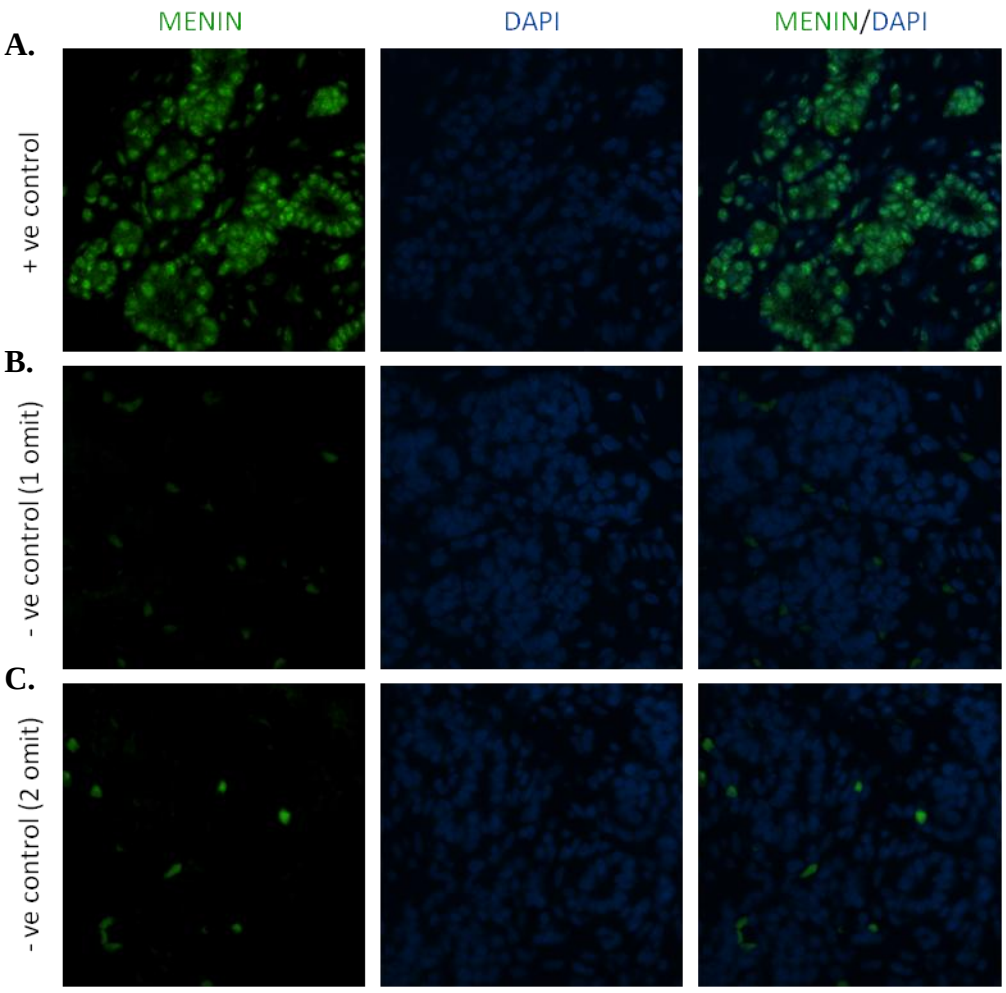

Supplementary Figure 1. Anti-Menin Antibody Control with Immunofluorescence Techniques.

Human fetal pancreata sections from 15 wks of development were used to test the Rabbit menin anti-human antibody by Bethyl Laboratories (Montgomery, TX, USA) for non-specific binding. **(A)** Normal immunofluorescence staining (+ve control) where sections were immunolabelled with anti-menin (primary) antibodies then visualized with Cy2 (green) conjugated secondary antibodies. Nuclei were labelled with DAPI (blue). Images display immunostaining for menin (green), DAPI (blue), and an overlay of the images. Omission of the **(B)** primary (1 omit) or **(C)** the corresponding secondary antibody (2 omit). Blood cells (containing no nucleus, indicated by DAPI staining) showed high non-specific binding with the menin antibody however blood cells bind all antibodies and can be distinguished by the lack of DAPI co-staining.

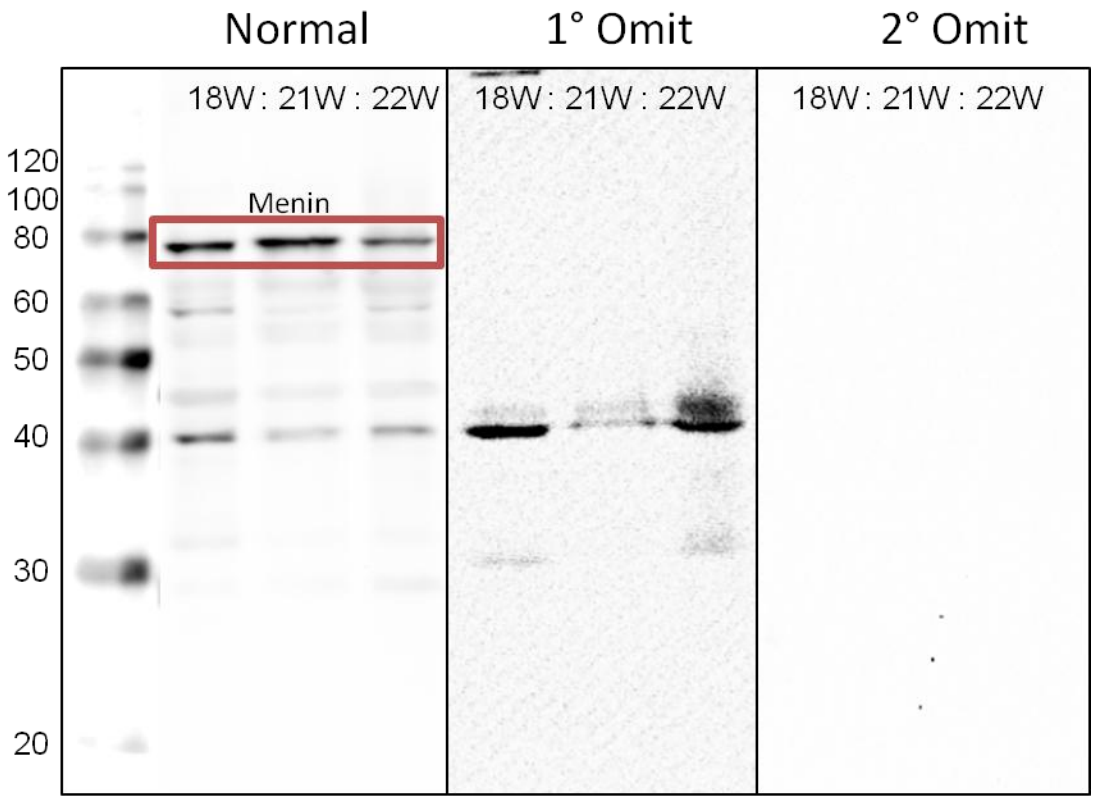

Supplementary Figure 2. Anti-Menin Antibody Control Using Western Blotting Techniques.

Whole protein extracts from human fetal pancreata at 18, 21, and 22 wks were used to test the western blotting specificity of the rabbit anti-human menin antibody from Bethyl Laboratories (Montgomery, TX, USA). The molecular weight of menin is predicted to be around 68 kDa. Normal menin antibody staining revealed multiple bands of non-specific binding. The second brightest band at 40kDa was predominantly shown to be due to the secondary antibody used (shown by 1° omit). The primary antibody had no background noise when the 2° was omitted. Thus the true menin band is observed around 75kDa. The protein extracts at each time point were taken from the same pancreatic aliquot and run on the same gel in triplicate. The membrane was then cut to allow for consistent membrane production conditions but different staining treatments.

A.

RNA Collection - siRNA

Treatment		Concentration	Purity Ratio
24hr	Ctrl	0.169	1.316
	MsiRNA	0.192	1.622
48hr	Ctrl	0.436	1.467
	MsiRNA	0.304	1.527
72hr	Ctrl	0.262	1.548
	MsiRNA	0.192	1.683

Sample: 15W 11H46 Wed June 1, 2011

B.

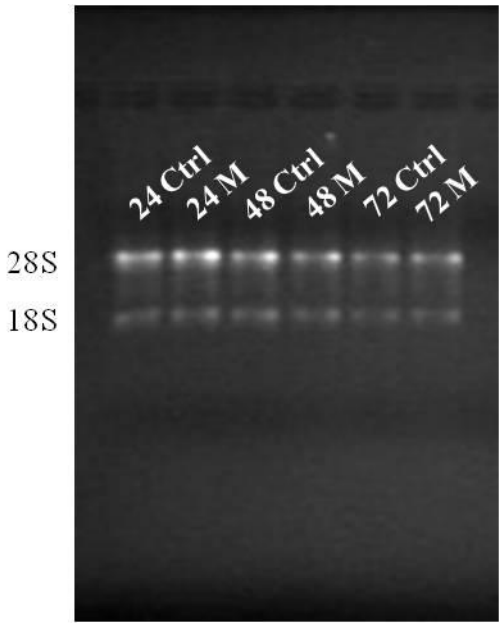

Supplementary Figure 3. RNA Collection and Quality Control.

Extracted RNA was tested to determine the concentration, purity, and quality of each sample and treatment group. A sample is shown where total RNA was extracted from Islet-epithelial cell clusters which had been transfected with either control siRNA (Ctrl) or *MEN1* siRNA (MsiRNA/M) for a treatment period of 24, 48, or 72 hrs. **(A)** 1µL of each treatment group was diluted and run through a spectrophotometer to determine the $O.D_{260}$ (total RNA concentration) and corrected OD ratio of A260/A280 (RNA purity). **(B)** 1 µL of each treatment group was run on a 1% agarose gel stained with ethidium bromide to test RNA Quality, two sharp and clear 28S and 18S rRNA bands were shown.

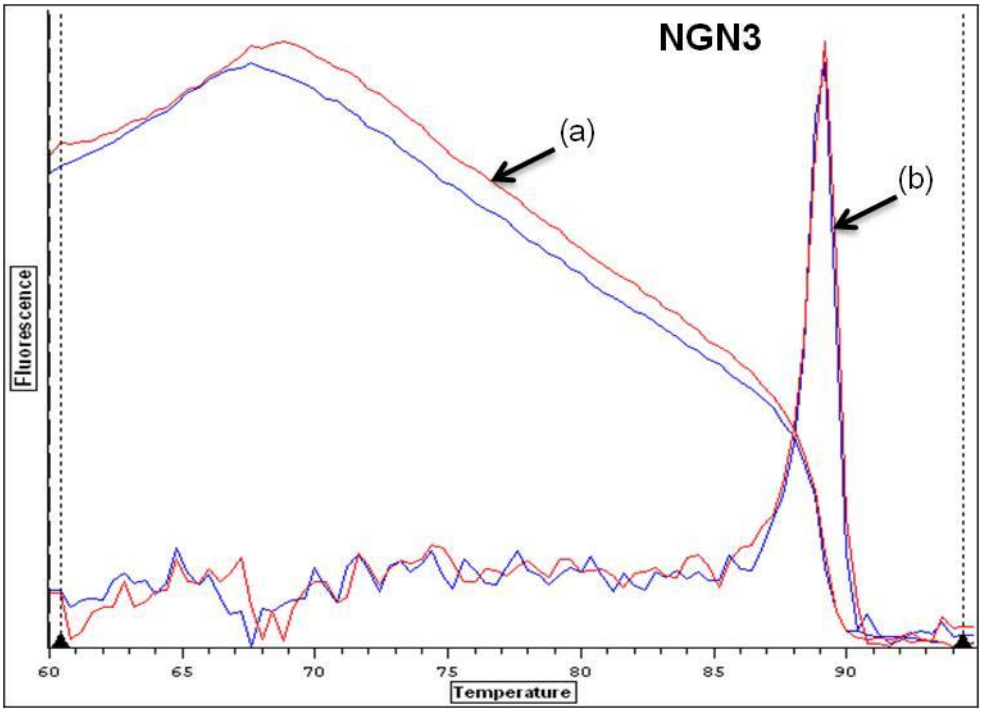

Supplementary Figure 4. Melting Curves and Derivative Melting Curves of qRT-PCR Products.

For each qRT-PCR reaction the melting curve and derivative melting curve was determined to ensure the quality of target sequence amplification. Shown is an example of a reaction amplifying NGN3 mRNA where the melting curves **(a)** and derivative melting curves **(b)** show that qRT-PCR assays have amplified the target sequences with excellent specificity.

A.

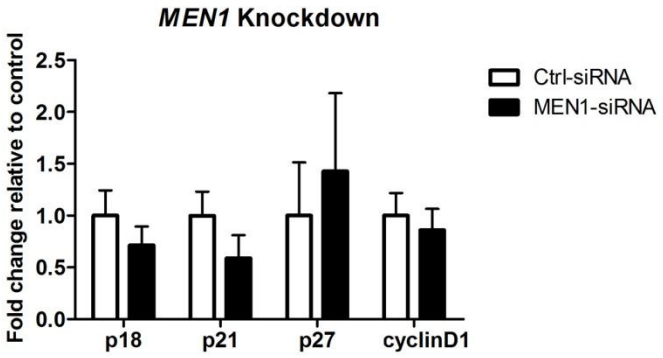

B.

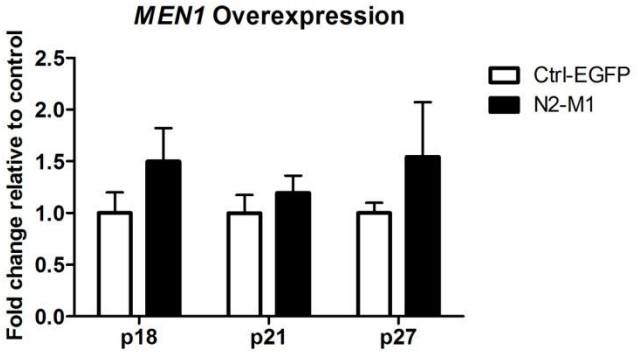

Supplementary Figure 5. Effect of *MEN1* Knockdown and *MEN1* Overexpression on *p18, p21, p27,* and *CyclinD1* Expression.

Islet-epithelial cell clusters were isolated from human fetal pancreata 15 to 19 wks. **(A)** Clusters were transfected with either control siRNA (Ctrl-siRNA) or *MEN1* siRNA (MEN1-siRNA) for a 48 hr treatment period. qRT-PCR analysis of total *p18*, *p21*, *p27*, and *CyclinD1* mRNA for control and *MEN1* siRNA treatments. **(B)** Clusters were transfected with either a control (Ctrl-EGFP) or a *MEN1* (N2-M1) vector and cultured for 48 hrs. qRT-PCR analysis of total *p18*, *p21*, and *p27* mRNA for control and N2-M1 treatment groups. Data were normalized to 18S rRNA and are expressed as means ± SEM where n=4-6 per experimental group.

A.

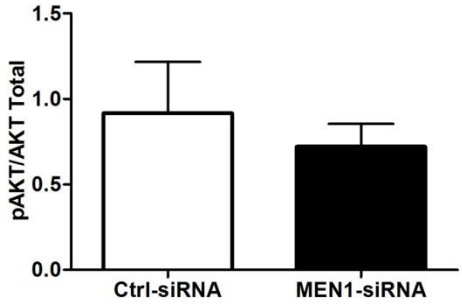

B.

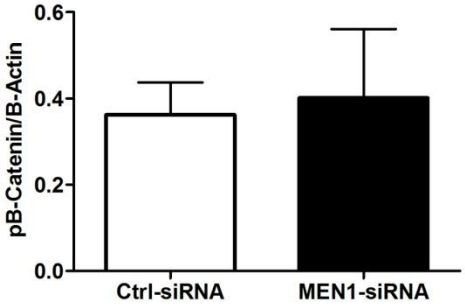

Supplementary Figure 6. Effect of *MEN1* siRNA on the AKT and Wnt/β-catenin Pathways.

Islet-epithelial cell clusters, isolated from human fetal pancreata 15 to 19 wks, were transfected with either control siRNA or *MEN1* siRNA for a 48 hr treatment. **(A)** Western blot analysis of total phosphorylated AKT (pAKT) expression (60 kDa) normalized to total AKT expression (60 kDa) for both treatment groups, n=3 per treatment group. **(B)** Western blot analysis of total phosphorylated β-catenin (pβ-catenin) expression (92 kDa) normalized to total β-Actin expression (42 kDa) for both treatment groups, n=3 per treatment group. Data were expressed as means ± SEM.

Supplementary Table 1: **List of Antibodies/Antisera Used for Immunofluorescence and Western-Blot Analyses.**

Primary antibody	Dilution	Company, Location
mouse monoclonal β –Actin	1:5000[a]	Sigma, St. Louis, MO, USA
rabbit polyclonal AKT	1:3000[a]	Cell signaling, Danvers, MA, USA
mouse monoclonal Phosphorylated AKT (Ser 473)	1:2000[a]	Cell signaling, Danvers, MA, USA
rabbit polyclonal Phosphorylated β-Catenin (Ser 675)	1:1000[a]	Cell signaling, Danvers, MA, USA

[a] dilution factor applied for western blot analysis. DSHB, Developmental Studies Hybridoma Bank; JRL, Jackson Immunoresearch Laboratories

Curriculum Vitae

Curriculum Vitae

Jessica Dubrick

Education

MSc Candidate 2010-present **University of Western Ontario, London, ON**

- Expected completion: June 2013

BSc 2004-2008 **University of Waterloo, Waterloo, ON**

- Bachelors of Science, Honours Biochemistry

Honours and Awards

- Western Graduate Research Scholarship (2010-2012)
- Schulich Graduate Scholarship (2011-2012)
- Pathology Research Day 2011 – 1st prize for Poster Presentation by a Graduate Student

Presentations and Posters

Pathology Research Day Poster Presentation – April 26, 2013

Elucidating the Role of Menin During Islet Cell Development in the Human Fetal Pancreas

Authors: Jessica Dubrick, Jinming Li, Rennian Wang

Pathology Research Day Oral Presentation – May 4, 2012

Role of *MEN1*/MENIN during Islet Cell Development in the Human Fetal Pancreas

Authors: Jessica Dubrick, Jinming Li, Rennian Wang

London Health Research Day Poster Presentation – March 22, 2012

Role of *MEN1*/MENIN during Islet Cell Development in the Human Fetal Pancreas

Authors: Jessica Dubrick, Jinming Li, Rennian Wang

Diabetes Research Day (Schulich School of Medicine & Dentistry) Poster Presentation – November 15, 2011

Role of *MEN1*/MENIN during Islet Cell Development in the Human Fetal Pancreas

Authors: Jessica Dubrick, Jinming Li, Rennian Wang

Pathology Research Day Poster Presentation – May 3, 2011

Role of *MEN1*/MENIN during Islet Cell Development in the Human Fetal Pancreas

Authors: Jessica Dubrick, Jinming Li, Rennian Wang

Margaret Moffat Research and Career Day Poster Presentation – March 29, 2011

Role of *MEN1*/MENIN during Islet Cell Development in the Human Fetal Pancreas

Authors: Jessica Dubrick, Jinming Li, Rennian Wang

Lawson Health Research Institute Research Day Poster Presentation – March 22, 2011

Role of *MEN1*/MENIN during Islet Cell Development in the Human Fetal Pancreas

Authors: Jessica Dubrick, Jinming Li, Rennian Wang